A STUDY ON DESIGN OF PILED RAFT FOUNDATION SYSTEMS

A THESIS SUBMITTED TO
THE GRADUATE SCHOOL OF NATURAL AND APPLIED SCIENCES
OF
MIDDLE EAST TECHNICAL UNIVERSITY

BY

NURULLAH SÖNMEZ

IN PARTIAL FULFILLMENT OF THE REQUIREMENTS
FOR
THE DEGREE OF MASTER
OF
SCIENCE IN CIVIL ENGINEERING

SEPTEMBER, 2013

Approval of the thesis:

A STUDY ON DESIGN OF PILED RAFT FOUNDATION SYSTEMS

submitted by **NURULLAH SÖNMEZ** in partial fulfillment of the requirements for the degree of **Master of Science in Civil Engineering Department, Middle East Technical University** by,

Prof. Dr. Canan Özgen _____
Dean, Graduate School of **Natural and Applied Sciences**

Prof. Dr. Ahmet Cevdet Yalçıner _____
Head of Department, **Civil Engineering**

Prof. Dr. M. Ufuk Ergün
Supervisor, **Civil Engineering Dept., METU** _____

Examining Committee Members:

Asst. Prof. Dr. Zeynep Gülerce _____
Civil Engineering Dept., METU

Prof. Dr. M. Ufuk Ergun _____
Civil Engineering Dept., METU

Asst. Prof. Dr. Nejan Huvaj Sarıhan _____
Civil Engineering Dept., METU

Dr. Onur Pekcan _____
Civil Engineering Dept., METU

M.Sc. CE A. Mengüç Ünver _____
Argem Geoteknik Müh. Müş. Ltd. Şti.

Date: **03.09.2013**

I hereby declare that all information in this document has been obtained and presented in accordance with academic rules and ethical conduct. I also declare that, as required by these rules and conduct, I have fully cited and referenced all material and results that are not original to this work.

Name, Last name: Nurullah Sönmez

Signature:

ABSTRACT

A STUDY ON DESIGN OF PILED RAFT FOUNDATION SYSTEMS

Sönmez, Nurullah
M.S., Department of Civil Engineering
Supervisor: Prof. Dr. Mehmet Ufuk Ergun

September 2013, 104 pages

Design concepts and load sharing mechanism of piled raft foundations have been studied in this thesis. In the conventional piled foundations, the load transferred only by the piles and the piles are used for the reducing of both total and differential settlements and the contribution of the raft is generally disregarded. In the first part of the thesis, design approaches in the literature have been discussed. In the second part of the thesis, parametric analyses have been conducted for typical foundation in overconsolidated Ankara clay and finite element analyses have been done for Messe-Torhaus building in Frankfurt. Three dimensional analyses have been made by the widely used commercial software of Plaxis 3D and Sap2000, which solve the models by using the Finite Element Method. The foundation settlement and the load sharing between raft and pile have been investigated to identify the contribution of raft to the total capacity of piled raft foundations. The results showed that the raft can carry up to the 40% of the total applied load for an optimum number of piles for acceptable settlement levels.

Keywords: Piled Raft Foundations, Plaxis 3D, Sap2000

ÖZ

KAZIKLI RADYE TEMEL SİSTEMLERİ ÜZERİNE BİR İNCELEME

Sönmez, Nurullah
Yüksek Lisans, İnşaat Mühendisliği Bölümü
Tez Yöneticisi: Prof. Dr. Mehmet Ufuk Ergun

Eylül 2013, 104 sayfa

Tez kapsamında, kazıklı radye temellerdeki tasarım yaklaşımları ve yük paylaşım mekanizması incelenmiştir. Klasik kazıklı temellerde sadece kazıkların yük taşıyacağı varsayımı yapılarak, toplam ve farklı oturmaların sadece kazıklar kullanılarak kontrolü sağlanarak ve radyenin katkısı göz ardı edilmektedir. Tezin birinci bölümünde, şimdiye kadar yapılan çalışmalardaki tasarım yaklaşımları incelenmiştir. Tezin ikinci kısmında ise aşırı sıkışmış Ankara kilinde tipik bir radyenin parametrik çözümü ve Frankfurt'taki Messe-Torhaus binasının sonlu elemanlar yöntemi ile çözümü yapılmıştır. Üç boyutlu analizlerde, yaygın olarak kullanılan ve çözümleri sonlu elemanlar metodu ile yapan Plaxis 3D ve Sap2000 ticari yazılımları kullanılmıştır. Oturmalar ve kazık-radye arasındaki yük paylaşımı incelenerek, radyenin toplam taşıma gücüne katkısı araştırılmış ve izin verilen oturma miktarlarında ve ideal kazık sayısı ile, radyenin toplam yükün %40'ına varan oranlarda taşıma kapasitesine katkı sağladığı bulunmuştur.

Anahtar Kelimeler: Kazıklı Radye Temeller, Plaxis 3D, Sap2000

TABLE OF CONTENTS

LIST OF TABLES

LIST OF FIGURES

CHAPTER 1

INTRODUCTION

1.1 Background

To carry the excessive loads that come from the superstructures like high-rise buildings, bridges, power plants or other civil structures and to prevent excessive settlements, piled foundations have been developed and widely used in recent decades. However, it is observed that the design of foundations considering only the pile or raft is not a feasible solution because of the load sharing mechanism of the pile-raft-soil. Therefore, the combination of two separate systems, namely “Piled Raft Foundations” has been developed (Clancy and Randolph (1993)).

Piled raft foundation system is verified to be an economical foundation type comparing the conventional piled foundations, where, only the piles are used for the reducing both total and differential settlements and the contribution of the raft is generally disregarded.

In this study, behavior of the piled raft foundation systems under axial loads has been investigated by comparing the traditional design approaches and the current design approaches by parametric analyses. In the literature, there are plenty of researches focusing of these parameters, like; the number of piles, length of piles, diameter of piles, pile spacing ratio, location of piles, stiffness of piles, distribution of load, level of load, raft thickness, raft dimensions and type of soil. However, through these parameters, the number of piles, length of piles and level of load are emphasized in this study. Effects of these parameters are discussed with the solutions of finite element models. To this end, parametric analyses are conducted via the software Plaxis 3D and SAP2000 with the comparisons.

1.2 Aim

This study aims to describe and clarify the load sharing mechanism of piled raft foundation systems by considering the ratio of raft /pile load sharing under variable conditions (load levels, pile lengths and number of piles). In addition it is purposed by the study to propose a new design methodology for the piled raft foundations.

For that reason, mainly two different cases have been studied, in which include sub-cases. These sub-cases are the outcomes of the previously mentioned variables. First case is an arbitrary case in Ankara clay and the second case is a real case of Messe-Torhaus building in Frankfurt. Parametric analyses are conducted for the cases. The second case has been particularly chosen to validate the outputs of the first case.

1.3 Research Methodology

A series of Plaxis 3D and Sap2000 analyses are carried out for two cases to examine the behavior of piled raft foundation. Deformations are directly calculated by three-dimensional meshing of the soil in Plaxis 3D. However, this is not the case for Sap2000, where the soil is characterized with Winkler springs. Therefore, the soil spring assignment and the values of these springs becomes the chief point for Sap2000 analyses. In current practical applications, only the pile springs are assigned to the models of Sap2000, which is not a realistic behavior of piled raft foundation. However, the contribution of raft should be taken into account. Hence, other than the Plaxis 3D analyses, a simplified method is presented for the piled raft foundations to find the settlements in Sap2000 by using the outputs of the Plaxis.

Using the embedded pile feature of Plaxis, pile loads are calculated and subtracted from the total applied load to find raft and pile load sharing. Settlements are calculated for each applied load level and equivalent load-settlement curves are plotted. Linear trend lines are plotted on these curves. Taking the constant of the slope of these trend lines as the total spring of elements, corresponding average spring constants are derived and assigned to the piles and raft in Sap2000. Method has been applied to an arbitrary case on Ankara clay. This method is also validated by an actual case of Messe-Torhaus in Frankfurt.

1.4 Outline

After this introduction of the Chapter 1, critical points of current knowledge and developments achieved in the design of piled raft foundation systems and the affecting parameters of the behavior of piled raft foundation systems are presented in Chapter 2. Details of the finite element analysis made by Plaxis 3D and Sap2000, geometry and material properties of the models of all cases and latest design approaches are described in the Chapter 3. Comparison

and discussion of results of Plaxis 3D and Sap2000 analyses and the proposed method are given in the Chapter 4. Lastly, the study is summarized and recommendations for further studies are given in the conclusion chapter of Chapter 5.

CHAPTER 2

LITERATURE REVIEW

2.1 Introduction

In the design of foundations, shallow foundation is the first option where the top soil has sufficient bearing strength to carry the superstructure load without any significant total and differential settlements to prevent damage of infrastructure and superstructure. However, in the last decades the need for high-rise buildings and high-loaded superstructures has been increased rapidly, even in the lands with poor subsoil conditions. Therefore, the need for foundations with high bearing capacity and showing low settlement values, both total and differential, has also been increased. These types of foundations can be constructed as a shallow foundation after the application of ground improvement techniques or as a piled foundation which transfers the excessive load to a deeper and stiffer stratum through the piles and reduces the settlements.

This chapter presents a brief review of previous researches on piles, rafts, pile groups and piled raft foundations. However, the main attention is on design methods and analyses of piled raft foundations. Chapter may be outlined as;

- Single Piles
- Pile Groups
- Raft Foundations
- Piled Raft Foundations
- Finite Element Programs: Plaxis 3D and Sap2000

As briefly mentioned in the Chapter 1; rafts are generally considered only as a “cap” which structurally connects the heads of the piles. However, the positive contribution of rafts to the load/settlement behavior is disregarded. As structural elements, rafts are mostly in contact with the soil, therefore has/have a capacity to transfer the load comes from the superstructure to the soil beneath. Considering this contribution (or load sharing), the total length of the piles may be significantly decreased. So, piled raft foundations become an alternative to the piled foundations or foundations with “settlement reducing piles” for an economic/feasible design.

Piled raft foundations consist of three elements; piles, raft and the subsoil. Therefore, it is essential to mention the behavior of piled raft foundations starting from the single piles, pile groups and the raft only. In this study, piled raft foundations with friction piles, which are subjected to static vertical compression load in cohesive soils, has been taken into account. Therefore, piles, rafts, pile groups and piled raft foundations in cohesionless soils and subjected to lateral/dynamic loadings are not mentioned.

Classification of Piles and Construction Techniques in Brief

Piles, which are used for the foundations, can be classified according to the material, size (diameter), installation technique and behavior. Piles can be made of timber, plane or reinforced concrete, precast concrete, cast in place concrete or steel/sheet. Considering the diameter, piles can be classified as small (d≤250mm), medium (300mm≤d≤600mm) and large (d≥800mm). According the installation technique, piles can be subdivided into two main categories as displacement piles and replacement piles (Viggiani et al. 2012). The displacement piles, which have been using prior than the replacement piles, are constructed by pushing, screwing or driving. Steel sections/columns or timber can be used as displacement piles, when it comes to concrete, as a material, the piles are to be precast. On the other hand, the replacement piles are constructed by the removal of the soil from the ground and pouring concrete or placing precast concrete units/steel sections into the hole. Considering the behavior, piles may be categorized as; floating/friction piles and end-bearing piles.

Installation/construction process of the replacement piles has a large number of details depending on the subsoil material, water level, equipment used and the excavation technique. Percussion or rotary drilling methods can be used for boring the soil. At the present, the most of the replacement piles are constructed by the rotary drilling, which is also valid for Turkey. If the soil profile consists of unstable material or water, a temporary steel casing or slurry is used to support the hole which called as wet method. In other case the soil is self-supporting. Therefore, the steel casing or slurry is not needed, which called as dry method.

2.2 Single Pile**Load Transfer Mechanism and Bearing Capacity of a Single Pile**

Under axial compression loads, load transfer mechanism of a single pile is as shown in the Figure 1. In the case of floating piles, the shaft friction "q_s" governs the capacity. However, as its name implies, capacity of end-bearing piles depends on tip resistance "q_b".

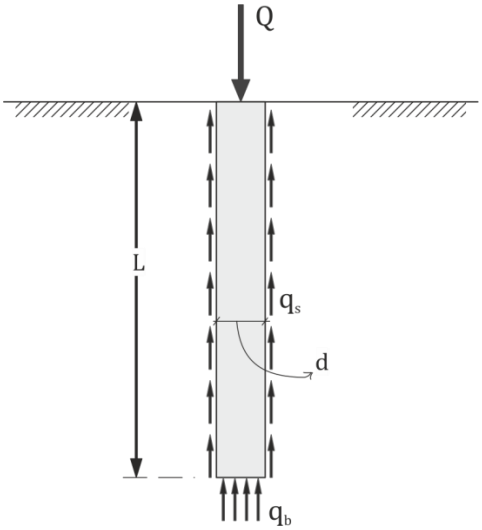

Figure 1 Load transfer mechanism of a single pile.

Considering the above mentioned load sharing mechanism of a pile, there are mainly three approaches for the calculation of the pile capacity; from fundamental soil properties, from in situ test (SPT, CPT, etc.) results and from full-scale load tests on a prototype pile. The general focus of this study will be on the first one; fundamental soil properties.

The general concept of the evaluation of the ultimate resistance of a pile is based on the shaft friction and base resistance. Thus, the total failure load is formulated as;

$$\overline{Q_u} = Q_u + W_p = Q_b + Q_f - W_p$$

where Q_u = load applied to the pile at failure
Q_b = base resistance
Q_f = shaft resistance
W_p = weight of the pile.

The general equation for the base resistance may be written as

$$Q_b = cN_c + q_0'N_q + \frac{1}{2}\gamma d N_\gamma A_b$$

where d = width or diameter of the shaft at base level
q_0' = effective overburden pressure at the base level of the pile
A_b = base area of pile
c = cohesion of soil
γ = effective unit weight of soil
N_c, N_q, N_γ = bearing capacity factors which take into account the shape factor.

In **cohesionless soils** $c = 0$ and the term ½ $\gamma d N_\gamma$ becomes insignificant in comparison with the term $q_0'N_q$ for deep foundations. Thus,

$$Q_b = q_0'N_qA_b$$

The net ultimate load in excess of overburden pressure load q_oA_b is

$$Q_u + W_p - q_oA_b = q_0'N_qA_b + W_p - q_0'A_b + Q_f$$

For all practical purposes, W_p and $q_0'A_b$ are assumed equal. Therefore;

$$Q_u = q_0'N_qA_b + Q_f$$

$$Q_u = q_0'N_qA_b + A_s\overline{q}_0'\overline{K}_s \tan\delta$$

where A_s = surface area of the embedded length of the pile

$\bar{q}_0'$ = average effective overburden pressure over the embedded depth of the pile
$\bar{K}_s$ = average lateral earth pressure coefficient
δ = angle of wall friction.

In the case of **cohesive soils,** such as saturated clays (normally consolidated), for ϕ=0, $N_q = 1$ and $N_\gamma = 0$.

The ultimate base load

$$\overline{Q_b} = (c_b N_c + q_0')A_b$$

The net ultimate base load

$$\overline{Q_b} - q_0' A_b = Q_b = c_b N_c A_b$$

Therefore, the net ultimate load capacity of the pile;

$$Q_u = c_b N_c A_b + \alpha \bar{c}_u A_s$$

where α = adhesion factor
$\bar{c}_u$ = average undrained shear strength of clay along the shaft
c_b = undrained shear strength of clay at the base level
N_c = bearing capacity factor

Bearing Capacity Factor N_c

The value of the bearing capacity factor N_c is accepted as 9 which is the value proposed by Skempton (1951) for circular foundations for a L/B ratio greater than 4. The base capacity of a pile in clayey soils may now be expressed as;

$$Q_b = 9 c_b A_b$$

Skin Resistance

by α –Method: For evaluating the adhesion factor α, Dennis and Olson (1983) developed a curve in Figure 2 giving a relationship between α and undrained shear strength c_u of clay. This curve is valid for the piles penetrating less than 30m. For embedment between 30 to 50m, a reduction factor should be applied linearly from 1.0 to 0.56 (Dennis and Olson, 1983).

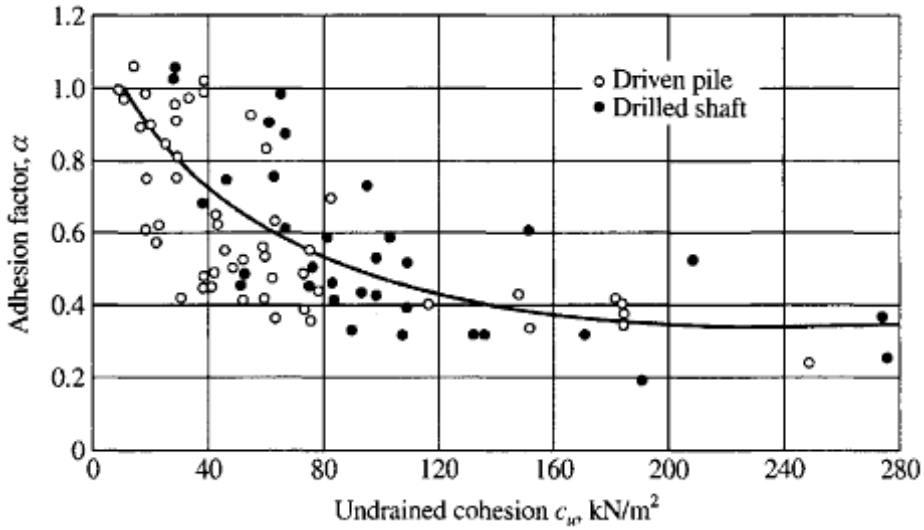

Figure 2 Adhesion factor α for piles with penetration lengths less than 50m in clay (Data from Dennis and Olson, 1983; Stas and Kulhawy, 1984)

by β Method or the Effective Stress Method of Computing Skin Resistance: Unit skin friction f_s is defined as

$$f_s = \bar{q}_0' \overline{K}_s \tan\delta = \beta \bar{q}_0'$$

by Meyerhof 's Method (1976): Meyerhof has suggested a semi-empirical relationship for estimating skin friction in clays. For bored piles

$$f_s = c_u \tan\phi'$$

where c_u= undrained shear strength of the soil
ϕ'= effective angle of internal friction

by Viggiani (1993): Viggiani et al. (2012) presents α values, depending on the pile type and c_u, as formulized in Table 1.

Table 1 - Values of α

Pile Type	cu	alfa
Displacement	$c_u \leq 25$	1
	$25 \leq c_u \leq 70$	$1 - 0.0011(c_u - 25)$

	$c_u \geq 70$	0.5
Replacement	$c_u \leq 25$	0.7
	$25 \leq c_u \leq 70$	$0.7 - 0.008(c_u - 25)$
	$c_u \geq 70$	0.35

Settlement of a Single Pile

For the settlement analyses of the single piles, there are plenty of methods in the literature. They are mainly based on empirical correlations or on the stress distribution along the pile. Meyerhof (1959), suggested an empirical formula for the settlement ρ of a single pile in sand, with a factor of safety FS on ultimate load not less than 3;

$$\rho = \frac{d_b}{30 * FS}$$

where d_b = diameter of pile base

Also Viggiani and Viggiani (2008) (in Viggiani et al. (2012)) suggested an empirical formula for the settlement w_s depending on the soil and pile type as;

$$w_s = \frac{d}{M}\frac{Q}{Q_{lim}} = \frac{d}{M} * \frac{1}{FS}$$

where d = diameter of pile

Q = applied load

Q_{lim} = bearing capacity of pile

M = constant depends on the pile and soil type, in Table 2.

Table 2 - Values of M

Pile Type	Soil type	M
Displacement	Cohesionless	80
	Cohesive	120
Small displacement	Cohesionless	50
	Cohesive	75
Replacement	Cohesionless	25
	Cohesive	40

Settlement of a pile can also be calculated by the load-settlement curves which are called as t-z curves. The basic idea of this method can be described as; the pile is divided into segments and assuming a linear variation of load in each segment, elastic deformations are calculated. Then, the displacement of the top of the pile is plotted against each increment of load. Curves depend on the relative strength values of the surrounding and underlying soil (Murthy (2002)) and

generally modeled by a set of independent Winkler springs (Viggiani et al. ((2012)). In addition, using Davisson's method, the ultimate pile capacity can be found by the help of load-settlement curves. A typical load-settlement curve for large diameter bored piles is shown in Figure 3.

Stiffness of a Single Pile

As illustrated in Figure 1, load is transferred by skin friction in addition to the end resistance of pile. Fleming et al. (1992) expressed the load settlement ratio i.e. stiffness of the shaft and the pile base as;

$$\frac{P_s}{w_s} = \frac{2\pi}{\zeta} L\bar{G}$$

and

$$\frac{P_b}{w_b} = \frac{2d_b G_b}{(1-v)}$$

The settlement of pile head w_t under the load P_t can be solved by combining both of the above equations;

$$\frac{P_t}{w_t d G_L} = \frac{2}{(1-v)}\frac{d_b}{d}\frac{G_b}{G_L} + \frac{2\pi}{\zeta}\frac{\bar{G}}{G_L}\frac{L}{d}$$

And the stiffness of a pile may be written as;

$$k_p = \frac{P_t}{w_t} = dG_L\frac{2}{(1-v)}\frac{d_b}{d}\frac{G_b}{G_L} + \frac{2\pi}{\zeta}\frac{\bar{G}}{G_L}\frac{L}{d}$$

where $\zeta = \ln[5\rho(1-v)L/d]$ for floating piles ($G_b = G_L$) and ρ is the ratio of shear modulus $\bar{G}$ at the center of pile over the shear modulus G_L at the end of the pile $\rho = \bar{G}\,/G_L$. General correlation of the shear modulus with E and $: G = E/2(1-v)$

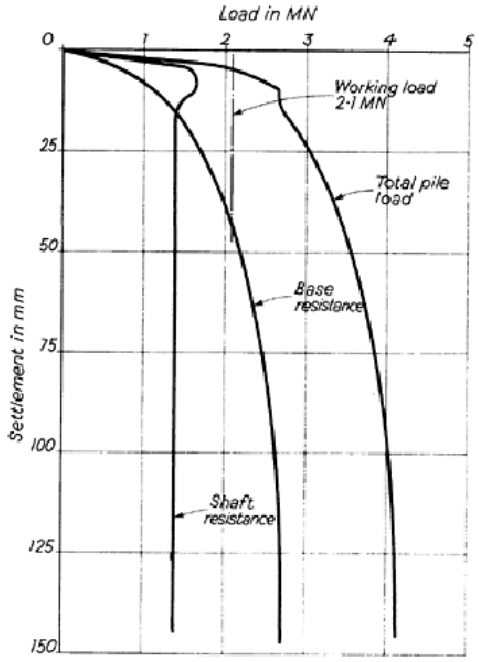

Figure 3 Load-settlement relationships for large-diameter bored piles in stiff clay (Tomlinson, 2004)

In addition to the empirical methods, some solutions, including analytical solutions, boundary element methods and finite element methods, have been suggested by various researchers (Randolph and Worth (1978), Poulos and Davis (1968), Ellison et al. (1971)) (Viggiani et al. (2012)).

Randolph and Worth (1978) suggested a widely used analytical solution for the settlement w of a single pile, assuming the pile in an elastic half space.

$$w = \frac{Q}{EL} I_w$$

where Q = total load on pile

E= Young's modulus of pile

L= length of pile

I_w= displacement influence factor

$$I_w = \frac{2L(1+\nu)}{r_0} \frac{1 + \frac{4}{1-\nu}\frac{\eta}{\xi}\frac{\tanh(\mu L)}{\mu L}\frac{L}{r_0}}{\frac{4}{1-\nu}\frac{\eta}{\xi} + \frac{2\pi\rho}{\zeta}\frac{\tanh(\mu L)}{\mu L}\frac{L}{r_0}}$$

where $\eta = \frac{r_b}{r_0}$ ($\eta = 1$ for cylindrical piles)

r_o= radius of the pile

r_b= radius of the pile base

$\xi = \frac{G_L}{G_b}$ ($\xi = 1$ for homogeneous layer where G is the shear modulus)

$\rho = \frac{\bar{G}}{G_L}$ for piles crossing soil with variable stiffness ($\bar{G}$ is the average shear modulus along pile length)

$\mu L = \sqrt{\frac{2}{\zeta \lambda}} \frac{L}{r_0}$

$\lambda = \frac{E_p}{E_L}$ pile soil relative stiffness

The parameter ζ is expressed by Viggiani et al. (2012) as;

$$\zeta = \ln\left\{[0.25 + \langle 2.5\rho(1-\nu) - 0.25\rangle\xi]\frac{L}{r_0}\right\}$$

2.3 Pile Foundations

Load Transfer Mechanism and Bearing Capacity of Pile groups

As load-bearing structural elements, piles are mostly installed in groups. Based on the connectivity of the pile cap with the underlying soil, pile groups can be divided into two main types as; free-standing groups, in which the piles cap is not in contact with underlying soil and piled foundations, in which the cap is in contact with the underlying soil (Poulos and Davis (1980)). For both types of the pile groups, it is naturally expected from piles to interact and to affect each other's capacity. Interaction between the piles in a group is indicated by Fleming et al. (1992) as shown in Figure 4. Pile slenderness ratio, pile spacing ratio, pile stiffness ratio, homogeneity of soil and Poisson's ratio are the factors which creates the interaction of piles in a group.

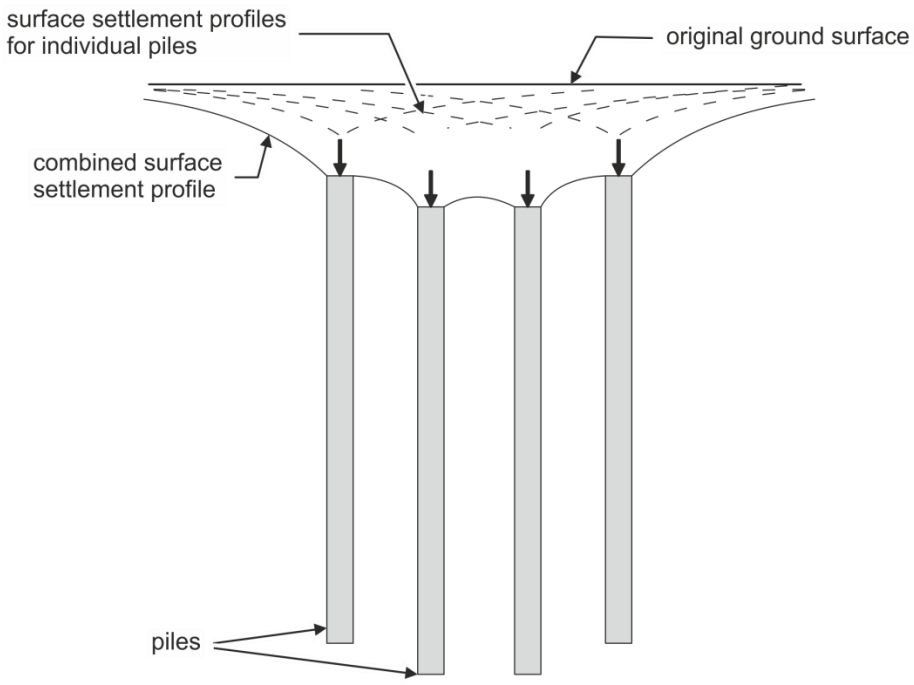

Figure 4 Interaction of piles in a pile group (after Fleming et al., 1992)

Due to the interaction effects within a group, bearing capacity of the group becomes lower than the total capacity of the individual piles. As a result, the bearing capacity of pile groups is described as the sum of the bearing capacity of the single piles, which was summarized in the previous section, multiplying with an efficiency coefficient E, and formulated as below:

$$Q_{Gu} = EnQ_u$$

where Q_{Gu}= bearing capacity of pile group

Q_u= bearing capacity of the single piles

n= number of piles

Efficiency of the pile group can be found by Feld's Rule, which reduces the capacity of each pile by $1/16$ for each adjacent pile, by the empirical expression of Converse-Labarre or by the group reduction formula of Terzaghi and Peck (1948).

In Feld's Rule, effect of the spacing of the piles is not taken into consideration. Widely used Converse-Labarre formula, for the efficiency E of the group, is expressed as;

$$E = 1 - \frac{\theta(n-1)m + (m-1)n}{90mn}$$

where m=number of columns of piles in a group.

n = number of rows,

θ= $\tan^{-1}\left(\frac{d}{s}\right)$ in degrees.

d= diameter of pile.

s= spacing of piles center to center.

In the group reduction formula of Terzaghi and Peck (1948), group capacity is the lesser of the bearing capacity for block failure of the group or the sum of the ultimate capacities of the individual piles (nQ_u). Block failure formula of Terzaghi and Peck (1948);

$$Q_{Gu} = B_r L_r c N_c + 2(B_r + L_r)L\bar{c}$$

where B_r= overall width of the group

L_r= overall length of the group

L= depth of the piles below ground level

c= undrained cohesion at the base of group

N_c= bearing capacity factor, in Figure 5.

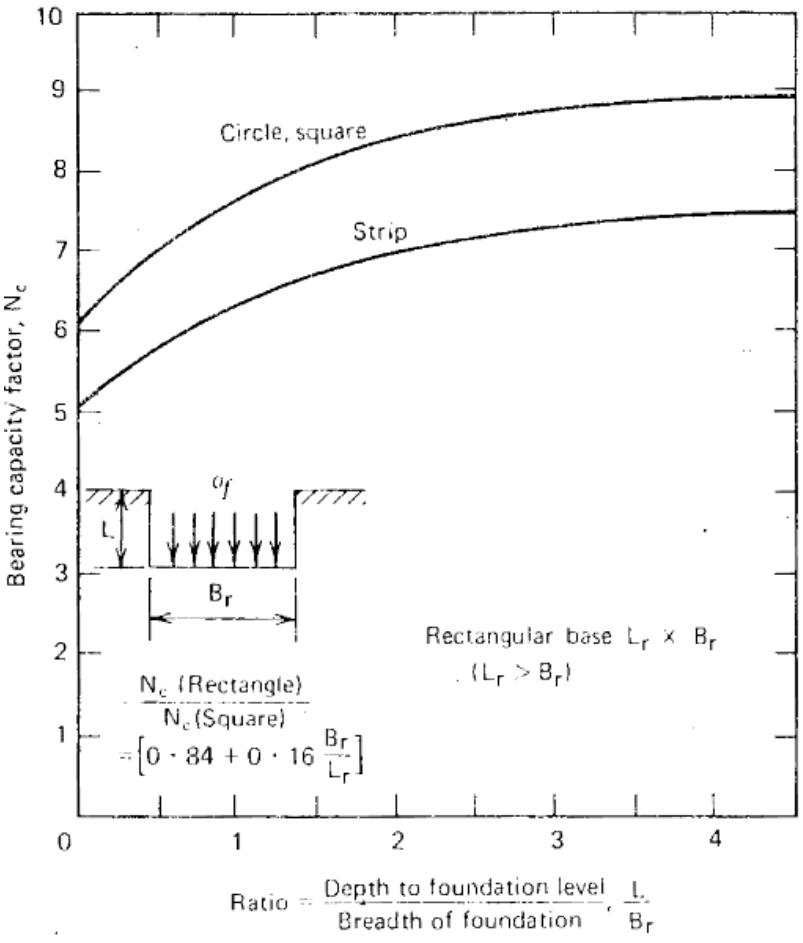

Figure 5 Bearing capacity factors for foundations in clay ($\phi = 0$) (after Skempton, 1951)

Other than the above formula of Terzaghi and Peck (1948), Tomlinson (1994) presents the below formula for the ultimate bearing capacity Q_B of the block of soil covered by the pile group.

$$Q_B = 2L(B_r + L_r)\bar{c} + 1.3c_b s N_c B_r L_r$$

where B_r= overall width of the group

L_r= overall length of the group

L= depth of the piles below ground level

$\bar{c}$= average cohesion of the clay over the pile embedment depth

c_b= cohesion of the clay at the pile base level

N_c= bearing capacity factor, Figure 6.

s= shape factor, Figure 7.

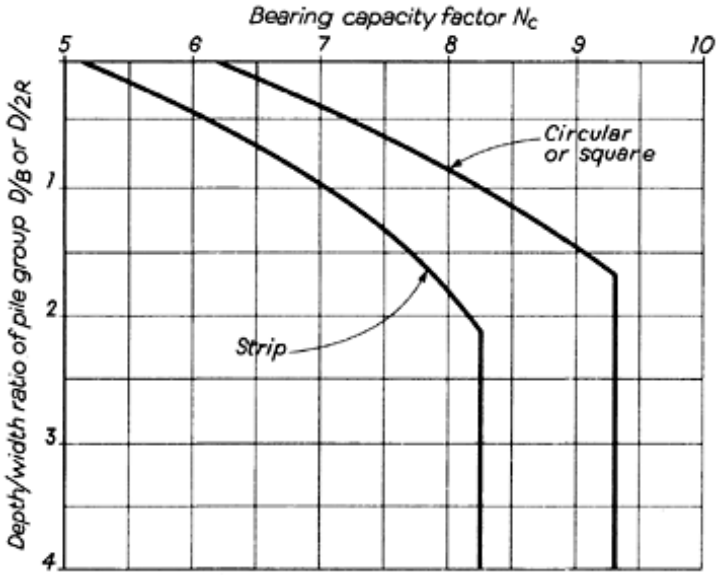

Figure 6 Bearing capacity factor N_c (Meyerhof (1992))

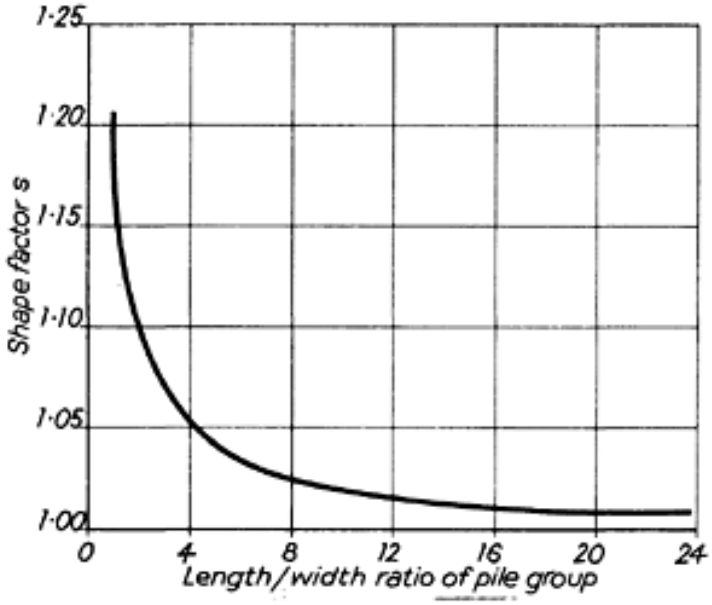

Figure 7 Shape factor for rectangular pile groups (Meyerhof(1992))

Settlement of Pile Groups

For the settlement calculation of pile groups, there has been a quite number of approaches, including, empirical, analytical and numerical methods. Some of the mostly used methods will be discussed, namely; (i) interaction factors method, (ii) equivalent pier method and (iii) equivalent raft method.

i- Interaction Factors Method

Settlement of pile groups has been basically reported by the interaction analysis of Poulos and Mattes (1971) with simplified model of two adjacent piles. They proposed an interaction factor α, which can be defined as the ratio of additional settlement caused by adjacent pile to the settlement of pile under its own load.

$$\alpha = \frac{\text{additional settlement caused by an adjacent pile under load}}{\text{settlement of pile under its own load}}$$

For groups of rigid piles, Randolph and Wroth (1979) proposed the below formula for the total pile head settlement P_t;

$$P_t = \delta_t \left(\frac{P_b}{\delta_b} + \frac{P_s}{\delta_l}\right)$$

arranging the above equation, interaction factor α has been included as;

$$\delta_t = \frac{(1+\alpha)}{G_L r_o} P_t$$

where δ_t= settlement at pile head due to load at pile head, P_t

δ_b= settlement at pile base due to load at pile base, P_b

δ_l= settlement due to shaft resistance in response to load along pile shaft, P_s

G_L= shear modulus of soil at the pile base

r_o= radius of pile

Poulos and Mattes (1971) figured the interaction factors α for various L/d ratios. They also showed that the interaction increases with increasing L/d and K. Where, K is the stiffness factor of the single pile and defined by Poulos and Davis (1980) as;

$$K = \frac{E_p}{E_s} R_A$$

where E_p= Young's modulus of pile

E_s= Young's modulus of soil

R_A= Ratio of the area of pile section to area bounded by outer circumference of pile

ii- Equivalent Pier Method

Equivalent pier method has been firstly suggested by Poulos and Davis (1980). Method approximates the group of piles into a single pier as shown in Figure 8. This equivalent pier can be same in size with the circumference of the group of piles, as a rectangle, and an equivalent length L_e or same in length with an equivalent circular area with diameter d_e. The latter approximation is more appropriate in layered and nonhomogeneous soils Poulos and Davis (1980).

The diameter of the equivalent pier may be calculated as $d_e = 1.13\sqrt{A_g}$, where A_g is the area of pile group. Similarly, Young's Modulus of the equivalent pier E_{eq} is given by Randolph (1994) as;

$$E_{eq} = E + (E_p - E)\left(\frac{A_p}{A_g}\right)$$

where E= Young's modulus of soil

E_p= Young's modulus of pile

A_p=sum of the area of each pile, $A_p = n\,\pi d^2/4$

For the floating piles groups, the ratio of L_e/L depends on L/d and s/d. In addition, the ratio of d_e/B also depends on s/d. Figures, representing L_e/L and d_e/B, have been illustrated by Poulos and Davis (1980) for various stiffness.

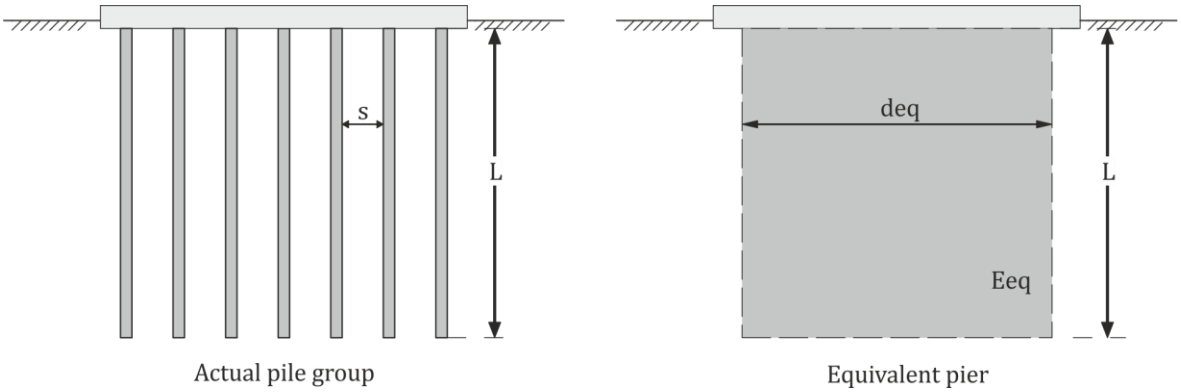

Figure 8 Equivalent pier method

As a result of the interactions between piles, stiffness of each pile k_1 needs to be reduced. Fleming et al. (1992) presented an efficiency factor η which is the inverse of the group settlement ratio R_s;

$$\eta = \frac{1}{R_s} = \frac{k_p}{n\,k_1}$$

this results a group stiffness $k_p = n^{1-e}k_1$, where e is the efficiency exponent, depends on the slenderness ratio of pile and correction factors $(c_1, c_{2,}, c_3, c_4)$. Design charts for the group efficiency and for the correction factors have been shown in Figure 9 by Fleming et al. (1992) Corrected e can be calculated as;

$$e = e_1(L/d) * c_1(E_p/G) * c_2(s/d) * c_3(\nu) * c_4(\rho)$$

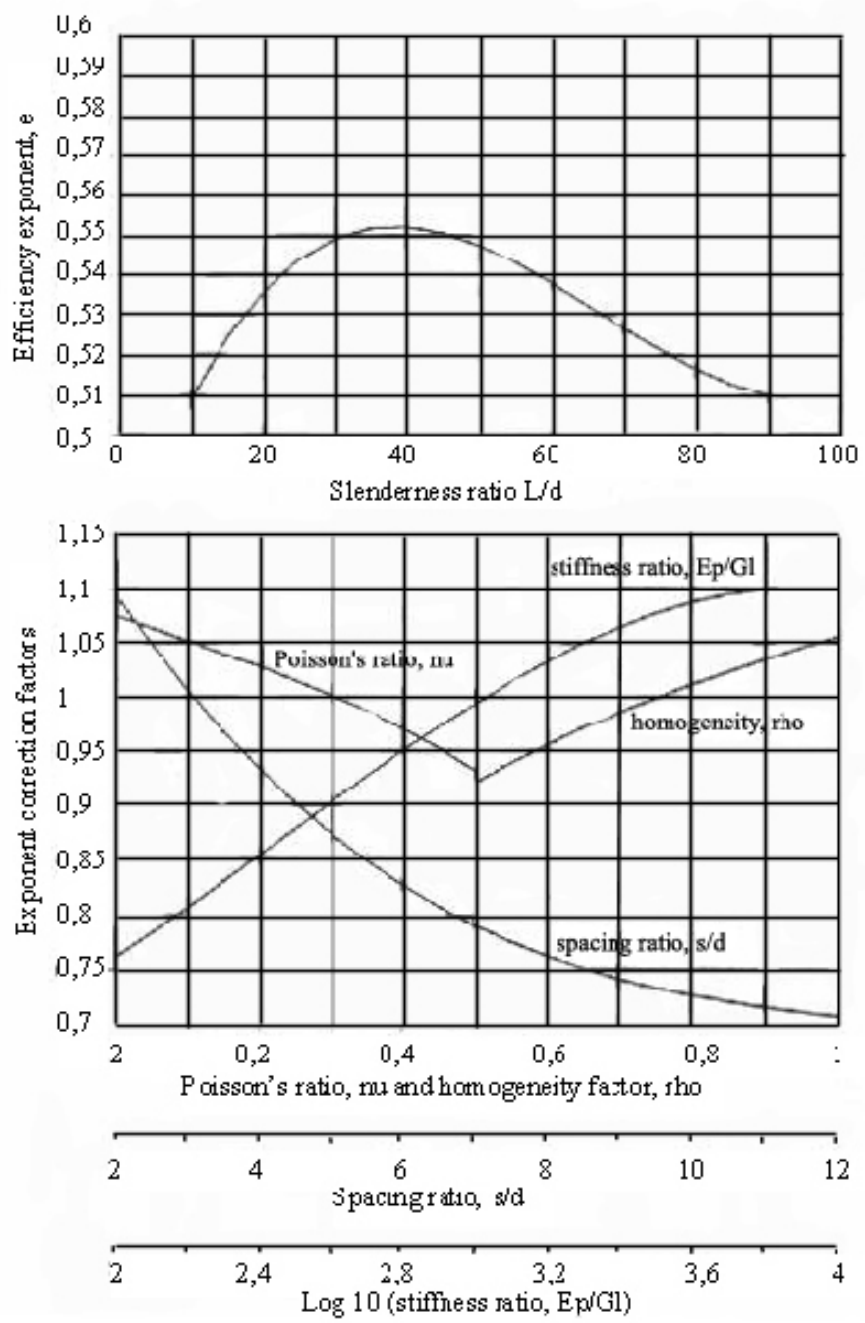

Figure 9 Design charts for the group efficiency and for the correction factors (after Fleming et al, 1992)

The settlement of the equivalent pier can be calculated as a single pile, using the Randolph and Worth (1978) approach stated under “Stiffness of a Single Pile” or similar elastic solutions.

iii- Equivalent Raft Method

In this method, the pile group is idealized as an equivalent flexible raft, which is a widely-used technique for the calculation the settlement of groups of piles. The pressure is assumed to be distributed a slope 2 vertical to 1 horizontal. Adopted depth of the equivalent raft, which was given by Tomlinson (1994) in Figure 10, depends on the nature of the soil profile.

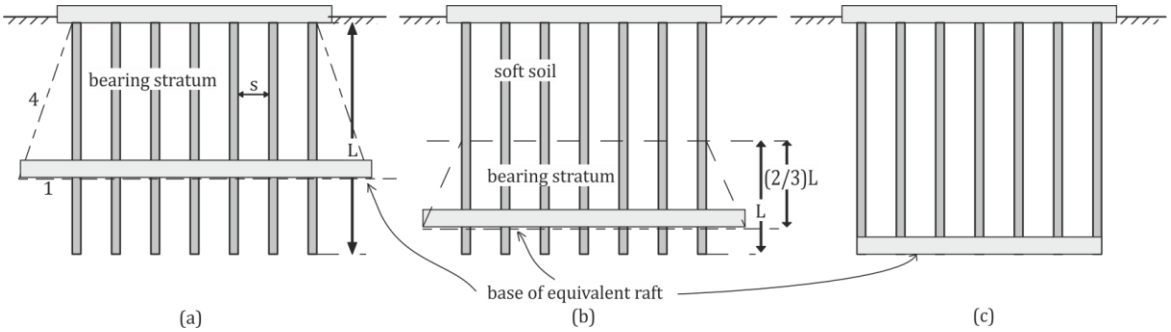

Figure 10 Adopted depth of the equivalent raft. (a) Piles supported mostly by skin friction, (b) Piles supported with a combination of skin friction and end bearing, (c) Piles supported mostly by end bearing.

Tomlinson (1994) gives the general equation for the average immediate/undrained settlement of a flexible foundation on clay, with an assumption for the undrained Poisson's ratio for clay is equal to 0.5, at depth D as;

$$\rho_i = \frac{\mu_i \mu_0 q_n B}{E_u}$$

Where μ_i and μ_0 are the influence factors, depend on the H B and D, shown in Figure 11. These values are for the soils, which have a constant deformation modulus with depth and result in the overestimation of settlements. Burland (1973), however, developed a formula for the settlement calculation of the equivalent raft for more realistic deformation modulus, which increases with depth.

$$E_u = E_f(1 + kH/B)$$

and

$$\rho_i = \frac{q_n B I_p'}{E_f}$$

where ρ_i= settlement at the corner of the loaded area

q_n= net foundation pressure

B=width of the equivalent raft

k=slope of the line for the deformation modulus increment
H= depth of the compressible soil layer
E_f= modulus of deformation at the base of the equivalent raft
I_p'=influence factor, see Figure 12.

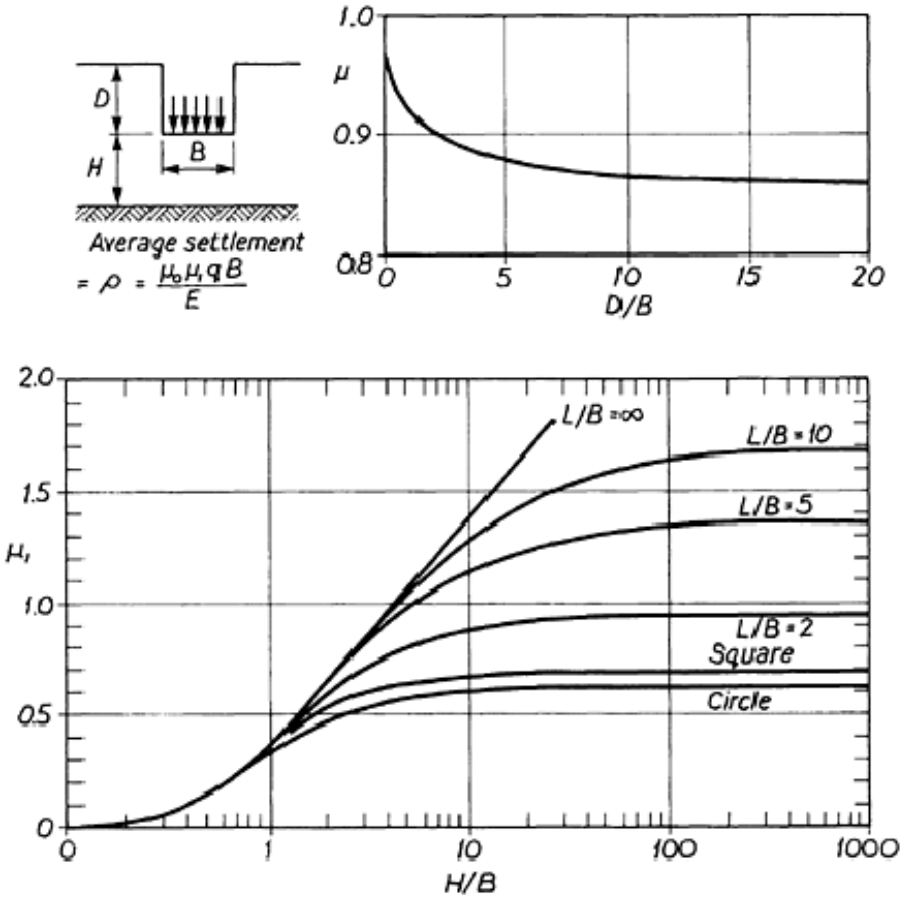

Figure 11 Influence factors for calculating immediate settlements of flexible foundations (after Christian and Carrier, 1978)

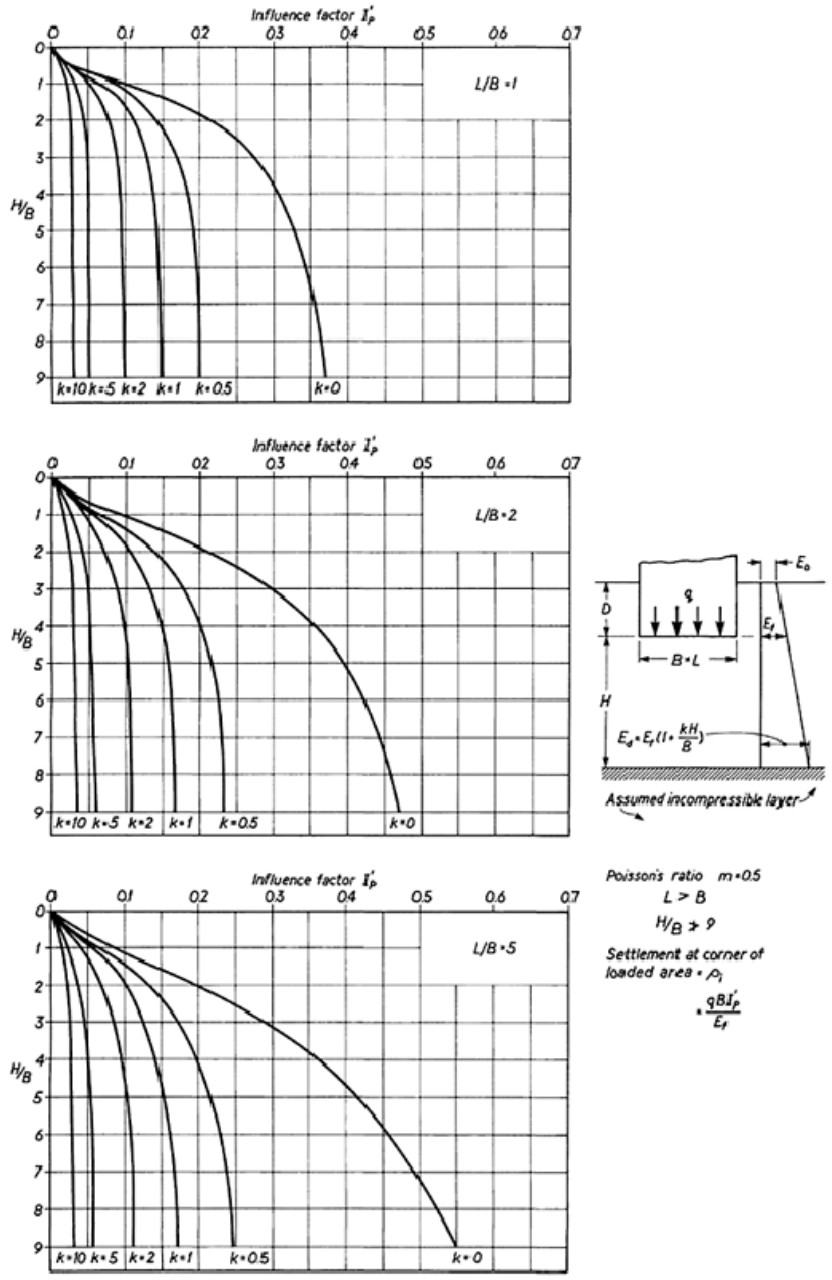

Figure 12 Influence factors for deformation modules increasing linearly with depth (after Burland, 1973)

Randolph (1994) states that the distinction of the equivalent pier and equivalent raft method is made by an overall aspect ratio "*R*";

$$R = \sqrt{\frac{ns}{l}}$$

where n= number of piles

s= spacing of piles

l= length of embedment

According to Randolph (1994), equivalent raft method is more suitable for values of R which are greater than 4 and the equivalent pier is more logical for the smaller values of R. This is because of the differential settlement pattern of the group is similar to the pattern of a raft foundation, assuming the group has a fully flexible cap.

Tomlinson (1994) considers that the equivalent raft method is sufficiently reliable for most routine settlement predictions. However, Viggiani et al. (2012) suggest that the equivalent raft method is more suitable for large pile groups, where the breadth B of the group is larger than the length of the piles L, and the equivalent pier method is suitable for small pile groups.

Both the equivalent pier method and the equivalent raft method assume the same diameter and length of piles, by disregarding the effect of pile interactions. Therefore, these methods may not be suitable for the foundations with variable lengths and diameter of piles.

2.4 Raft Foundations

Raft foundations are commonly one-piece structural elements and cover an area at least equal to the projection of the structure. These types of foundations are suitable when large differential settlements are expected or the underlying soils have low bearing capacity. Due to large size of raft foundations, generally the differential settlements govern the design.

Basically two approaches have been suggested for analyzing the behavior of raft foundations as;

1. Rigid foundation approach
2. Flexible foundation approach

Rigidity or flexibility of a raft depends on the relative stiffness of itself and the subsoil. The behavior of the foundation also depends on the rigidity of the superstructure (Gupta (1997)). It should be noted that the contribution of the rigidity of the superstructure to the rigidity of the foundation is not considered within this study.

Raft Stiffness

Assuming a rigid raft, the raft stiffness k_r has been given by Poulos and Davis (1974) as;

$$k_r = \frac{2.25\ G\ B}{(1-\nu)}$$

In addition to the above formula for the raft stiffness, various authors suggested different relative stiffness (K) factors for the raft foundations. Gupta (1997) relates the stiffness of raft with the underlying soil for;

- rectangular rafts: $K = \frac{E_r}{12E_s}\left(\frac{t}{B}\right)^3$
- circular rafts: $K = \frac{E_r}{12E_s}\left(\frac{t}{2R}\right)^3$

where E_r= Young's modulus of the raft

E_s= Young's modulus of the subsoil

B= length of the section in the bending axis

t= thickness of the raft

R= radius of the raft

With the inclusion of the Poisson's ratio of raft ν_r and soil ν, Fraser and Wardle (1976) suggest for rectangular rafts of width B;

$$K = \frac{4}{3}\frac{E_r}{E_s}\frac{(1-\nu^2)}{(1-\nu_r^2)}\left(\frac{t}{B}\right)^3$$

For different values of width and breadth, Horikoshi and Randolph (1997) propose the relative stiffness as;

$$K = \pi^{3/2}\frac{E_r}{E_s}\frac{(1-\nu^2)}{(1-\nu_r^2)}\left(\frac{B}{L}\right)^{1/2}\left(\frac{t}{L}\right)^3$$

where B= breadth of the raft

L= length of the raft

$\pi^{3/2} = 5.57$, this expression can be also modified for the circular rafts

Gupta (1997) considered raft as "rigid" if the $K > 0.5$. Fraser and Wardle (1976) assumed that the raft is fully flexible for $K < 0.01$ and rigid for the values of K greater than unity. Furthermore, Horikoshi and Randolph (1997) reported that the raft is fully flexible for $K = 0.001$ and is rigid for $K = 1{,}000$.

Depending on the raft geometry, relative stiffness of the raft can be found using the above equations. After the determination of relative stiffness K of the raft, settlement ρ of the rectangular raft may be found by the expression suggested by Fraser and Wardle (1976) as;

$$\rho = pb\frac{(1-\nu_s^2)}{E_s}\,I$$

where p= applied uniform pressure

I= influence factor, see Figure 13.

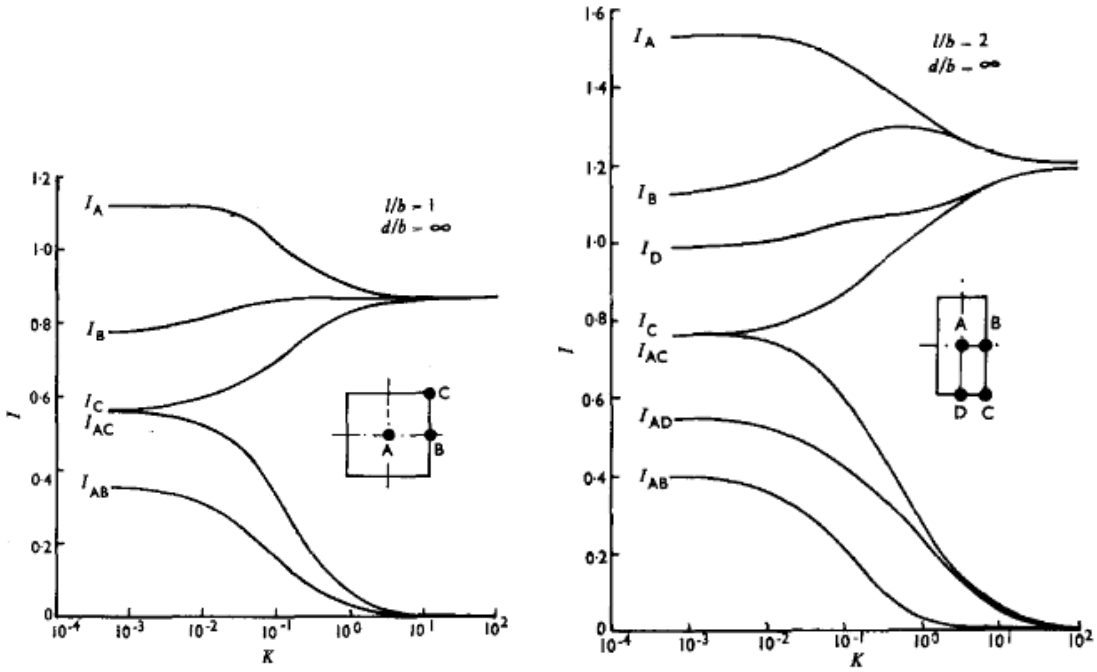

Figure 13 Settlement influence factor I for $l/b = 1$ and $l/b = 2$ (Fraser and Wardle (1976))

In Figure 13, ρ and I is associated with the central and differential settlements. Fraser and Wardle (1976) presented an influence factor "M" (see Figure 14) for the maximum bending moment "m" in the raft.

$$m = plbM$$

where l= raft length ($l > b$)

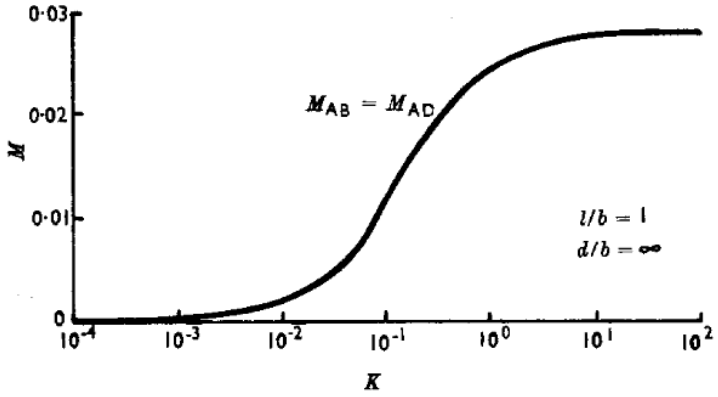

Figure 14 Bending moment influence factor M

In addition to the influence factors I and M, for the effect of layer depth, correction factors S and R to the settlement and to the moment, have been suggested by Fraser and Wardle (1976). These factors can be used if the ratio d/b is not assumed as infinite.

Load Bearing Capacity

Terzaghi's (1943) well-known expression may be used for the ultimate load bearing capacity of the raft foundations;

$$q_{ult} = cN_c s_c + qN_q + 0.5B\gamma N_\gamma s_\gamma$$

where c= cohesion

s_c= shape factor for cohesion

q= overburden pressure (γD)

B= least lateral dimension of the raft

γ= unit weight of soil

s_γ= shape factor for soil wedge

N_c, N_q, N_γ are the coefficients of bearing capacity as a function of internal friction angle of the soil ϕ which are tabulated by Terzagi (1943) as;

Table 3 - Terzaghi's bearing capacity factors

ϕ	N_c	N_q	N_γ
0	5.3	1.0	0.0
5	7.3	1.6	0.5
10	9.6	2.7	1.2
15	12.9	4.4	2.5
20	17.7	7.4	5.0
25	25.1	12.7	9.7
30	37.2	22.5	19.7
35	57.8	41.4	42.4
40	95.7	81.3	100.0
45	172.0	173.0	298.0

For square foundations, formula becomes;

$$q_{ult} = 1.3cN_c + qN_q + 0.4B\gamma N_\gamma s_\gamma$$

Settlement

The load-settlement behavior or the stiffness of the raft is governed by; raft dimensions c and d, soil shear modulus G_s and Poisson's ratio ν of the subsoil according to Tan and Chow (2004). For the rectangular rafts, Richart et al. (1970) give the stiffness of the raft acting alone, as;

$$k_r = \left[\frac{G_s}{1-\nu}\right]\beta_z(4cd)^{\frac{1}{2}}$$

Where β_z is the coefficient depending on the one-half of the raft dimensions c and d. Coefficient of β_z has been shown in Figure 15 and can be chosen as 2.2 for square rafts.

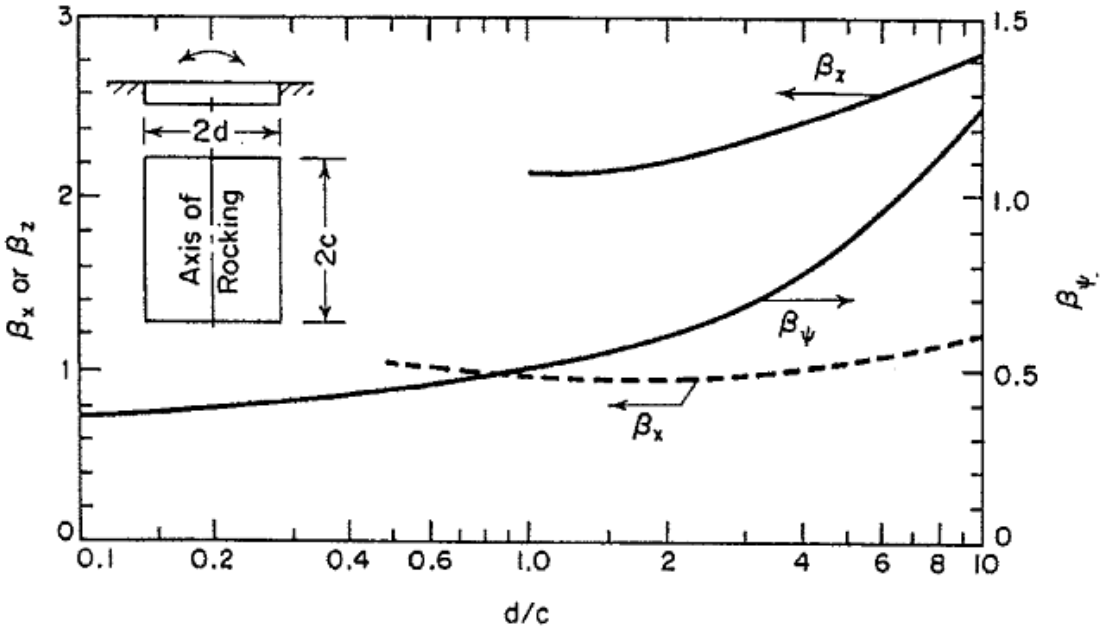

Figure 15 Coefficients of β_z, $\beta_x$and β_ψ for rectangular footings (after Richart et al., 1970)

Tomlinson (1994) gives the general equation for the immediate/undrained settlement of a flexible foundation on clay as;

$$\rho_i = q_n * 2B * \left(\frac{1-\nu}{E_u}\right) * I_p$$

where ρ_i= settlement at the center of the flexible loaded area

q_n= net foundation pressure

B=width of the equivalent foundation raft

ν=undrained Poisson's ratio for clay

E_u= undrained deformation modulus

I_p= Steinbrenner's influence factor.

I_p depends on the ratios on $H/B$and L/B. Where, H is the depth of compressible soil layer, B is the equivalent raft breadth.

2.5 Piled Raft Foundations

Piled raft foundations are the composite structures which consist of three elements; piles, raft and the subsoil. Applied loads are transferred to the subsoil both through the raft and the piles. This load transfer mechanism can be simply shown in Figure 16. Load sharing between raft and piles is the main distinctive feature that diversifies this type of foundation from other type of piled foundations' design.

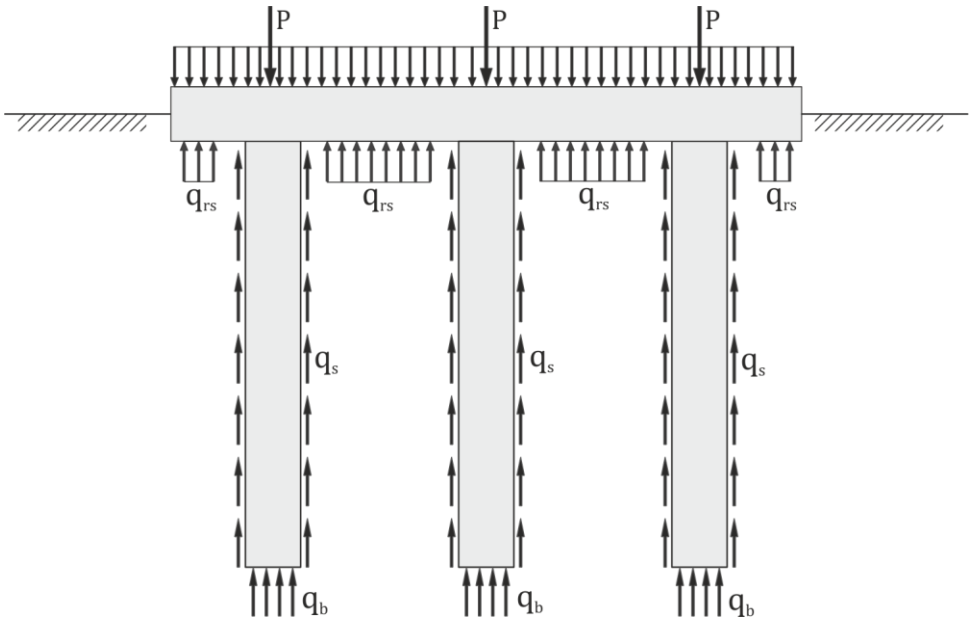

Figure 16 Simplified load transfer mechanism of piled raft foundations.

Randolph (1994) has presented three design approaches for the piled raft foundations in his state-of-the-art report as:

1. The Conventional Approach: Piles are designed to carry the majority of the load.
2. Differential Settlement Control: Piles are located in order to reduce the differential settlement, rather than the overall average settlement.
3. Creep Piling: Piles are designed to operate at a working load (70-80% of the ultimate capacity) at which significant creep occurs.

In conventional design approach, loads are assumed to be carried only by the piles or by the raft. However, in the design of piled raft foundations, the load sharing between piles and the raft is taken into account (Reul and Randolph (2003)). Naturally, this load sharing improves the underestimated load capacity of the foundation comparing with the conventional approach,

considering the properties of the piles and the raft remain unchanged. In addition, the piles may be used to control the settlement rather than carry the entire load (Linag et. al. (2003)) in the piled rafts. Tan and Chow (2004) illustrated the usage benefit of piles and raft together in the design of foundations in Figure 17.

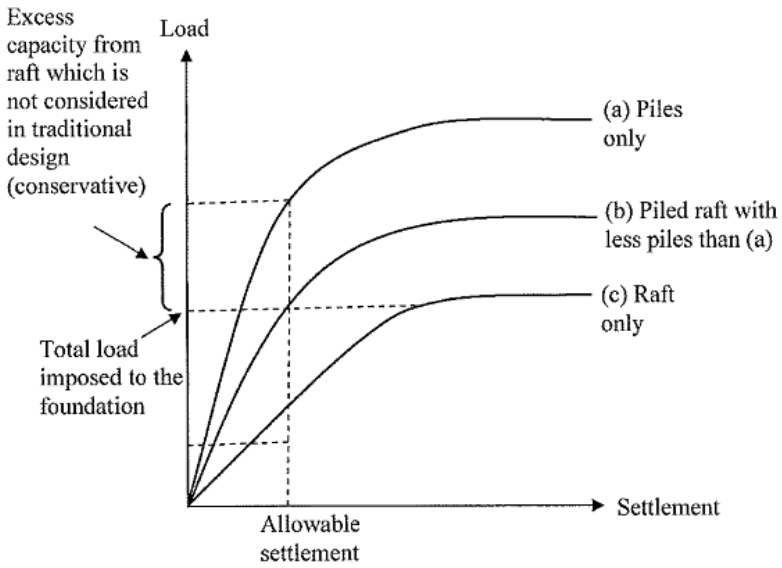

Figure 17 Concept of piled raft (Tan and Chow, 2004)

2.5.1 Methods for the Analysis of Piled Raft Foundations

Poulos (2001) categorized the methods of analysis of piled raft foundations into three classes;

I. Simplified calculation methods
II. Approximate computer-based methods
III. More rigorous computer-based methods

I. Simplified calculation methods

Some of the simplified methods are those of Randolph (1994) and Burland (1995).

In Randolph's (1994) approach, only the interaction between the piles and the raft is taken into account with the factor of α_{cp} and the interaction between piles in the pile group is not considered (Nguyen et. al. (2013)). This may be because of the consideration of the non-linearity of the soil has relatively small effect on pile group response. For the components of pile group and raft, Randolph (1983) (in Randolph (1994)) relates the settlements by tagging subscripts of p for the pile group and r for the raft as;

$$\begin{Bmatrix} w_p \\ w_r \end{Bmatrix} = \begin{bmatrix} 1/k_p & \alpha_{pr}/k_r \\ \alpha_{rp}/k_p & 1/k_r \end{bmatrix} \begin{Bmatrix} P_p \\ P_r \end{Bmatrix}$$

where α_{rp} and α_{pr} are the interaction factors, P and k are the loads and stiffness. By Maxwell's Reciprocal Theorem (diagonal terms are equal) and considering the equality of the average settlement of raft and pile group, overall stiffness k_{pr} and the proportion of load carried by the raft X are calculated as;

$$k_{pr} = \frac{k_p + k_r(1 - 2\alpha_{rp})}{1 - {\alpha_{rp}}^2 \left(\frac{k_r}{k_p}\right)}$$

where the stiffness of the pile group k_p and the raft k_r can be calculated by the elastic theory using the methods of equivalent pier and Fraser & Wardle (1976) respectively, as described in the previous section.

$$X = \frac{P_r}{P_t} = \frac{P_r}{P_r + P_p} = \frac{(1 - \alpha_{rp})k_r}{k_p + (1 - 2\alpha_{rp})k_r}$$

The load carried by the raft is P_r and the total load is P_t. α_{rp} is the raft-pile interaction factor and approximated by Randolph (1983) for single piles, which may be used for the large groups with an equivalent radius r_c, with circular caps;

$$\alpha_{cp} = 1 - \frac{\ln(\frac{r_c}{r_0})}{\zeta}$$

where r_c = average radius of pile cap

r_0 = radius of pile

$\zeta = \ln\left(\frac{r_m}{r_0}\right)$

$r_m = \{0.25 + \xi[2.5\rho(1 - \nu) - 0.25] * L\}$

$\xi = \frac{E_{sl}}{E_{sb}}$

$\rho = \frac{E_{sav}}{E_{sl}}$

L = length of pile

E_{sl} = Young's modulus of soil at level of pile tip

E_{sb} = Young's modulus of soil at bearing stratum below pile tip

E_{sav} = average Young's modulus of soil along pile shaft

Randolph (1994) reported that the raft-pile interaction factor α_{rp} has a tendency to be equal to 0.8 for large group of piles, even for 6x6 pile groups. Therefore, the overall stiffness k_{pr} may be simplified to;

$$k_{pr} = \frac{1 - 0.6\,(k_r/k_p)}{1 - 0.64\,(k_r/k_p)} k_p$$

and the proportion of load carried by the raft P_r over load carried by the pile group P_p;

$$\frac{P_r}{P_p} = \frac{0.2}{1 - 0.8(k_r/k_p)} \frac{k_r}{k_p}$$

According to Poulos (2001) overall stiffness equation k_{pr} is operative up to the fully mobilization of pile capacity, which is point A in Figure 18.

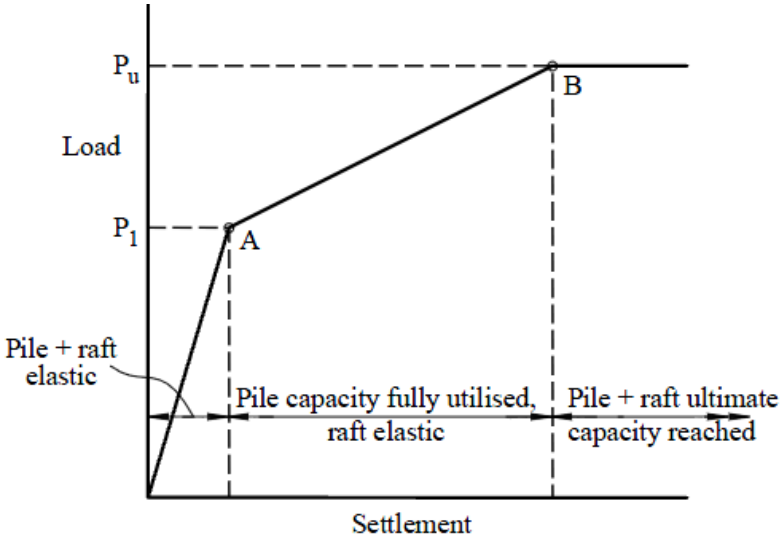

Figure 18 Simplified load-settlement curve of piled raft foundation (Poulos, 2001)

Burland (1995) considered the piles as settlement reducers, and suggested that, if the piles are located below the columns, excess load P_{su} corresponding the difference of the design load P_0 and the load carried by the raft P_1, is equal to the fully mobilized shaft resistance of these piles times a mobilization factor of 0.9. Therefore, foundation can be analyzed as a raft, which only subjected to the reduced load Q_r.

$$Q_r = Q - 0.9P_{su}$$

For the estimation of settlement, Poulos (2001) suggested an adaptation for the Randolph's (1994) approach as;

$$S_{pr} = \frac{S_r * K_r}{K_{pr}}$$

where S_{pr} = settlement of the piled raft

S_r = settlement of the raft without piles under the total load

K_r = stiffness of the raft

K_{pr} = stiffness of piled raft

II. Approximate computer-based methods

The approximate computer-based methods are based on elastic theory and mainly have two approaches (Poulos 2001) as; strip on springs and plate on springs. In these approaches, the raft is treated as a strip and as a thin plate respectively. Additionally, piles are treated as springs and the soil as an elastic continuum, which are also simplified into springs, for the foundation-structure interaction analyses. Furthermore, the combination of these two methods is also possible. Sonoda et al. (2009) modeled of a raft of a building in Japan, composed of a mat having a thickness of 0.6m and beams having height of 1.2m, by a combination of thin plates and beams and as a combination of pile springs and soil springs as shown in Figure 19.

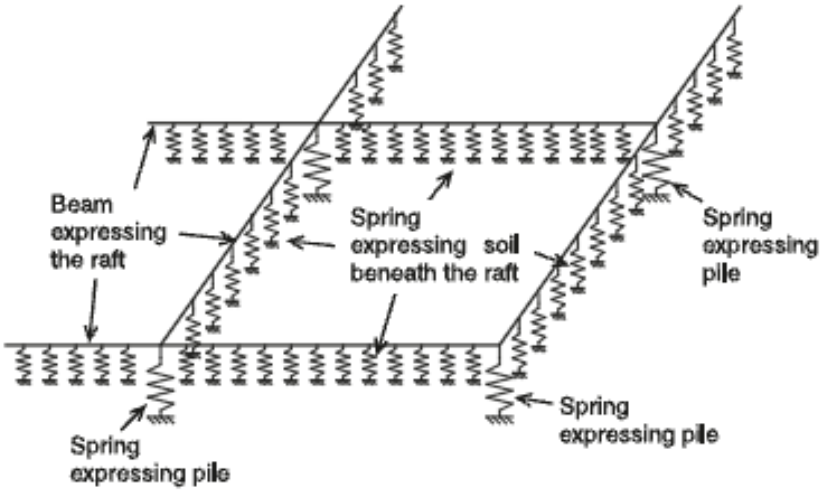

Figure 19 Strip on springs approach (Sonoda et al, (2009))

.

III. More rigorous computer-based methods

More rigorous methods mainly include boundary element methods and finite element methods. Besides, for the different members of the foundation, combination of these methods has been applied.

The piled raft coefficient α_{pr}, is defined as the ratio of the sum of all pile loads P_{pile}, to the total applied load on the foundation P_{tot};

$$\alpha_{pr} = \frac{\sum P_{pile}}{P_{tot}}$$

$\alpha_{pr} = 1$ denotes the foundation as free standing pile group, ignoring the existence of the raft and $\alpha_{pr} = 0$ represents a shallow foundation or an unpiled raft. Therefore, the coefficient of piled rafts must be $0 < \alpha_{pr} < 1$.

The coefficient of the maximum settlement ξ_s, is defined as the ratio of the maximum settlement of the pied raft, s_{pr}, to the maximum settlement of the corresponding unpiled raft, s_r ;

$$\xi_s = \frac{s_{pr}}{s_r}$$

The coefficient of differential settlement, $\Delta\xi_s$, is the difference of the settlement of the center of the raft and the middle of the shorter side of the raft.

Poulos (2001) pointed out that the two-dimensional finite element analyses may lead to over estimation of settlements and the pile loads, due to the plain strain assumptions and therefore the most accurate numerical method of analysis for piled raft foundations is the three-dimensional finite element methods. Reul and Randolph (2003) also modeled the piled rafts in overconsolidated clay with the three-dimensional finite element method, which allows the most precise treatment of the soil-structure interaction. Sales et al. (2010) indicated that most piled raft analyses using boundary element method programs only consider the interaction between two piles at a time, neglecting the presence of other piles which lead to a higher settlement compared with finite element analysis of the same foundation.

For the vertical bearing capacity $Q_{PR,ult}$ of piled rafts, Poulos (2000) suggested as the smaller of the following values:

- The ultimate capacity of the portion of the raft outside of the boundary of the pile group and adding the ultimate capacity Q_{BF} of the block containing the piles.
- The sum of the ultimate loads of all the piles $Q_{G,ult}$ and the raft$Q_{R,ult}$:

$$Q_{PR,ult} = Q_{G,ult} + Q_{R,ult}$$

As mentioned before, the design of piled rafts differs from traditional foundation design, where the loads are assumed to be carried either by the raft or by the piles, considering the safety factors in each case

Russo and Viggiani (1998) have categorized the piled raft foundations based on the purpose of the piles as:

1. Small piled rafts, in which the primary reason of the usage piles is to increase the insufficient bearing capacity of unpiled raft. These rafts are generally 5 to 15 m in width and the ratio over the length of piles is less than unity ($B/L < 1$). In this

category of piled raft, the differential settlement is not a significant problem comparing with the overall average settlement.

2. Large piled rafts, on the other hand, have sufficient bearing capacity to carry the load, so the piles are used to reduce the settlement. The ratio over the length of piles is higher or equal than unity ($B/L \geq 1$). Both the differential and the overall average settlement are important for an optimum design.

For square rafts, Russo and Viggiani (1998) have defined the relative flexural stiffness K_{rs} of the raft as;

$$K_{rs} = \frac{4}{3}\frac{E_r(1-{\nu_s}^s)^2}{E_s(1-{\nu_r}^s)^2}\left(\frac{t}{B}\right)^3$$

where E_r= Young's modulus of raft
E_s= Young's modulus of soil
ν_r= Poisson's ratio of raft
ν_s= Poisson's ratio of soil
t= thickness of raft
B= breadth of raft

The characterization of the distribution of the piles has been embraced by the ratio A_g/A (Sanctis et al. (2002)). A_g and A is the area of the pile group and the area of the raft respectively. A_g was formulated as;

$$A_g = \left[\left(\sqrt{n}-1\right)s\right]^2$$

where n= number of piles
s= spacing of piles

Viggiani et al. (2012) reported the load sharing between the raft and the piles as a function of A_g/A with respect to L/B for various relative raft stiffness K_{rs} for small and large piled rafts (*see Appendix I*).

2.5.2 Factors affecting the Behavior of Piled Raft Foundations

Many researchers have examined the behavior of piled rafts. The following factors can be listed as the main determinants of the behavior:

1. The number of piles,
2. Length of piles,
3. Diameter of piles
4. Pile spacing ratio,
5. Location of piles
6. Stiffness of piles
7. Distribution of load,
8. Level of load,
9. Raft thickness
10. Raft dimensions.
11. Type and stiffness of soil

Sales et al. (2010) stated that the total piled-raft stiffness is directly related with the stiffness of piles and the settlement performance of the foundation is a direct consequence of the individual stiffness of all involved elements and the raft-soil-pile interaction. With the combination of geometric properties; diameter and length of piles, number of piles and spacing ratio, the relative stiffness of pile group may be derived. Long (2010) conducted an experimental study with large-scale field models and found that the larger the loads taken by piles, the smaller the settlement occur. According to Lin and Feng (2006), the outer most piles take higher axial loads (1.25 P_{ave}) than the inner piles (0.8 P_{ave}) with even distribution of piles. Some researchers investigated the effect of the length of piles. Leung et al. (2010) found that the differential settlements can be reduced by using longer piles under central part and shorter piles in the periphery of raft and optimization benefits are augmented with increased Ep/Es (pile stiffness / soil stiffness) ratio and reduces pile spacing. Lee et al. (2010) concluded that, at low load levels, pile load of the center pile is generally smaller than corner pile, whereas at higher load levels, pile load of center pile is slightly larger than corner pile. Lee et al. (2010) also found that end-bearing capacity is almost same under the same pile configuration and length, irrespective of loading types, furthermore, it was resulted that the proportion of the load taken by the raft at failure was not highly dependent on the pile configurations. To examine the group effect of piles, Gök and Toğrol (2009) conducted a numerical study for piled rafts and obtained that the shaft friction developed by piles within a piled raft can be significantly greater than that for a single pile or a pile in a group of piles.

Behavior of piled rafts also depends on the type of soil beneath the raft. Oh et al. (2009) conducted a modeling study with numerical analysis by two case studies, which were in sandy soil and in soft clay. They came up with these results; for sandy soils, maximum settlement depends on pile spacing and number of piles, raft thickness does not have significant effect, for clayey soils, raft thickness has obvious effect on differential settlement.

Lin and Feng (2006) stated that the thickness of the raft displays a minor effect on normalized settlement in the case of the smaller raft dimension (15mx15m) and for differential settlements; thin raft appears more prominent than thick, as expected. Leung et al. (2010) stated that optimization benefits of piled rafts reduce as the load level is increased and increase with a thicker raft but not significantly. In addition, Cunha et al. (2001) investigated design alternatives for a piled raft case history. Main outcomes of their study can be summarized as; by increasing raft thickness; maximum displacements (both total and differential) decrease, maximum pile load decreases, more load is taken by the raft. According to Lin and Feng (2006) bending moment of a thick piled raft is higher than a thin piled raft and larger the raft dimensions, higher the bending moment. Cunha et al. (2001) also found that by decreasing the number of piles, displacements and contact pressures increase.

In brief, as Randolph (1994) stated that the key questions are; what is the relative proportion of load carried by raft and piles and what is the effect of additional pile support on total and differential settlements?

2.6 Finite Element Programs: Plaxis 3D and Sap2000

Plaxis 3D

Plaxis is a company based in the Netherlands, developing software under the same brand name; Plaxis. The Plaxis 3D program is a three-dimensional finite element program used to make deformation and stability analysis for various types of geotechnical applications (Reference Manual, Plaxis). The user interface of the Plaxis 3D consists of two sub-programs as Input and Output. Properties of soil and other elements (boreholes, embedded piles, plates etc.) are assigned to the elements by using material data sets by the Input interface. The basic soil elements of the 3D finite element mesh are the 10-node tetrahedral elements (Figure 20).

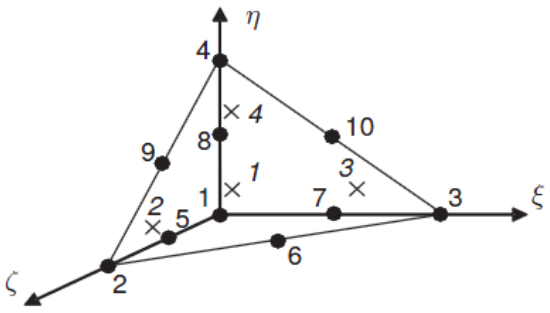

Figure 20 3D soil elements (10-node tetrahedrons) zone (Reference Manual, Plaxis)

Sap2000

Sap2000 is general-purpose civil-engineering software for the analysis and design of any type of structural system developed by Computers and Structures, Inc. based in Berkeley, California.

Frame elements, shell elements and spring supports are used in this study to define the model in Sap2000. As stated in the Reference Manual of Sap2000, the Frame element uses a general, three-dimensional, beam- column formulation which includes the effects of bi axial bending, torsion, axial de formation, and bi axial shear deformations. In this study, piles are modeled using the frame section properties.

Shell elements are used to model the raft behavior. In Sap2000, three-node or four-node shell elements are available. Both the four-node and three-node shell element may be used in this study; however, the four-node shell elements are chosen. The main difference of four-node element is that, it does not have to be planar. The raft thickness is directly in the center of the axis line which can be seen in Figure 21. Shell elements involve three types; membrane, plate and shell. Within these types, shell type of shell element is chosen, which supports all type of forces. However, plates support only the bending moments and the transverse forces and membranes support only the in-plane forces and the normal (drilling) moments (Sap2000 Reference Manual). In addition, shell type elements involve thin and thick types. Shear strain is assumed to be zero for the thin type elements. Therefore, thick shell elements are used in this study. The piles (frame elements) and the raft (shell elements) has been connected without any constrains in the joints. The bottom of the model is supported by the spring supports, which is one of the possible joint connections shown in Figure 22.

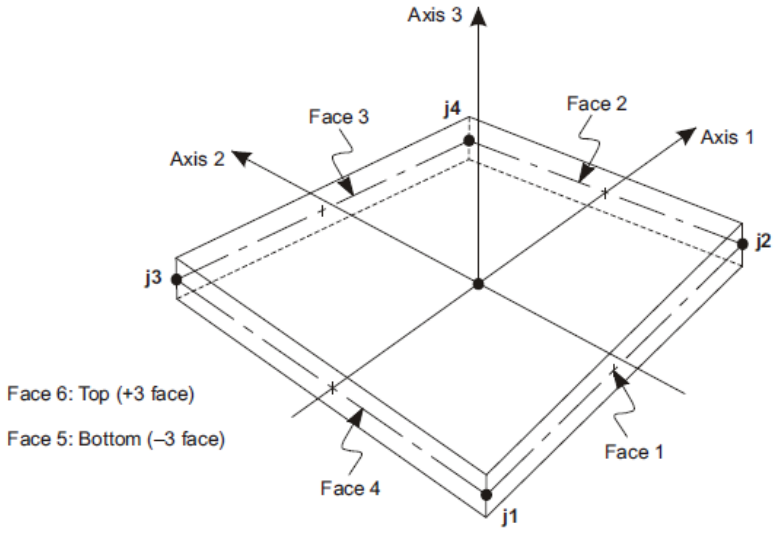

Figure 21 Four-node Quadrilateral Shell Element (reference manual, Sap2000)

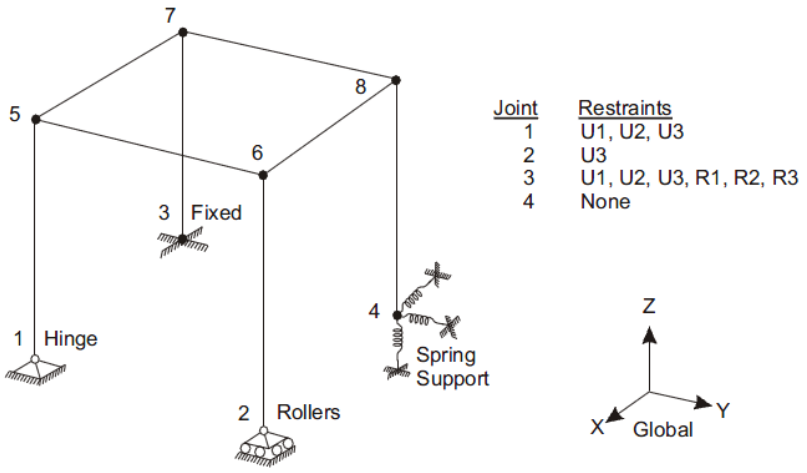

Figure 22 3D frame structure and possible joint connections in Sap2000 (reference manual, Sap2000)

CHAPTER 3

FINITE ELEMENT ANALYSES OF PILED RAFT FOUNDATIONS

3.1 Introduction

Behavior of the piled raft foundation systems under axial loads has been investigated by comparing the traditional design methods and the latest design approaches by parametric analyses. Sales et al. (2010) states that the most piled raft analyses using boundary element method (BEM) programs only consider the interaction between two piles at a time and do not take into account the presence of other piles in the group that will affect the interaction calculated. This may lead to higher settlements when compared with FEM analysis of the same foundations. To this end, finite element programs Plaxis 3D and Sap2000 have been used in this study to analyze the selected cases. Mainly, two different piled rafts were analyzed in this study. The first one is a typical 50-storey building in Ankara, Turkey. The second one is the Messe-Torhaus Building in Frankfurt, Germany. Both regions have a common type of clay as overconsolidated.

Special types of elements are used to model structural behavior of the piled raft foundation. For the raft, plate elements are used. Plate elements are the 6-node triangles with six degrees of freedom per node (three translational and three rotational). In this study, embedded piles are used for the model of piles. Embedded piles are structural elements developed by Plaxis which are modeled like beam elements. The main benefit of the embedded piles is the interaction with the continuum as the skin resistance and the foot resistance. The embedded piles can be placed in any direction within the subsoil without any alteration of the mesh. This is achieved by crossing through a 10-node tetrahedral soil element while creating virtual nodes (blank grey circles) as shown in Figure 23.

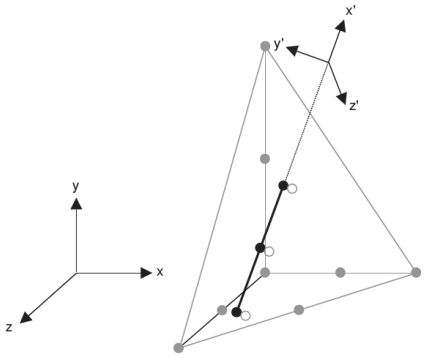

Figure 23 Embedded beam element denoted by the solid line within a 10-node tetrahedral soil element. (Scientific Manual, Plaxis)

Embedded piles do not have a “real” volume and a “real” interface. However, a virtual elastic zone, is shown in Figure 24, is created by assigning an equivalent pile diameter within the

material data set of the embedded pile. This virtual elastic zone disregards the plastic behavior of the soil within the zone (Reference Manual, Plaxis) and approaches to the actual volume pile behavior. On the other hand, due to the "virtual" volume and interface, evaluation of the effect of strength reduction factor (R_{inter}) cannot be realized. R_{inter} is taken as rigid (1.0) with the assumption of the interface does not have a reduced strength with respect to the strength in the surrounding soil. As a result, for the practical usage for the calculation of pile load and raft load sharing, embedded piles are used in this study.

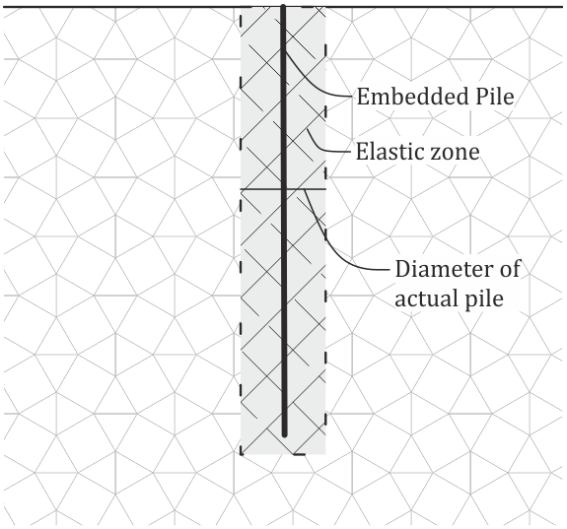

Figure 24 Virtual elastic zone of embedded pile.

3.2 Geotechnical and Material Parameters for Input

Two different piled rafts were analyzed in this study. The first one is a typical 50-storey building in Ankara. The second one is the Messe-Torhaus Building in Frankfurt.

Case 1: A typical 50-storey building in Ankara

Soil Properties: The SPT data was taken from a report for a construction site on Eskişehir Yolu, which is the popular place for the high-rises in Ankara, where the soil is commonly overconsolidated clay. Raw SPT-N values for four different boreholes are shown in Figure 25.

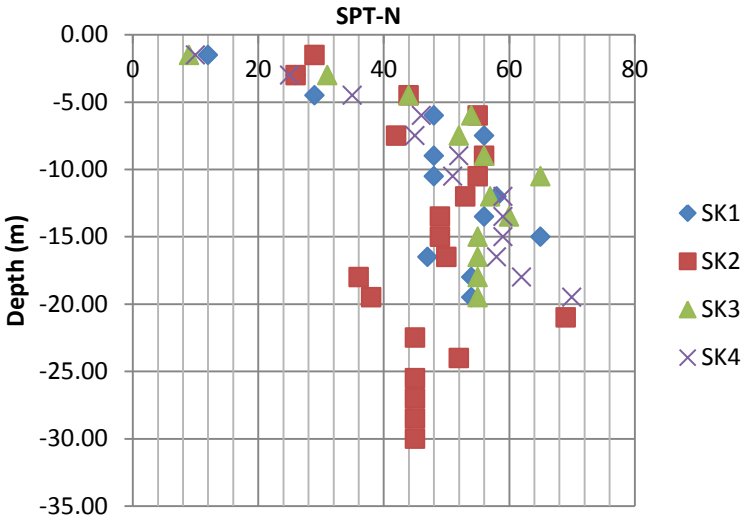

Figure 25 SPT-N values vs. Depth (m)

Average of the SPT-N values has been taken to derive a single corrected SPT value, N_{60}, which is shown in Figure 26. It is assumed that the stiffness of the soil is linearly increasing; therefore the profile of the corrected N values is deeper than the profile of raw SPT-N values.

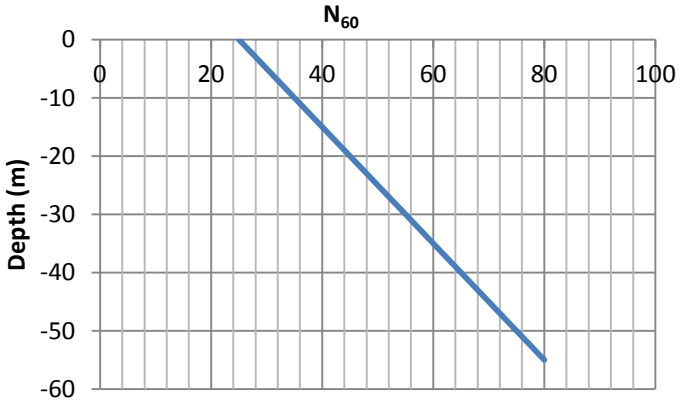

Figure 26 Corrected SPT-N values

For the input parameters of the Plaxis 3D, it is needed to convert the SPT-N values to soil stiffness parameter E'. The correlation of Stroud (1975) has been used for the N_{60} - E' relationship.

$$E' = N_{60} * 0.8$$

where E' is in MPa

Corresponding E’ values vs. depth has been shown in the Figure 27. E’ increases averagely 0.800 MPa per one meter depth, starting from the 20.000 MPa at ground level.

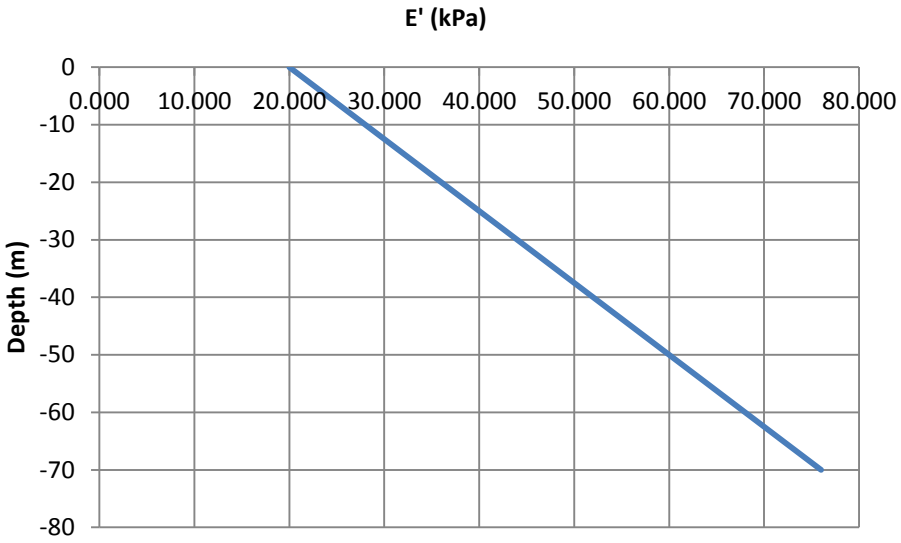

Figure 27 E' (kPa) vs. depth (m)

Required input parameters of the soil are tabulated in the Table 4. These parameters are assigned to the soil material data set and transferred to the model by a single borehole, which shows the information on the position of soil layers and the water table given. It is assumed that the water level is at -50m. This level indicates that the effect of water is not considered during the construction (and excavation) phase. Soil is modeled with Mohr-Coulomb failure criterion. The main reason for the usage of Mohr-Coulomb failure criterion is that the lack of required data/tests for soil stiffness parameters E_{50}^{ref}, E_{oed}^{ref} and E_{ur}^{ref}.

Table 4 - Soil Properties for Ankara Clay

Parameter	Symbol	Overconsolidated Clay	Unit
Material Model	-	Mohr-Coulomb	-
Unsaturated weight	γ_{unsat}	20	kN/m^3
Saturated weight	γ_{sat}	20	kN/m^3
Stiffness	E’	20,000	kN/m^2
Stiffness Increment	$E_{increment}$	800	$kN/m^2/m$
Cohesion	c'_{ref}	15	kN/m^2

Friction angle	φ’	25	-
Poisson ratio	ν'	0.25	-
Lateral pressure coefficient (K_{0x}=K_{0z})	K_0	0.8	-
Interface stiffness ratio	R_{inter}	1.0	-
Drainage Type	-	Drained	-

Structural Properties: The building is assumed as reinforced concrete building with 50-storey and 40x40m floor area. Piled raft foundation located at 5m below ground level. Raft thickness and the length of the piles are variable. Raft and pile properties used in the Plaxis 3D model are shown in Table 5 and Table 6. Piles are designed as embedded piles. Massive circular pile was selected among the predefined pile types for embedded piles. Skin resistance and the base resistance of embedded piles must be calculated and specified for the material input phase. The correlation of Stroud (1975), shown in Figure 28, has been used for the conversion of SPT-N values to shear strength of soil by taking the coefficient f_1 as 4.6. In addition the unit skin friction multiplier is taken as 0.35 of C_u. With the multiplication of these coefficients by related area and circumference values of piles, maximum skin resistance at the top (T^{top}_{max}) and the bottom (T^{bottom}_{max}) of the pile and the base resistance were calculated for the piles with a diameter of 1m. Material and section properties, used in Sap2000 Analyses, of raft and pile are shown in Table 7 and

Table 8 for Case-1.

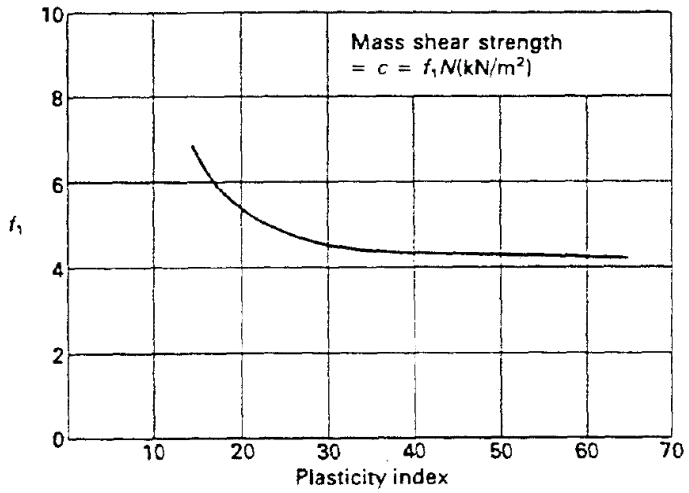

Figure 28 Relationship between Mass Shear Strength, Plasticity Index, and SPT-N values (after Stroud, 1975)

Table 5 Raft Properties for Case 1

Parameter	Symbol	Raft	Unit
Material Model	-	Linear-Isotropic	-
Unit weight	γ	25	kN/m^3
Stiffness	E_{ref}	3.000E+07	kN/m^2
Poisson ratio	ν	0.2	-
Thichness	t	2	m
Width - Breadth	WxB	40x40	m

Table 6 Embedded Pile Properties for Case 1

Parameter	Symbol	Embedded Pile		Unit
Material Model	-	Linear Elastic		-
Unit weight	γ	25		kN/m^3
Stiffness	E_{ref}	3.000E+07		kN/m^2
Diameter	d	1		m
Length	L	25	35	m
T^{top}_{max}	-	165	165	kN/m
T^{bottom}_{max}	-	255	300	kN/m
Base resistance	F_{max}	1,800	2,150	kN
# of piles	-	100 & 144		-

Table 7 Material and section properties of Raft in Case-1 for Sap2000 Analyses

Parameter	Symbol	Raft	Unit
Property	-	Shell Thick	-
Unit weight	γ	25	kN/m^3
Modulus of Elasticity	E	3.000E+07	kN/m^2
Poisson ratio	ν	0.2	-
Thickness	t	2	m
Width - Breadth	WxB	40 x 40	m

Table 8 Material and section properties of Pile in Case-1 for Sap2000 Analyses

Parameter	Symbol	Pile	Unit
Property	-	Frame - Pile	-
Unit weight	γ	25	kN/m^3
Modulus of Elasticity	E	3.000E+07	kN/m^2
Poisson ratio	ν	0.2	-
Diameter	d	1	m
Length	L	2.5	m
# of piles	-	100 & 144	-

Case 2: Messe-Torhaus Building

Messe-Torhaus has been constructed between 1983 and 1986 in Frankfurt, Germany. With a 130 m high and 30 floors, Torhaus is the first building in Germany with a foundation designed as a piled raft (Reul, O & Randolph, M.F. (2003))

Soil Properties:

Reul (2000) described the distribution of the Young's modulus of the Frankfurt clay with depth by the formula:

$$E = 45 + \left(\tanh\left(\frac{z-30}{15}\right) + 1\right) \times 0{,}7z$$

where E= Young's modulus (MPa)
z= depth below surface (m)

Stiffness of the Frankfurt Clay is shown in Figure 29 and calculated by using the suggested formula of Reul (2000). A stiffness increment of 1,545 kPa has been applied per one meter depth. In addition, different approaches to the stiffness value of Frankfurt Clay have been given in Figure 30.

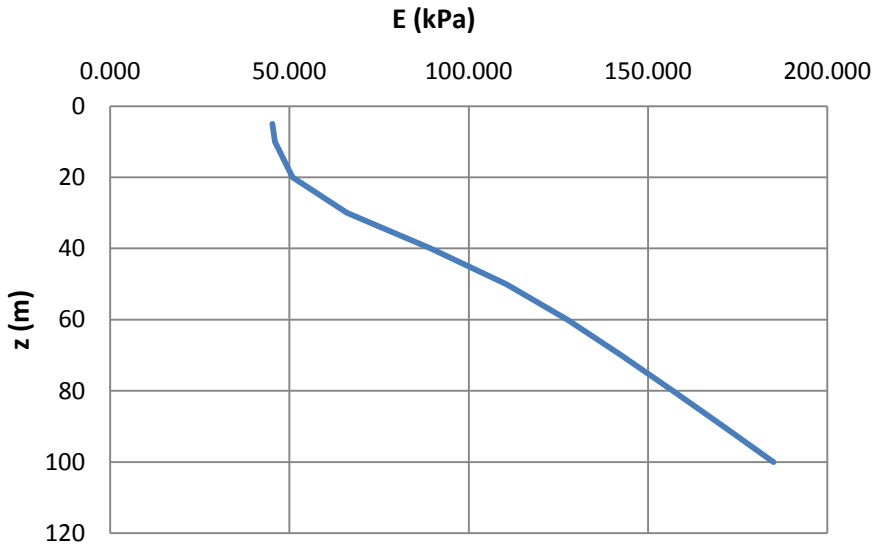

Figure 29 Variation of the stiffness of the Frankfurt Clay with depth.

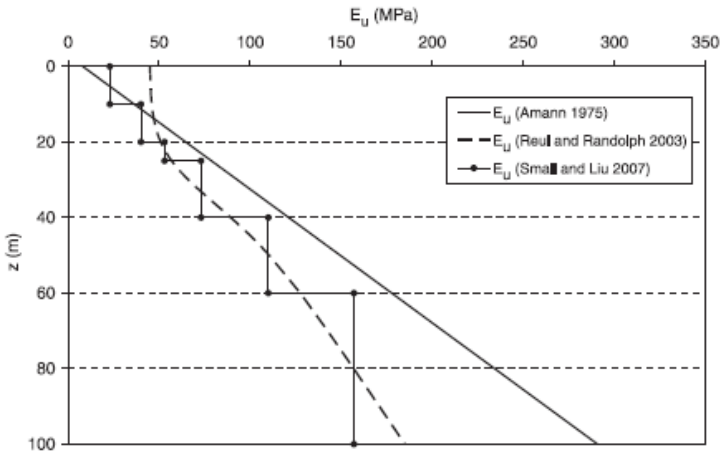

Figure 30 Different soil moduli for Frankfurt clay found in the literature. (Sales et. al. 2010)

Required input parameters of the soil are tabulated in the Table 9. These parameters are assigned to the soil material data set and transferred to the model by a single borehole, which

shows the information on the position of soil layers and the water table given. Groundwater level is just below the foundation, which is at -3m.

Table 9 - Soil Properties for Messe-Torhaus Building

Parameter	Symbol	Frankfurt Clay	Quaternary sand and gravel	Unit
Material Model	-	Mohr-Coulomb	Mohr-Coulomb	-
Unsaturated weight	γ_{unsat}	10	11	kN/m^3
Saturated weight	γ_{sat}	20	19	kN/m^3
Stiffness	E’	45,241	45,000	kN/m^2
Stiffness Increment	$E_{increment}$	1,545	0	$kN/m^2/m$
Cohesion	c'_{ref}	20	0.0001	kN/m^2
Friction angle	φ’	20	35	-
Poisson ratio	ν'	0.2	0.2	-
Lateral pressure coefficient ($K_{0x}=K_{0z}$)	K_0	0.8	0.426	-
Interface stiffness ratio	R_{inter}	1.0	1.0	-
Layer thickness	-	94.5, under the Quaternary layer	5.5, starting from the ground level	m

Structural Properties: The building was designed as reinforced concrete building with 30-storey and stands over two identical rafts with dimensions 17.5x24.5m. Distance between the rafts is 10m and each raft has 42 piles. Cross-sectional view and the plan of the building are shown in Figure 31.

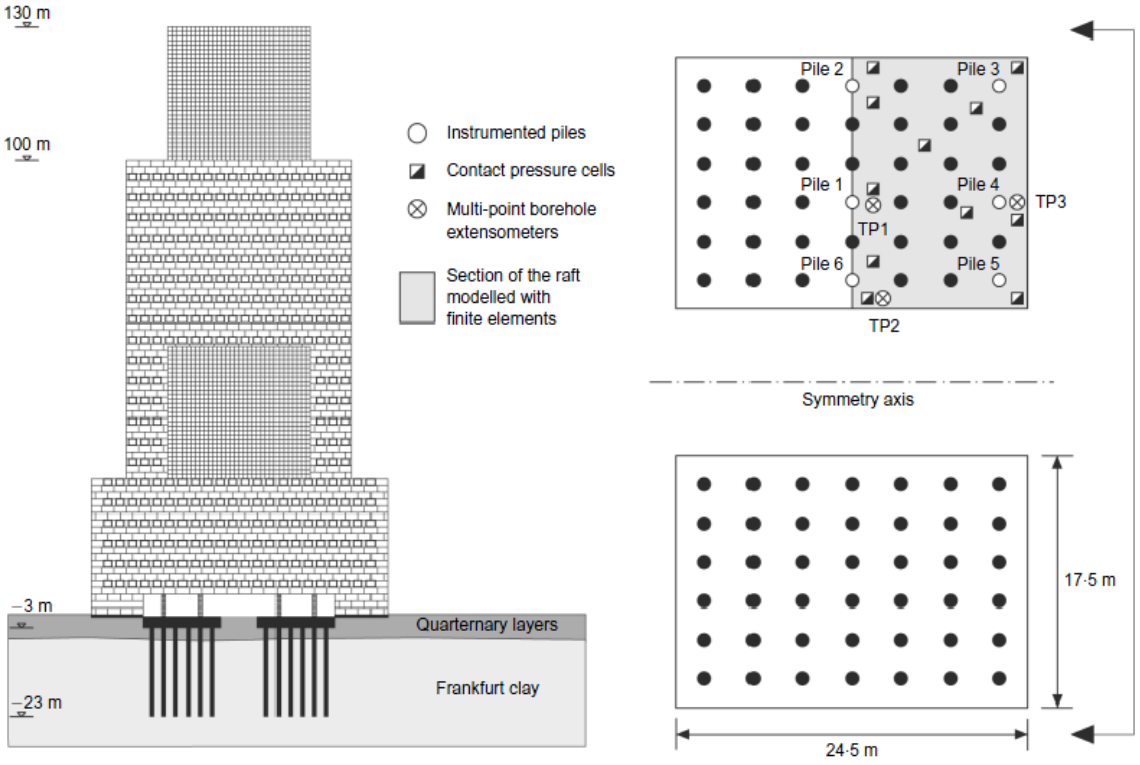

Figure 31 Messe-Torhaus Building cross-sectional view and piled raft layout with instrumentation (Reul, O & Randolph, M.F. (2003))

Piled raft foundation located at 3m below ground level. Raft thickness is 2.5m and the piles are identical with a length of 20m. Piles are designed as embedded piles. Raft and pile properties of Messe-Torhaus, used in the Plaxis 3D model are shown in Table 10 and Table 11. Due to loading and the shape/geometry of the structure and also the soil beneath the foundation only the half of the foundation has been taken into account along the symmetry axis. Massive circular pile was selected among the predefined pile types for embedded piles. Material and section properties, used in Sap2000 Analyses, of raft and pile are shown in Table 12 and Table 13 for Case-2. Maximum skin resistance at the top (T^{top}_{max}) and the bottom (T^{bottom}_{max}) of the pile is taken as equal. Parameters required for the input interface are tabulated in the Table 10.

Table 10 - Raft Properties of Messe-Torhaus

Parameter	Symbol	Raft	Unit
Material Model	-	Linear-Isotropic	-
Unit weight	γ	25	kN/m^3
Stiffness	E_{ref}	3.700E+07	kN/m^2
Poisson ratio	ν	0.2	-
Thickness	t	2.5	m
Width - Breadth	WxB	17.5 x 24.5	m

Table 11 Pile Properties of Messe-Torhaus

Parameter	Symbol	Embedded Pile	Unit
Material Model	-	Linear Elastic	-
Unit weight	γ	15	kN/m^3
Stiffness	E_{ref}	2.350E+07	kN/m^2
Poisson ratio	ν	0.2	-
Diameter	d	0.9	m
Length	L	20	m
T^{top}_{max}	-	453	kN/m
T^{bottom}_{max}	-	453	kN/m
Base resistance	F_{max}	1,200	kN
# of piles	-	42	-

Table 12 Material and section properties of Raft of Messe-Torhaus for Sap2000 Analyses.

Parameter	Symbol	Raft	Unit
Property	-	Shell Thick	-
Unit weight	γ	25	kN/m^3
Modulus of Elasticity	E	3.700E+07	kN/m^2
Poisson ratio	ν	0.2	-
Thickness	t	2.5	m
Width - Breadth	WxB	17.5 x 24.5	m

Table 13 Material and section properties of Piles of Messe-Torhaus for Sap2000 Analyses.

Parameter	Symbol	Pile	Unit
Property	-	Frame - Pile	-
Unit weight	γ	15	kN/m^3
Modulus of Elasticity	E	2,350E+07	kN/m^2
Poisson ratio	ν	0.2	-
Diameter	d	0.9	m
Length	L	2	m
# of piles	-	42	-

3.3 Definition of the Models, Geometries and Loading Conditions

Default boundary conditions were applied for all the models of Plaxis 3D, which was given in the Reference Manual of Plaxis as:

- The ground surface is free in all directions.
- Vertical model boundaries with their normal in x-direction are fixed in x-direction and free in y- and z-direction.
- Vertical model boundaries with their normal in y-direction are fixed in y-direction and free in x- and z-direction.

- Vertical model boundaries with their normal neither in x- nor in y-direction are fixed in x- and y-direction and free in z-direction.
- The model bottom boundary is fixed in all directions.

The deflection of the structural model is controlled by the displacements of the joints in the Sap2000 analyses. Each joint of the structural model have six displacement components, as: translations (U1, U2, and U3) and rotations (R1, R2, and R3). One or more of these components may have a zero value. In the SAP2000 model, only the bottom of the structure is supported by the springs. Area sections have area springs and pile ends have joint springs. All these springs have a spring constant for translation in direction of gravity i.e. U3. However, no constrain has been applied for other displacement components.

Case 1: A typical 50-storey building in Ankara

The building is a reinforced concrete building with 50-storey and 40x40m floor area. Piled raft foundation located at 5m below ground level (assuming two basements). Lengths of the piles are variable. Due to loading and the shape/geometry of the structure and also the soil beneath the foundation only a quarter of the foundation has been taken into account and the center of the model foundation has been placed in alignment with the z-axis the as shown in Figure 32. For the parametric analyses of the Case 1, sub-cases have been used, which are listed in the Table 14.

Table 14 Sub-cases of Case 1

Case	Number of piles*	Pile length (m)	Distributed load (kPa)
1-a	25	25	500
1-b	25	25	700
1-c	25	35	500
1-d	25	35	700
1-e	36	25	500
1-f	36	25	700
1-g	36	35	500
1-h	36	35	700

*number of piles represents the piles in the model which is a quarter of the actual model.

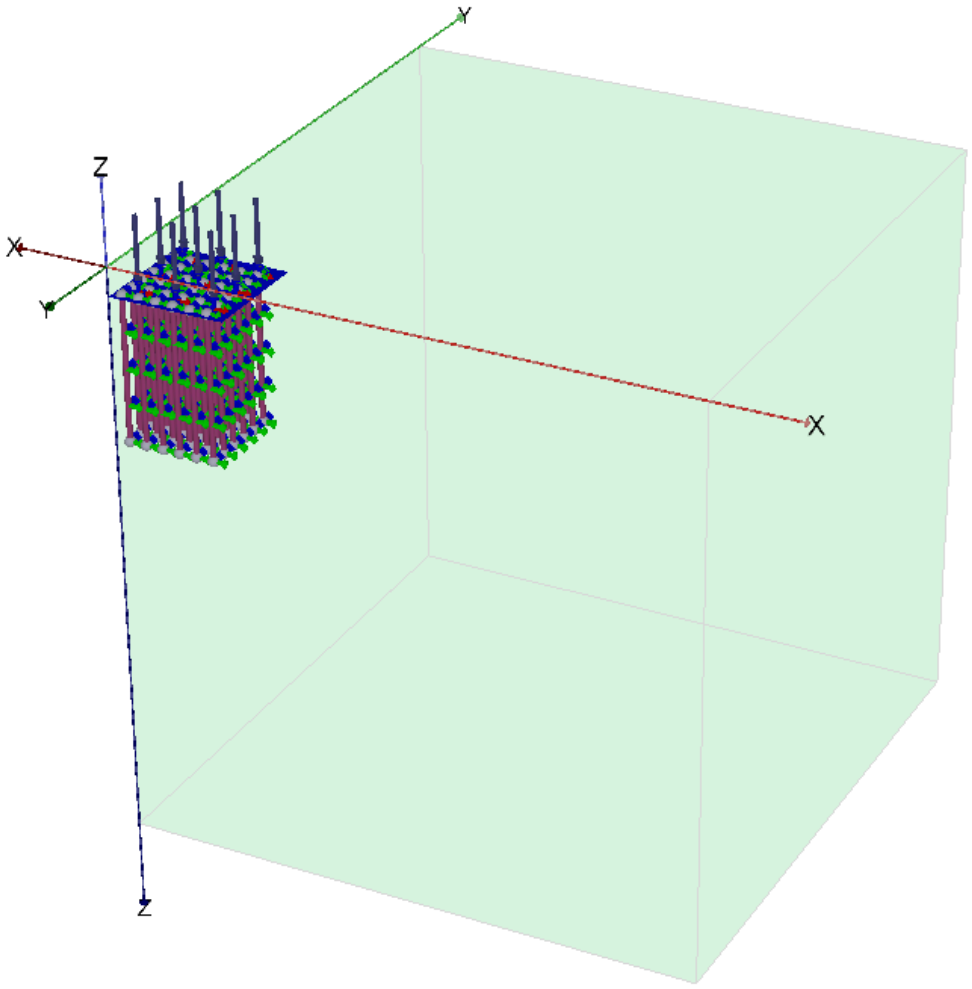

Figure 32 Finite Element model of the piled raft foundation of Case 1 in Plaxis 3D.

Raft and pile properties, including the geometrical properties, were previously tabulated in Table 5 and in Table 6. The raft thickness is taken as 2m. Ultimate capacity of 25m and 35 m length piles are 7,162kN and 10,522kN respectively.

The maximum total (dead and live) load has been taken as 14kN/m^2/floor. Therefore, the maximum total design load of the structure becomes 1,120MN for the selected case with 50-storey building. Total 500 kN/m^2 and 700 kN/m^2 loads applied to the foundation in the direction of gravity as distributed load. In other words, the weight of the building becomes 800MN and 1,120MN respectively.

Vertical excavation surfaces have been aligned (2h/5v) to solve the “soil body collapse” errors, which are occurred at the edges of the surface.

It is important to mention that the weight of excavated soil and the weight of the foundation must be taken into account to prevent heave of the soil where the settlements are observed lower

than the expected values and generally created in the deeper layers. This phenomenon is shown in the Figure 33. The calculations based on the exclusion of the weight of the excavated soil and raft can be found in the Appendix II. Steps of the analyses of the construction and calculation process in the Plaxis are outlined in the Table 15.

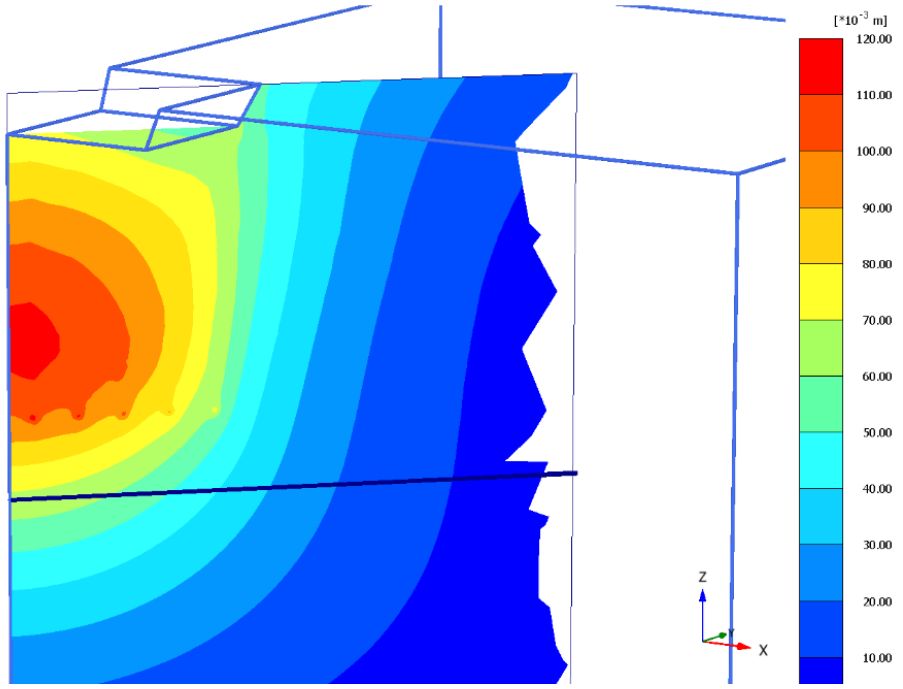

Figure 33 Heave of the soil.

Table 15 –Steps of the FE Analyses

Step	Description	Type
1. Initial Phase	Initial stress state calculated.	K_0 procedure
2. Excavation	Excavated up to -5m. **100kPa** applied to prevent heave.	Plastic
3. Construction	Raft and Pile activated (i.e. constructed). **60kPa** applied to prevent heave.	Plastic
4. Loading	**500kPa** and **700kPa** distributed loads are applied on Raft.	Plastic

3.4 Evaluation of mesh dependency

In the finite element calculations, the model has to be divided into elements which compose the "finite element mesh". In order to analyze the influence of mesh coarseness, other than the default coarseness of "Medium", three types of coarseness have been applied to the mesh of all eight sub-cases additionally. The generated number of elements and the nodes are shown in Table 16 with the resulting settlements at the critical points of foundation (locations of points are shown in Figure 42). It can be seen that the settlements are increasing with the finer mesh, which is reliable with the mesh dependence. However, in preliminary design stages, it may not be necessary to use the "very fine" mesh, considering the excessive time consumption of the analyses. Moreover, the mesh should be fine enough to get the accurate numerical analysis. The mesh is auto-created to be denser in the center line of the embedded pile and area under the raft, where the deformations and stresses are expected to have major variations.

During the analyses of the "very fine" coarseness, for the sub cases e, f, g and h (where 12x12 pile pattern applied), Plaxis failed to calculate the excavation, construction and loading steps with an error "*Picos_Back: error in call to Picos. [205]*". This problem has been solved by changing the default solver from "Picos (multicore iterative)" to "Classic (single core iterative).

Table 16 Mesh generation for Case 1-a (100piles, 25m, 500kPa)

			Settlement (mm)			
Mesh Coarseness	Number of elements	Number of nodes	A	B	C	D
Coarse	11,101	17,300	195	186	166	135
Medium	19,901	30,112	195	188	165	136
Fine	36,016	53,318	196	188	166	137
Very fine	84,103	120,839	197	189	169	142

Another point of interest in the mesh dependency is the extension of the model width in both horizontal directions and the depth. Extension of the model is important to avoid any influence of the boundary. Three different model sizes have been used in the analyses; 3x (60m), 5x (100m) and 8x (160m) by fixing the depth of the model at -100m.

The generated number of elements and the nodes are shown in Table 17 for the Case 1-a, under medium coarseness. As observed, for a wider model, only the differential settlement has a slight increase. However, comparing with the refinement of mesh, extension of the model has a lower influence on settlements. It is also observed that, the number of elements and the number of nodes of 8x model are less than the 5x model. This is because of the automatic creation of larger elements in the opposite direction of the foundation within the model. Please refer to the Appendix III and Appendix IV for the meshing information of all sub-cases.

Table 17 for Case 1-a (100piles, 25m, 500kPa)

			Settlement (mm)			
Model size	Number of elements	Number of nodes	A	B	C	D
3x (60m)	14,653	22,875	196	188	167	139
5x (100m)	19,901	30,112	195	188	165	136
8x (160m)	19,690	29,845	195	186	166	130

Further results and discussions of Plaxis are made for the model with 5x size and medium coarseness of mesh.

3.5 Sap2000 Analyses

Simplified Method (Using the outputs of Plaxis):

Sap2000 software has been used for back analyses of the model. As mentioned before, the main supports are joint springs and area springs in Sap2000. The stiffness of soil is modeled by the joint and area springs. A sample of a 3D view of the Sap2000 model is shown in Figure 34. Raft settlements are taken as average by the suggested formula of Davis & Taylor (1962) as following;

$$s_{avg} = \frac{1}{3}(2s_{centre} + s_{corner})$$

To find the spring constant of raft and pile separately, a linear trend line has been drawn as shown in Figure 35 and Figure 36 for Case 1-d and Case 1-h, respectively. Disregarding the constant in the formula, the multipliers of the x values in the Figure 35 are chosen as the spring constant of this structural element after dividing by the number of elements or area. As an example, the soil spring of total 25 numbers of piles is 738,320kN/m. This results in a soil spring of 29,533kN/m per pile. Also, similarly, soil spring of whole 400m^2 raft is taken as 465,050kN/m. This also results in to a soil spring of 1,163kN/m per one square meter of raft. 280MN (700kN/m^2) has been applied on the foundation (shell element).

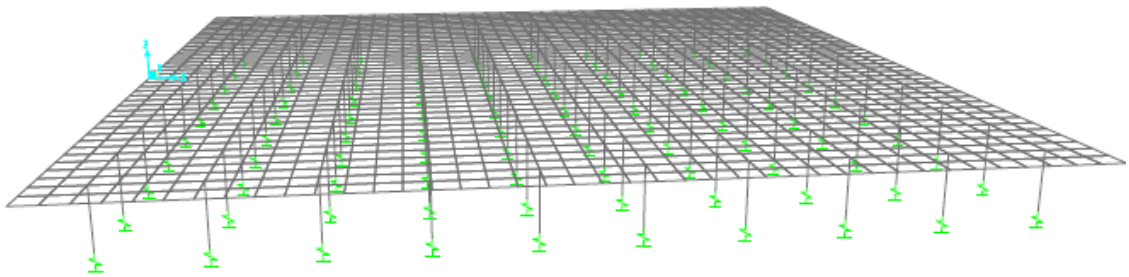

Figure 34 3D view of the Sap2000 model for Case 1

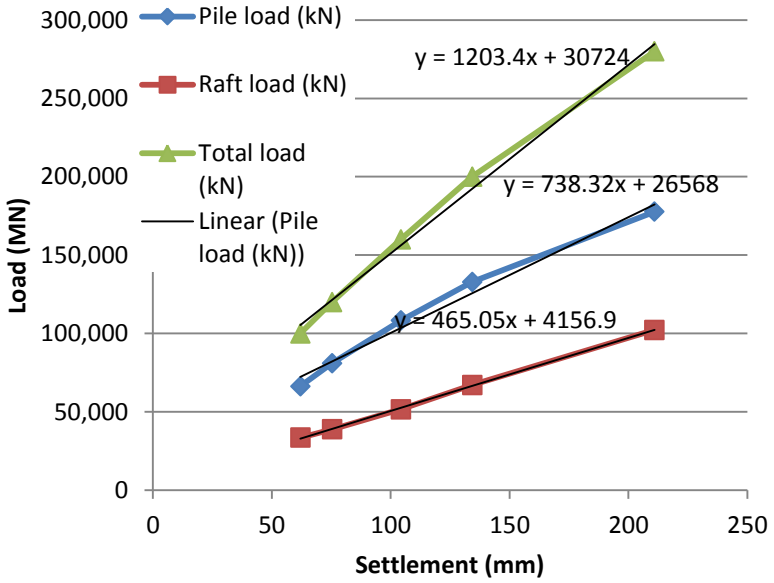

Figure 35 Load-settlement behavior of Case 1-d (100piles, 35m, 700kPa)

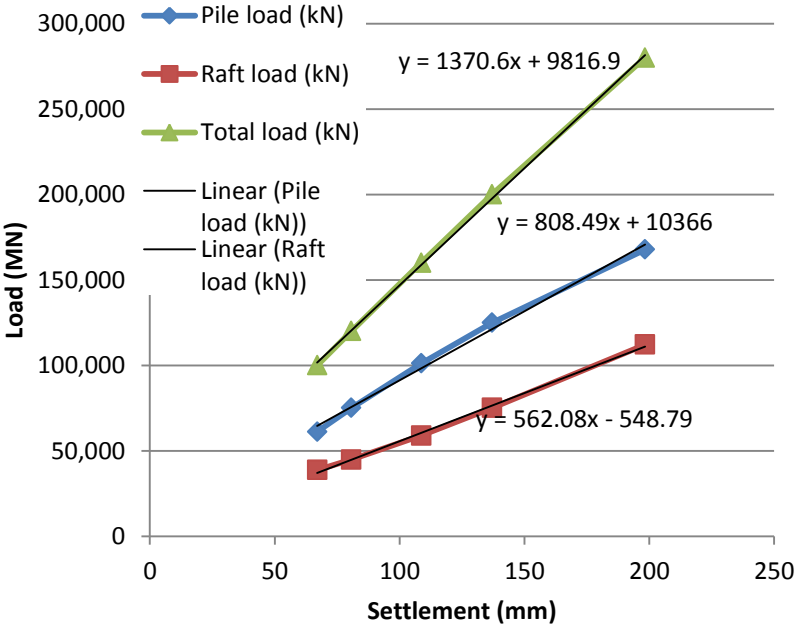

Figure 36 Load-settlement behavior of Case 1-h (144piles, 35m, 700kPa)

Disregarding the outputs of Plaxis

Separate analyses have been conducted to observe the behavior of piled raft by disregarding the outputs of Plaxis. In these analyses, allowable loading capacities of piles have been divided to the variable allowable settlements (at the top of the pile) to the usage of spring stiffness of piles. Initially, maximum allowable settlement is taken as 0.01m. This results in to a spring constant of 358,000kN/m and 526,100kN/m for 25m and 35m length piles, respectively. Also, to analyze the effect of raft contribution, raft springs have been used as; 0, 1000, 2000, 5000, 10000 kN/m/m2. This process has been repeated for the allowable settlements; 0.1m, 0.015m and 0.005m. All results are listed in Appendix V. Critical piles' loads are listed in Table 18 and the locations of piles are shown in a quarter of the piled raft in Figure 37.

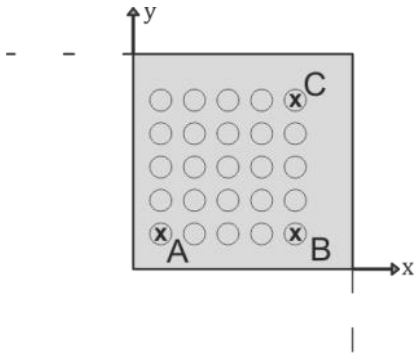

Figure 37 Piles taken as reference shown in a quarter of the piled raft.

Table 18 Comparison of pile loads

		Springs		Pile Loads (kN)			
		Pile (kN/m)	Raft (kN/m/m2)	A	B	C	Ref.
SAP 2000	k for 0.010m	526,100	10,000	9040.5	9177.3	9292.7	50 S
	k for 0.015m	350,733	10,000	8109,3	8213.7	8303.5	90 S
	k for 0.005m	1,052,200	10,000	10226.9	10417.4	10573.1	130 S
	k from Plaxis	29,533	1,163	7351.1	7390.8	7429.4	200 S
Plaxis				6266.4	7469.0	7497.5	204

Case 2: Messe-Torhaus Building

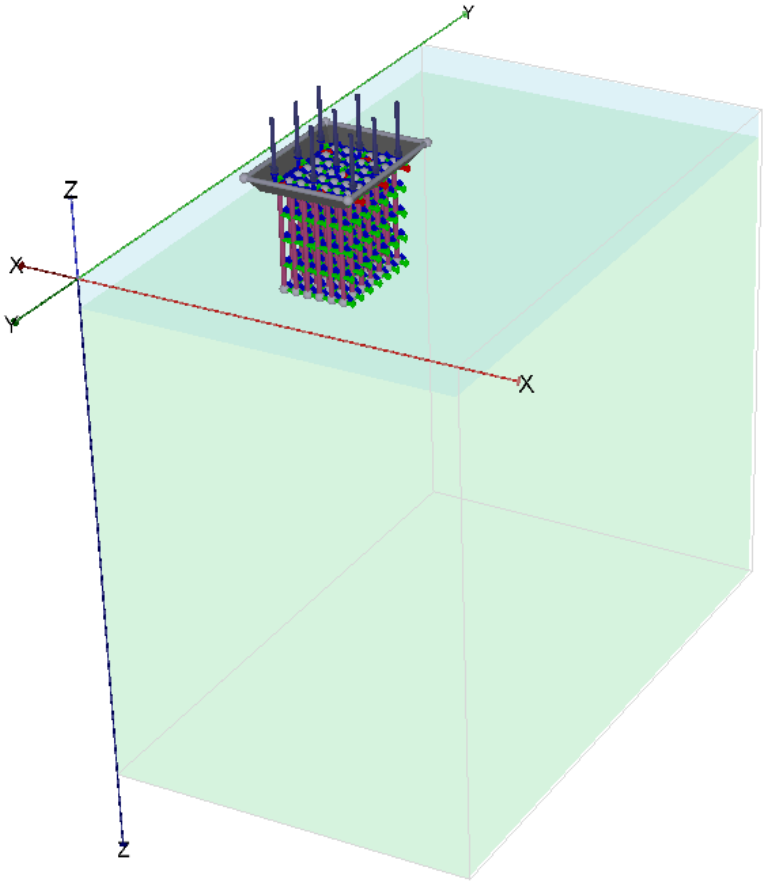

Figure 38 Finite Element model of the piled raft foundation of Case 2 in Plaxis 3D.

Messe-Torhaus Building is a reinforced concrete building with 30-storey and stands over two identical rafts with dimensions 17.5x24.5m. Distance between the rafts is 10m and each raft has 42 piles. Due to loading and the shape/geometry of the structure and also the soil beneath the foundation only the half of the foundation has been taken into account.

As seen in the Figure 38, the model width is extended up to 50 meters from the edges of the foundation except the symmetry axis. This side has been taken as 5m to show the actual behavior of the symmetric foundation. The depth of the model is also extended to -100 m, in order to minimize the boundary effects.

Total design load of the structure was given as 400 MN. This corresponds to a load of 12 kN/m^2/floor (assuming a rectangular shape in line with foundation boundary). For the half of the foundation, 466 kN/m^2 load has been applied to the foundation as distributed load in the direction of gravity.

Vertical excavation surfaces have been aligned (2h/5v) to solve the “soil body collapse” errors, which are occurred at the edges of the surface as shown in Figure 39 with the exploded view of the mesh of Plaxis 3D model.

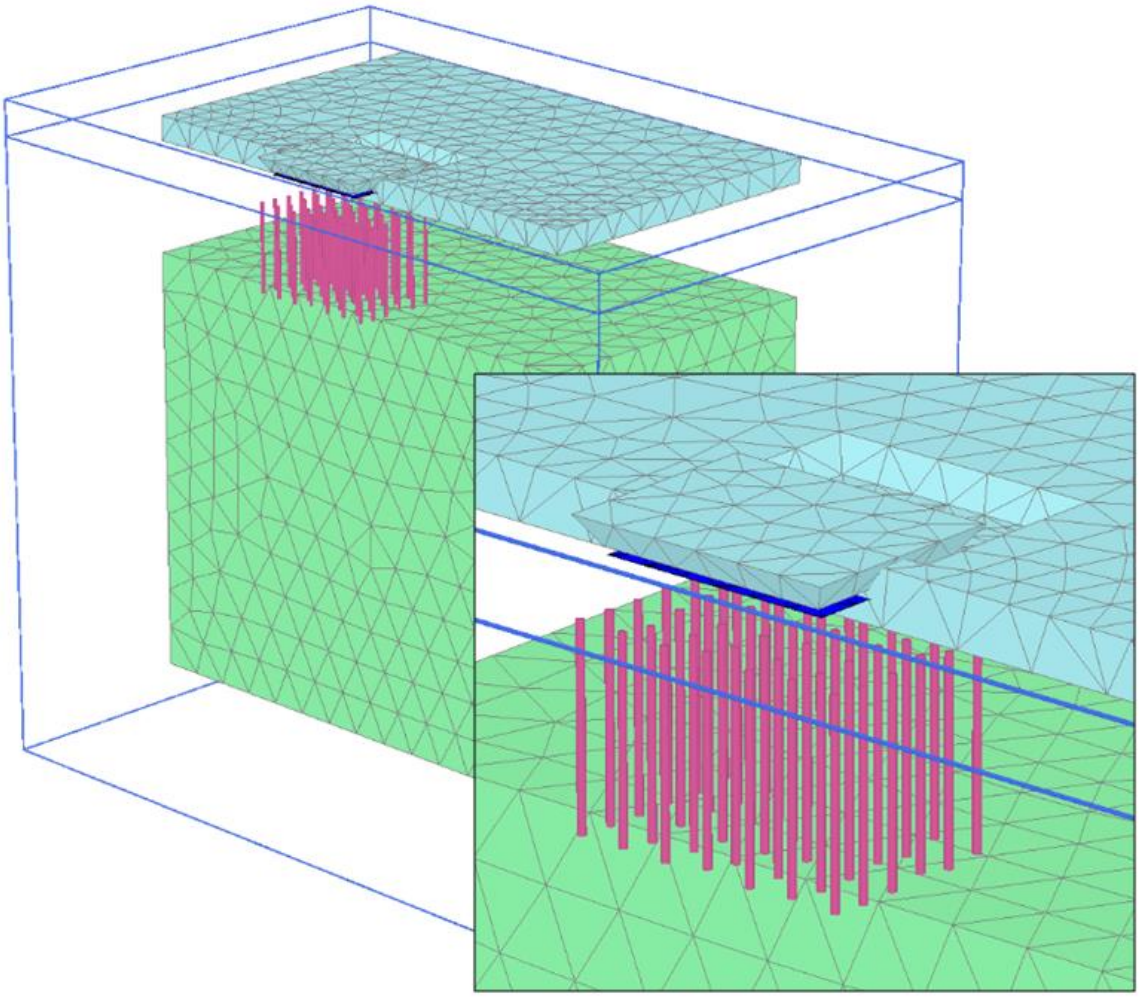

Figure 39 Exploded view of the 3D mesh of Messe-Torhaus foundation (42 piles).

Sap2000 Analyses

Usage of Sap2000 has been described for Case 1. Therefore, it will not be detail for Case 2. Using the proposed simplified method, load-settlement curves are plotted in Figure 40 with the linear trend lines for soil springs and the 3D view of the Sap2000 model is shown in Figure 41

Soil spring of a pile is calculated as 54,286 kN/m. Also, the soil spring of raft is calculated as 1,116 kN/m per one square meter.

200MN (466kN/m^2) has been applied on the foundation (17.5m x 24.5m) (shell element). Besides, it should be noted that, as derived from the measurements of Katzenbac the maximum total load could not reach to the design load as shown in Figure 40.

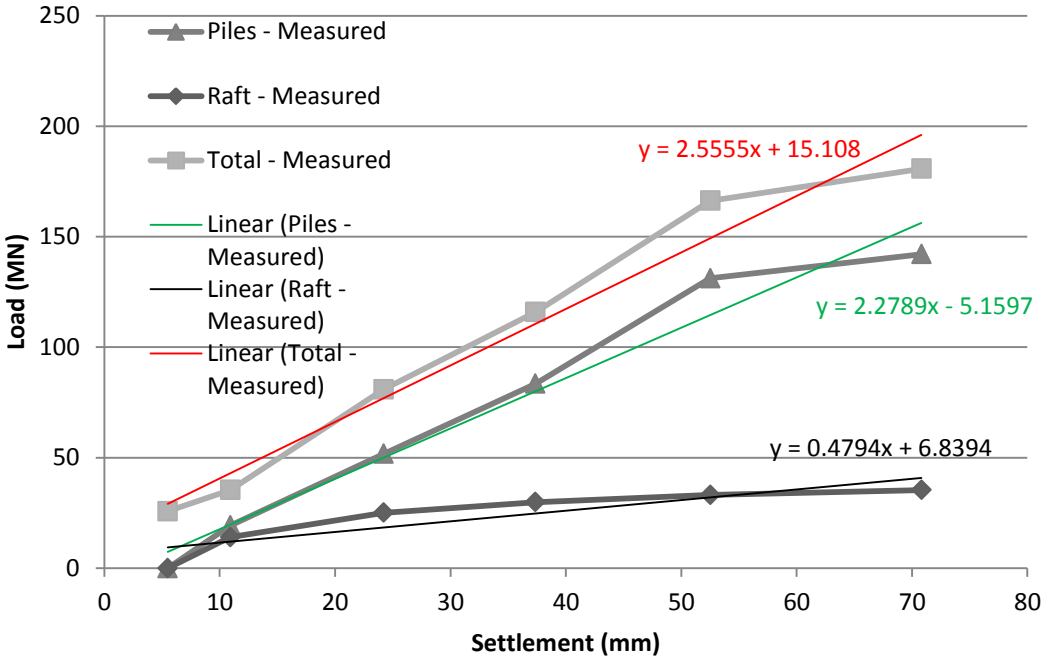

Figure 40 Load-settlement behavior of Case 2 and the linear trend lines. (modified after Katzenbach et al. (2000))

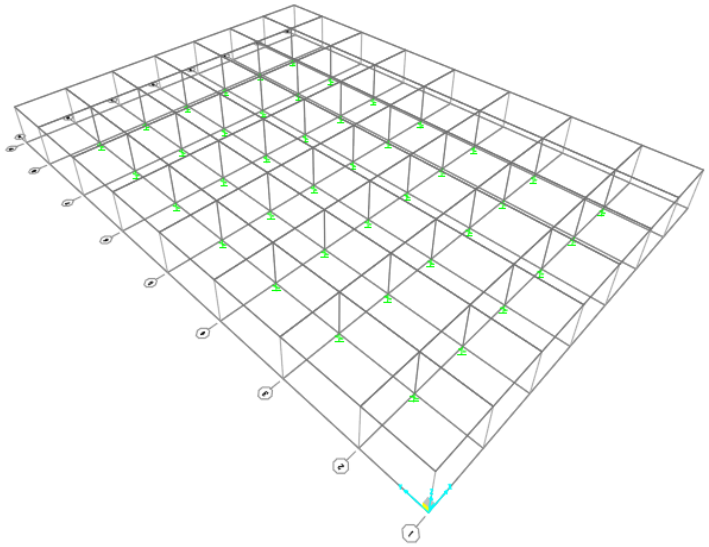

Figure 41 3D view of the Sap2000 model for Case 2

CHAPTER 4

DISCUSSION OF RESULTS

In this study, behavior of the piled raft foundation systems under axial loads has been investigated by modeling a real case study and an artificial case with parametric analyses. Some variables for the parametric analyses are pile number, pile length and level of the load applied. To this end, parametric analyses are conducted via the finite element software Plaxis 3D. SAP2000 software has been used as a structural back analysis. Discussions are made on settlements, pile load distributions and share of load by raft.

4.1 Settlements

Case 1: A typical 50-storey building in Ankara

After all of the analyses have been carried out, the settlements of the raft under two vertical loading of 500 kPa and 700 kPa are monitored. The related settlements values are taken from the explicit points on raft as quarterly, shown in the Figure 42 with coordinates (x.y) at the foundation level -5m. Calculated settlements are tabulated in Table 19 for different number of piles, pile length and load level.

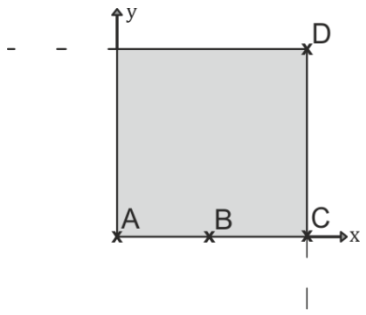

Figure 42 Settlement points; A (0,0), B (10,0), C (20,0), D (20,20) on the quarter of the piled raft.

Settlements are variable between 94 mm to 343 mm, which includes some excessive/unacceptable settlements for the selected building's piled raft foundation. This is mainly due to the higher s/d ratios (3 for 144 piles and 4 for 100 piles cases) of pile group and the overestimated loading conditions (700kPa which gives 14kN/m^2 for each floor).

It is obvious that the maximum settlements are occurred at the center of raft. It is not the case for the analyses disregarding the weight of soil excavated and the raft, in which the highest settlements occur at point C (i.e. midpoint of the edge of raft).

Table 19 Settlement values for variable number of piles, pile length and load level

				Settlement (mm)			
Case 1-	Number of piles*	Pile length (m)	Dist. Load (kPa)	A	B	C	D
a	25	25	500	-195	-188	-165	-136
b	25	25	700	-343	-330	-290	-239
c	25	35	500	-153	-146	-122	-94
d	25	35	700	-234	-226	-200	-164
e	36	25	500	-189	-182	-166	-145
f	36	25	700	-277	-271	-266	-238
g	36	35	500	-151	-143	-127	-109
h	36	35	700	-213	-204	-188	-169

*number of piles represents the piles in the model which is a quarter of the actual model.

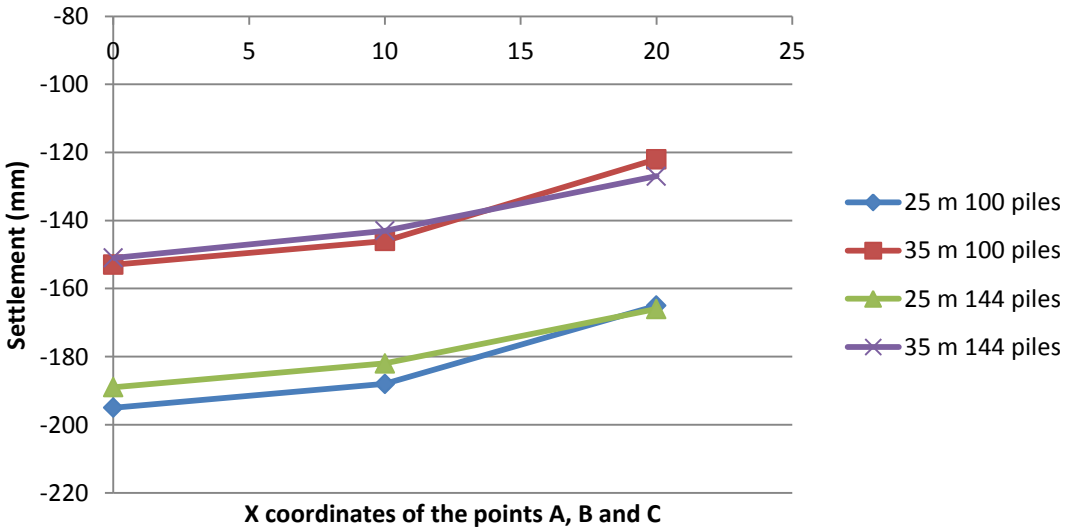

Figure 43 Settlements along raft for load level of 500 kPa

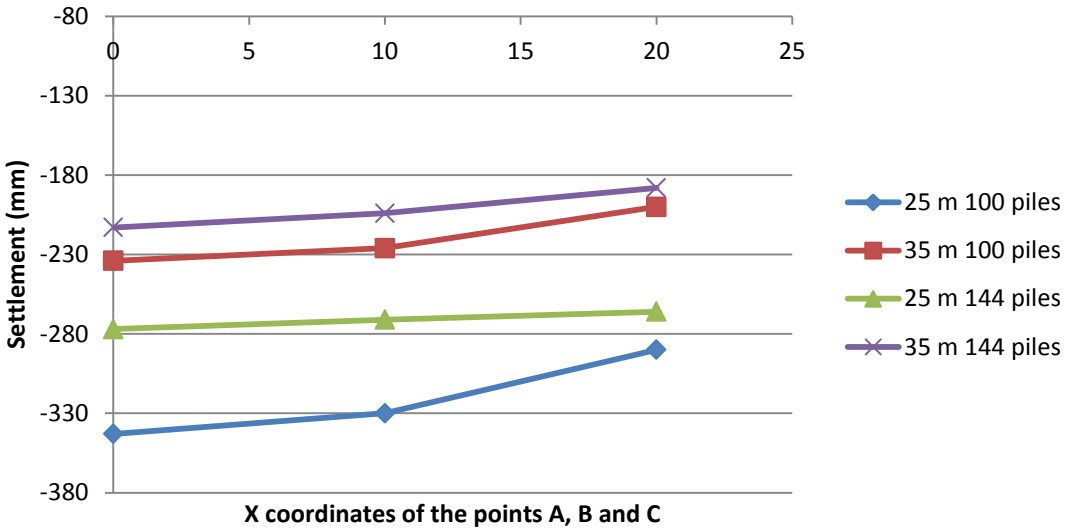

Figure 44 Settlements along raft for load level of 700 kPa

The settlements calculated along the x-axis on raft are shown in Figure 43 and Figure 44 for load levels of 500 kPa and 700 kPa. It is observed that the number of piles in the model does not have a significant effect on the settlements for low load levels. However, in higher loads, increasing number of piles has a decreasing effect on settlements only for shorter piles (25 m). In addition, using longer piles reduced the differential settlement of raft in higher load levels.

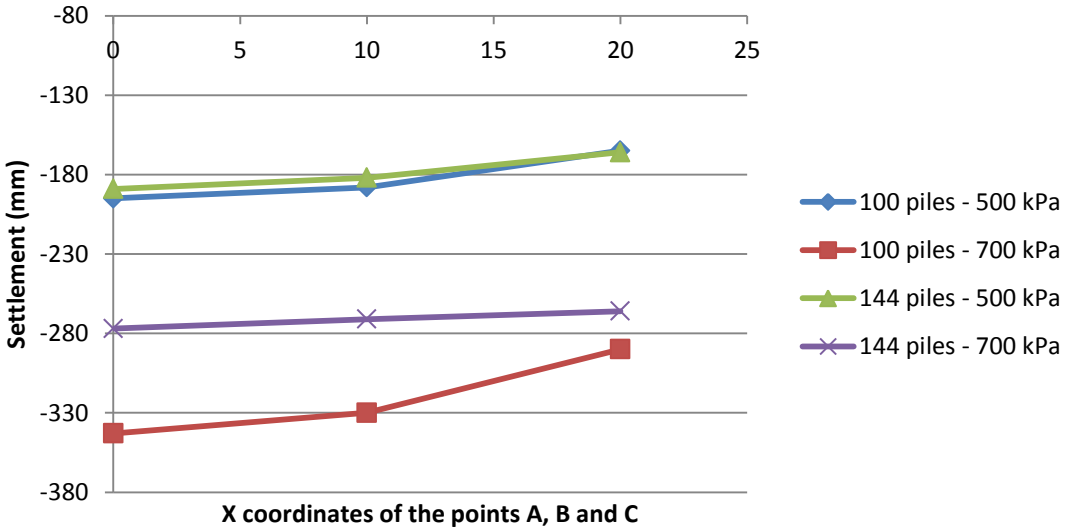

Figure 45 Settlements along raft for piles length of 25 m

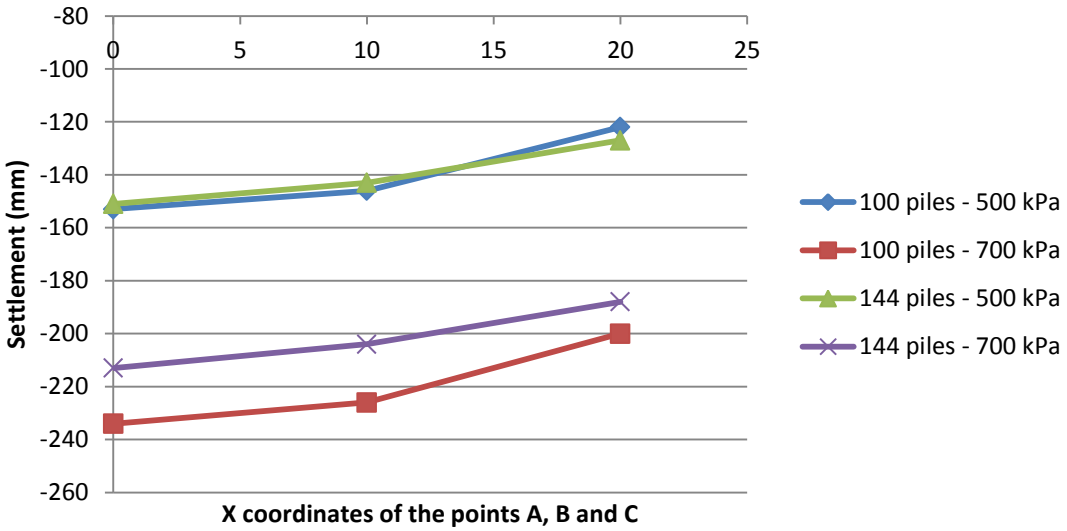

Figure 46 Settlements along raft for piles length of 35 m

To analyze the effect of pile length, settlement values are shown in Figure 45 and Figure 46. It is observed that, longer piles create more parallel settlement patterns comparing with the shorter piles at higher load levels in case of increasing number of piles in the model.

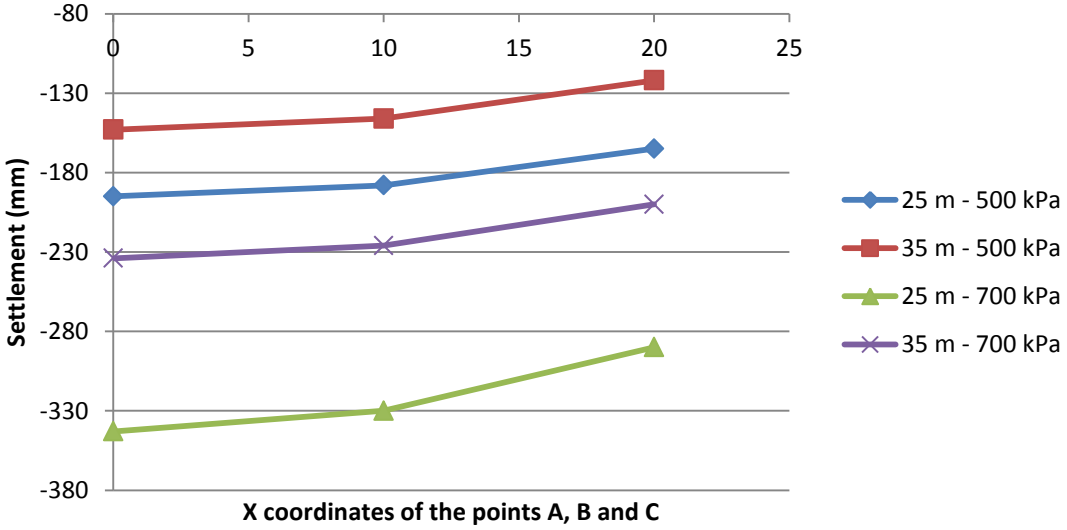

Figure 47 Settlements along raft for 100 piles (in model 25 piles)

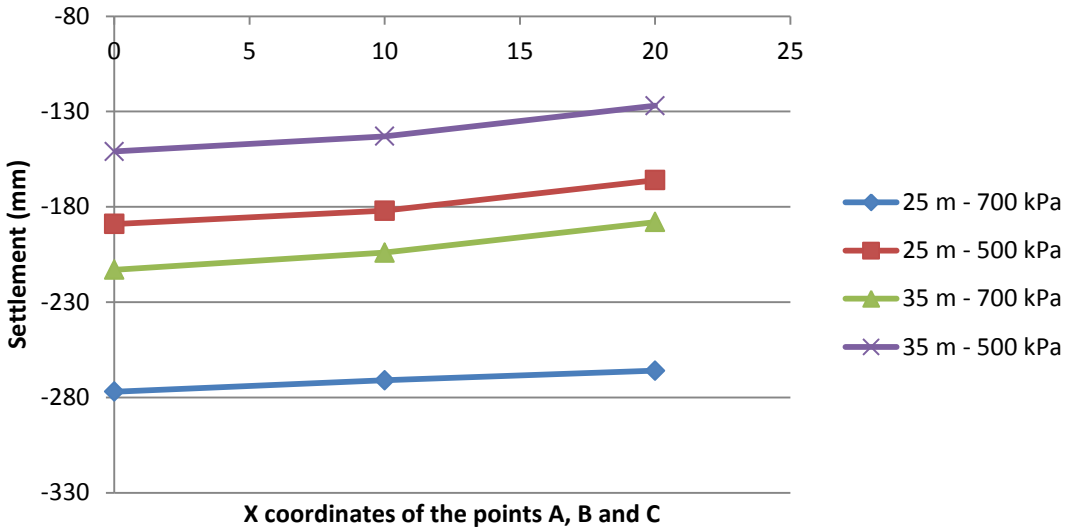

Figure 48 Settlements along raft for 144 piles (in model 36 piles)

In the case of using same number of piles, it is basically outlined that the both total and differential settlements are proportional with the load level and inversely proportional with the length of piles. These results are derived from the Figure 47and Figure 48. As a general conclusion, bowl shape settlement occurs in all cases.

Case 2: Messe-Torhaus Building

After the FE analyze of the piled raft foundation of Messe-Torhaus Building with Plaxis, load-settlement curves have been plotted in Figure 49. Analyses have been made for 100MN, 150MN and final design load of 200MN. Figure shows that, at the final design load of the structure, the calculated settlements are quite close to the measured values. However, the raft load sharing appears to be lower than the actual case at the lower loads. At the final design load, raft carries %19.2 of the total load in addition the measured values gives %19.6. Differential settlement pattern is shown in Figure 50 which is logical, considering the symmetry axis of the model is close to the edge of the raft.

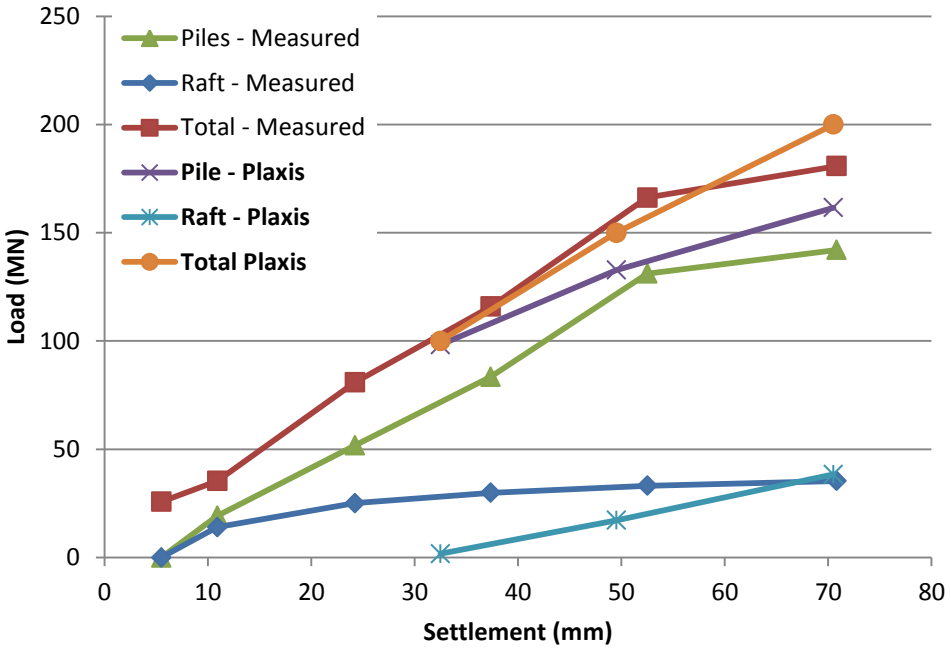

Figure 49 Measured load-settlement curves of Katzenbach et al. (2000) and the calculated load-settlement curves through Plaxis 3D.

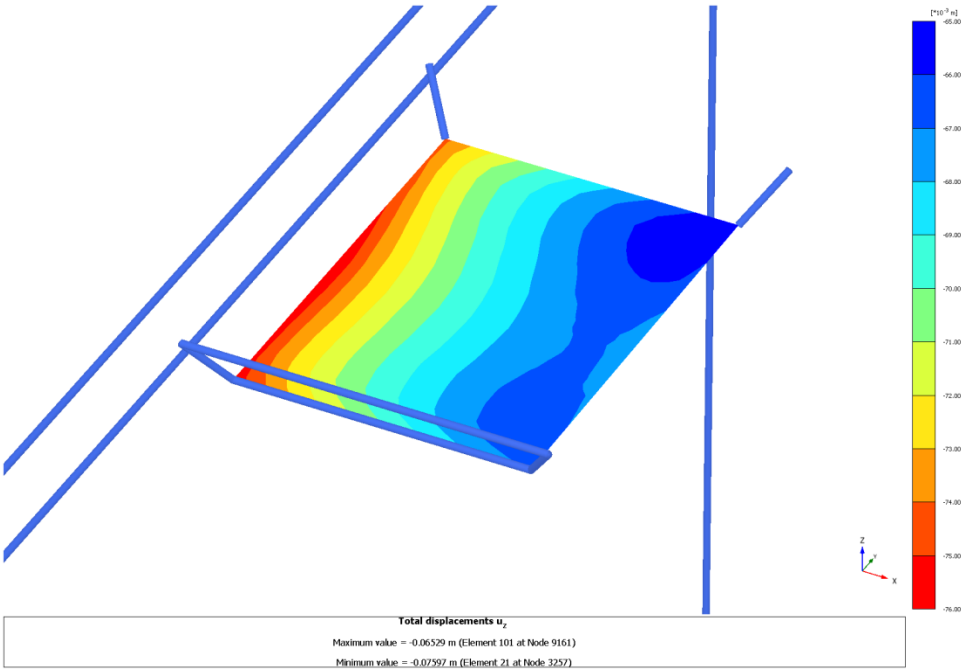

Figure 50 Total displacement of the raft in Plaxis 3D for Messe-Torhaus

4.2 Pile load distributions

Case 1: A typical 50-storey building in Ankara

Axial load distributions are plotted in Figure 51. All the piles are 25 m length. It is observed that the center piles have lower axial loads on both 100 piles and 144 piles situations. This is because of the pile group effects. However, for 144-pile case, it is observed that the axial load of the center pile is almost half of the outer piles. Center pile can approach to the load level of outer piles after the depth of 23m and moves parallel after this point. This may be the effect of small ratio of pile spacing and pile diameter, which causes the block movement of soil just beneath the center of raft. Therefore, considering the movement of the soil beneath the center of raft, shown in Figure 52 and Figure 54, the behavior of the center and corner piles is in reasonable.

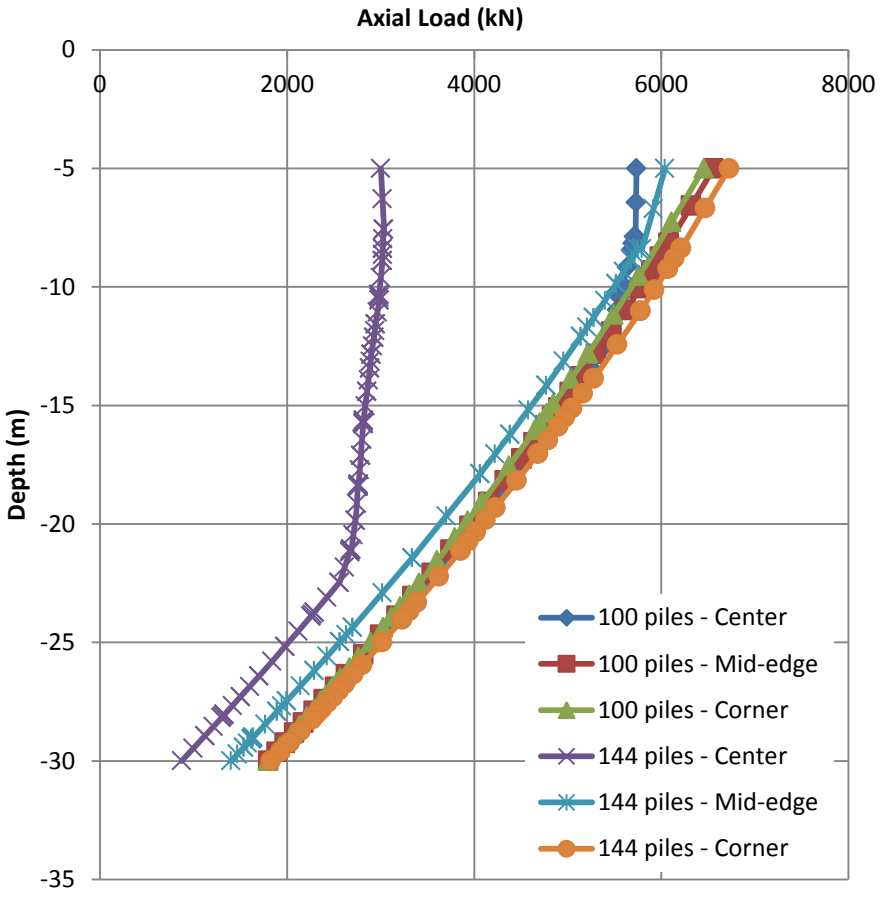

Figure 51 Comparison of axial load distributions along piles for different number of piles (Case 1-a (100piles, 25m, 500kPa) vs. Case 1-e (144piles, 25m, 500kPa))

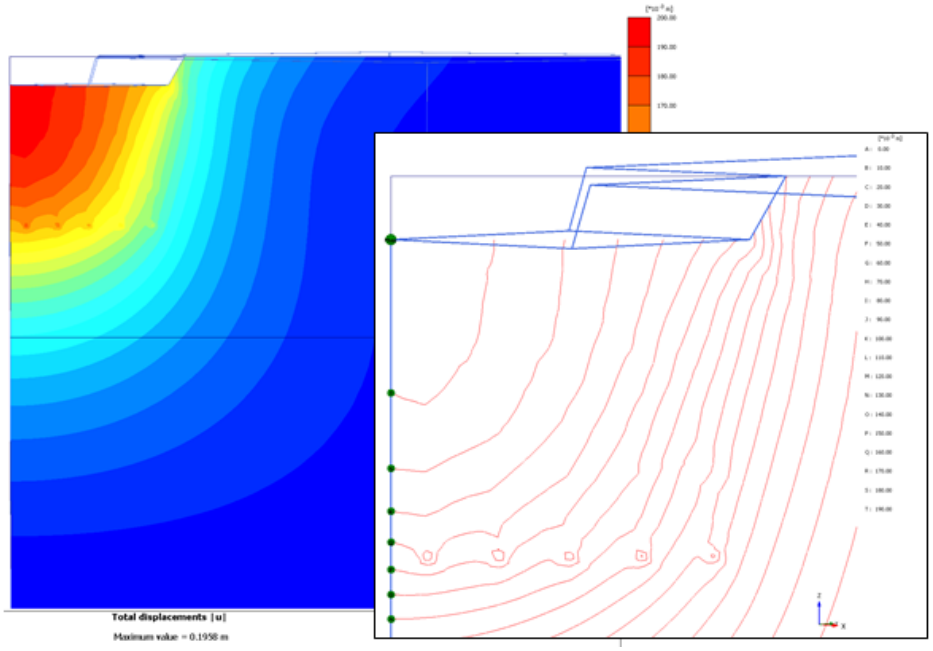

Figure 52 Total displacement of Case 1-a (100piles, 25m, 500kPa) as shadings and counter lines

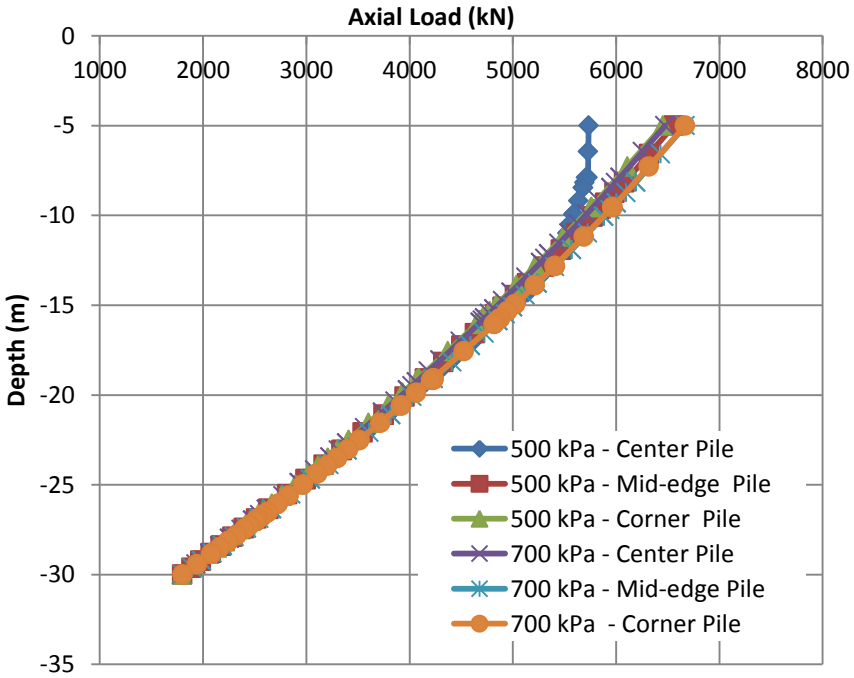

Figure 53 Comparison of axial load distributions along piles for different load levels (Case 1-a (100piles, 25m, 500kPa) vs. Case 1-b (100piles, 25m, 700kPa))

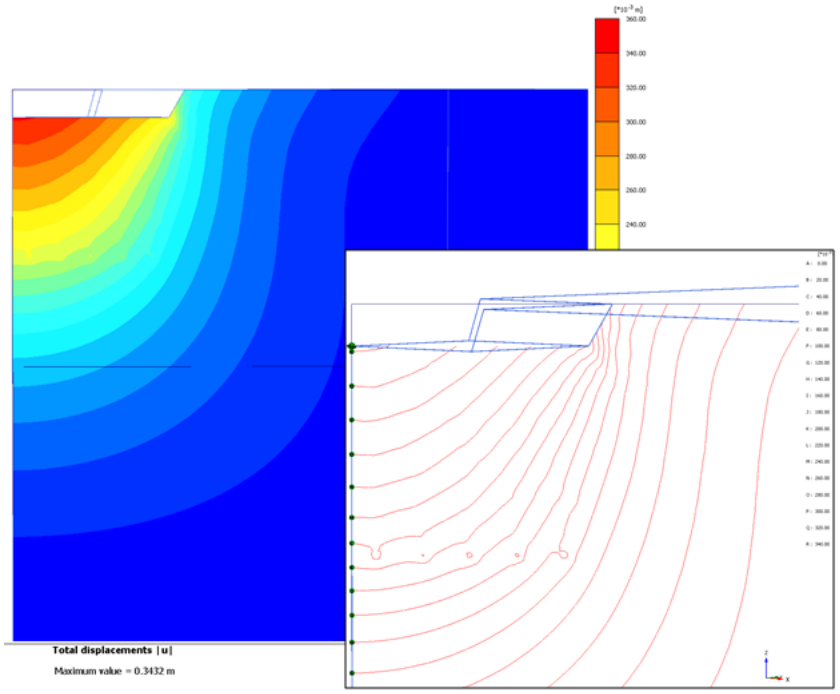

Figure 54 Total displacement of Case 1-b (100piles, 25m, 700kPa) as shadings and counter lines

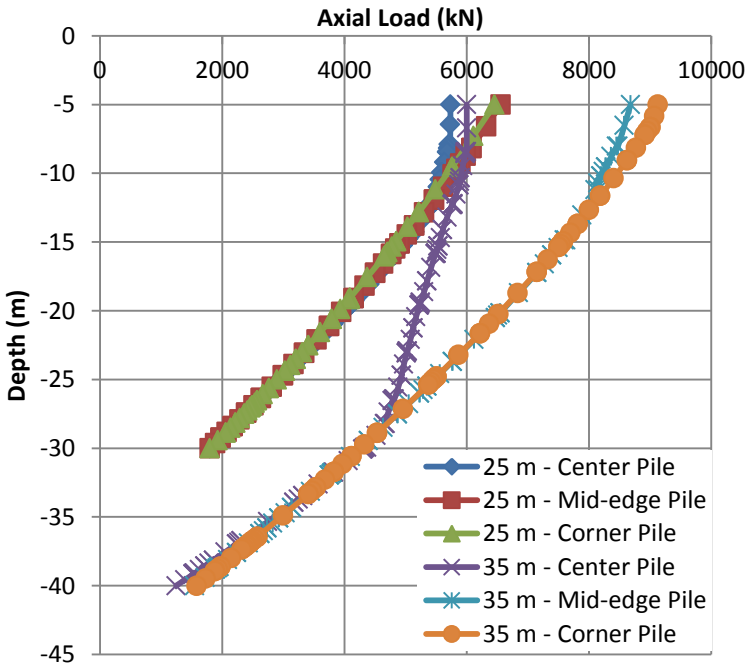

Figure 55 Comparison of axial load distributions along piles for different length of piles (Case 1-a (100piles, 25m, 500kPa) vs. Case 1-c (100piles, 35m, 500kPa))

At higher levels of load, center pile tends to be identical with the outer piles in distribution of axial load. In other words, at low load level; pile load of the center pile is smaller than the corner pile and at higher load level; pile load of the center pile is almost same with the corner pile. This may be because of the block movement of the soil between the piles in the projection of raft or due to the increase in the load sharing of raft. Figure 54 shows the pattern of soil movement

For the same level of loads, center piles of the both 25m and 35m length configuration have almost same axial load distribution up to a depth of 10m. However, the total loads on outer piles for 35m length are higher than 25m length piles as shown in Figure 55. Therefore, it can be concluded that the usage of longer piles increases the shared load of piles.

For the Case 1-b (100piles, 25m, 700kPa), where the highest settlement occurs among 100-pile cases, outer most pile has almost same axial loads (0.97 Pave) with inner piles (1.01 Pave) (Pave=4,801kN).

For the Case 1-c (100piles, 35m, 500kPa), where the lowest settlement occurs among 100-pile cases, outer most pile take higher axial loads (1.42 Pave) than inner piles (0.89 Pave) (Pave=5,320kN). This result is in line with the study of Lin and Feng (2006).

Case 2: Messe-Torhaus Building

Axial load distributions are plotted in Figure 56. It is observed that the center pile (TP 1) has lower axial load than the outer piles (TP 3 and TP 5). As explained in the Case 1, this is a outcome of the pile group effect. Measured axial pile loads are plotted to compare with the calculated pile loads in Figure 57. Cross-section of the vertical settlement along symmetry axis of the model is shown in Figure 58. Considering the movement of the soil beneath the center of raft, the behavior of the center and corner piles is in reasonable.

Calculated pile loads are compared with the measured values and with the calculations of Engin & Brinkgreve (2009). Most of the Plaxis results, which are made in this study, present close agreement as shown in Figure 59. However, for the piles TP3 and TP4, calculated results show almost 10% variations with the results of Engin & Brinkgreve, (2009). The main reason for this difference is the soil model of this study is Mohr-Coulomb failure criterion whereas the Engin & Brinkgreve, (2009) model is Hardening Soil Model.

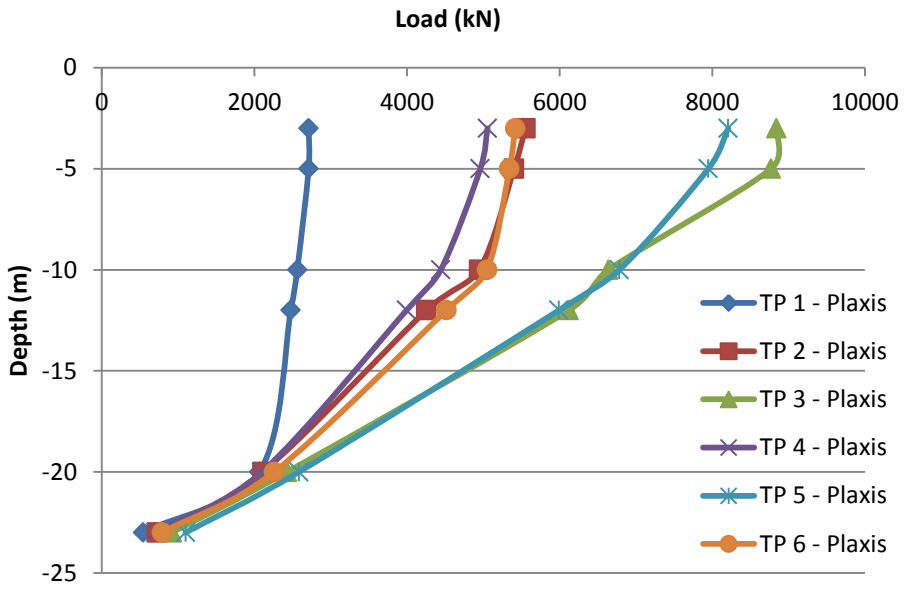

Figure 56 Calculated axial load distributions for chosen piles

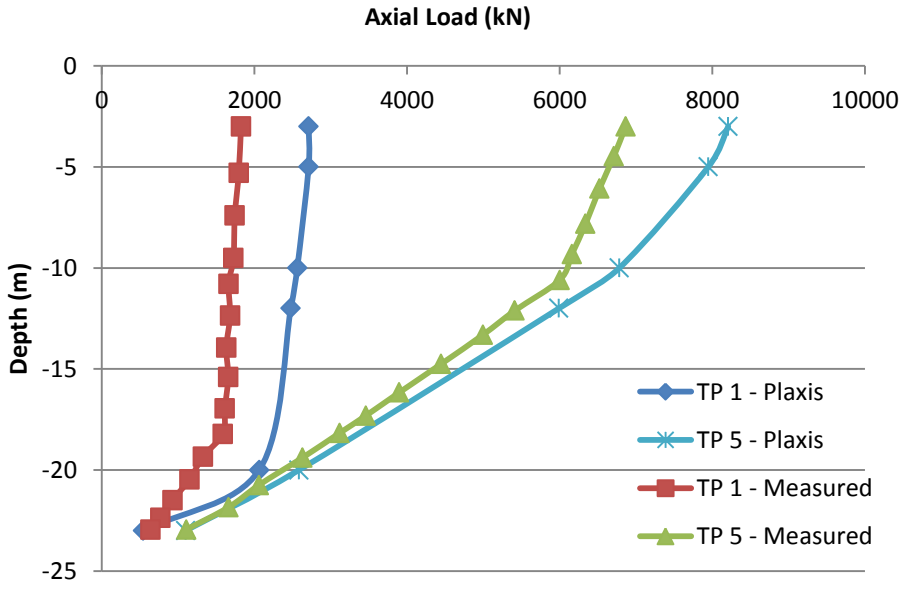

Figure 57 Measured and calculated axial loads along piles TP 1 and TP 5 (after Katzenbach et al. 2000)

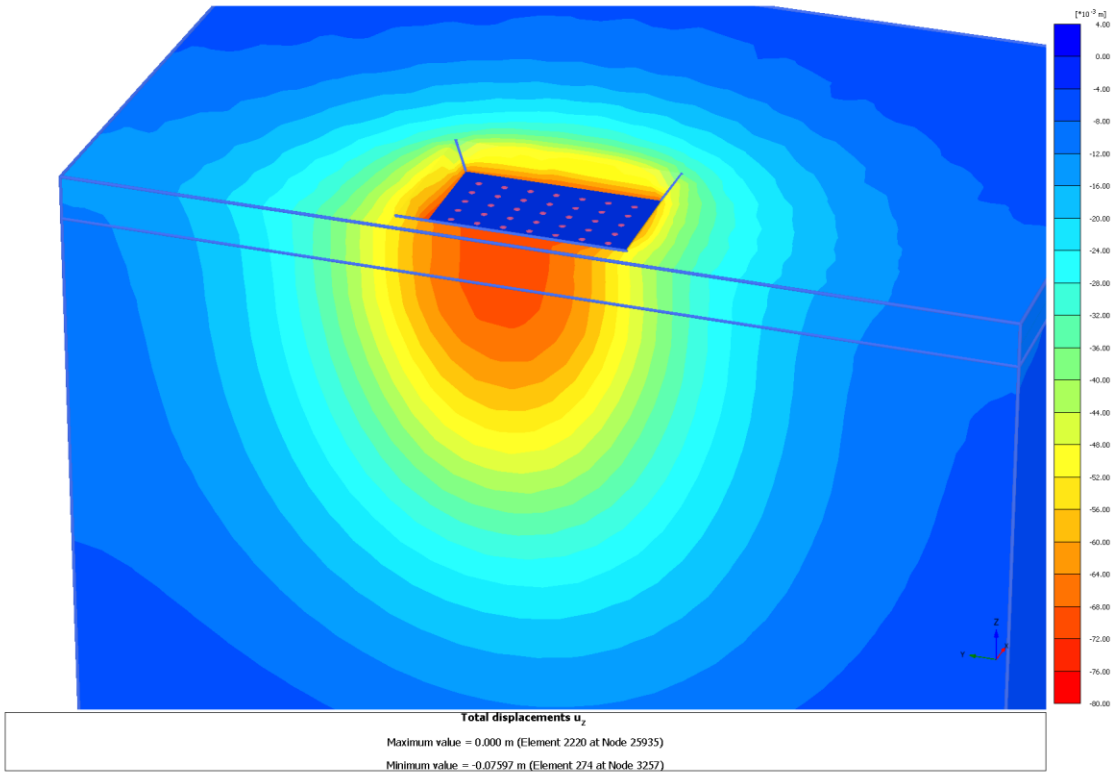

Figure 58 Vertical settlement shadings of Messe-Torhaus

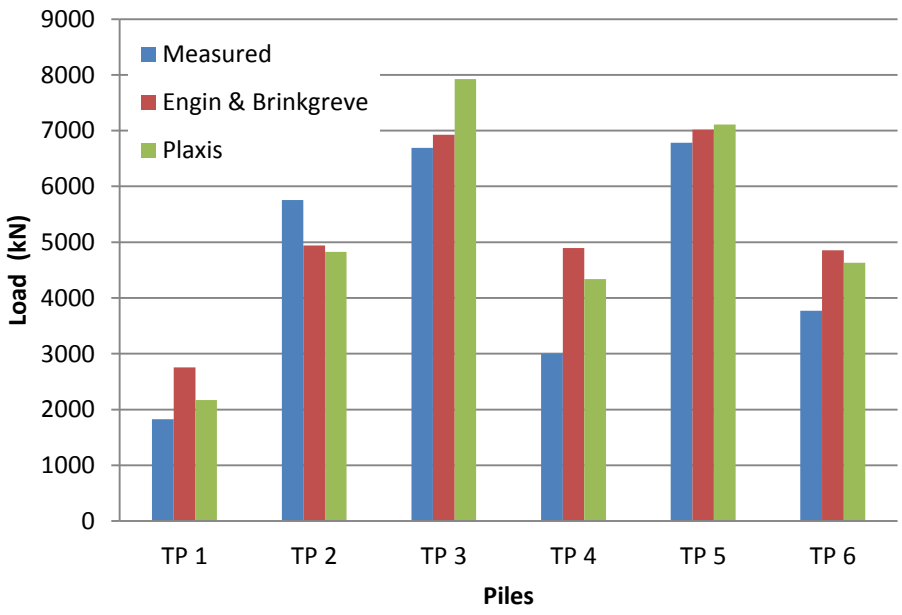

Figure 59 Comparison measured and calculated pile loads for Messe-Torhaus (after Engin & Brinkgreve, 2009)

4.3 Load Sharing of Raft

After all of the analyses have been carried out, the loads on each pile are added and subtracted from the total applied load to find the total load carried by the raft. The values are tabulated in Table 20. As stated in the previous subject, the usage of longer piles increases the shared load of piles. Other points can be listed as; total load carried by the raft increases in higher load levels and it also increases in higher number of piles for longer piles. However, the load on raft is decreased by the higher number of piles for shorter piles.

Load sharing ratio of raft is shown concisely in Figure 60 for all sub cases of Case 1. Up to 57% of the total load is carried out by the raft for the Case 1-b (100piles, 25m, 700kPa), in which the shorter piles are used with a pattern 10x10 under 700 kPa. However, this ratio seems like excessive comparing with the average percentage of 42.4% for the selected cases. This may be because of the excessive settlements in which the average load (4,801kN) on individual piles exceeds the allowable capacity of piles (for 25m-length piles with a F.S. 2, $Q_{all} = Q_{ult}/2 = 7{,}162/2 = 3{,}581kN$). For the Case 1-c (100piles, 35m, 500kPa), where the raft has the lowest load sharing, the average load (5.320kN) on an individual pile is slightly over the allowable capacity of piles (for 35m-length piles with a F.S. 2, $Q_{all} = Q_{ult}/2 = 10{,}522/2 = 5{,}261kN$). Therefore, it may be concluded that the load sharing ratio of raft is the most ideal (or realistic) ratio when the load on pile approaches to the allowable capacity of pile with F.S.=2.00.

For the Case 2 - Messe-Torhaus, at the final design load, raft carries %19.2 of the total load in addition the measured values gives %19.6.

Table 20 Sub-cases for Case 1 with variable number of piles, pile length and load level

Case 1-	Number of piles*	Pile length (m)	Dist. Load (kPa)	Total load (kN)	Pile load (kN)	Raft load (kN)	Load on piles	Load on raft
a	25	25	500	200,000	111,150	88,850	55.6%	44.4%
b	25	25	700	280,000	120,028	159,972	42.9%	57.1%
c	25	35	500	200,000	133,009	66,991	66.5%	33.5%
d	25	35	700	280,000	177,665	102,335	63.5%	36.5%
e	36	25	500	200,000	114,357	85,643	57.2%	42.8%
f	36	25	700	280,000	147,084	132,916	52.5%	47.5%
g	36	35	500	200,000	124,930	75,070	62.5%	37.5%
h	36	35	700	280,000	167,819	112,181	59.9%	40.1%

*number of piles represents the piles in the model which is a quarter of the actual model.

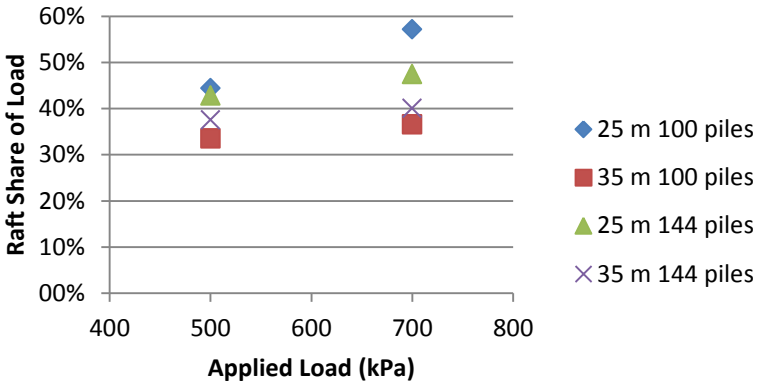

Figure 60 Load carried by raft vs. applied load for Case 1

4.4 Sap2000 Analyses

In general design application of foundations, soil springs are assigned to the end of the piles. However, actual behavior of a piled raft foundation differs by the load sharing between raft and piles. Therefore, the additional soil springs should be added to the shell (area) elements. Previously explained method of analysis, in Chapter 3.5, becomes more realistic with the additional soil springs connected to the raft. Settlements and pile load shares are shown in Table 21 for Case 1-d (100piles, 35m, 700kPa) and Case 1-h (144piles, 35m, 700kPa). It is observed that the contribution of raft support is significant and raft share is the 39-36% of total applied load.

Table 21 Settlements and pile loads for Case 1-d (100piles, 35m, 700kPa) & Case 1-h (144piles, 35m, 700kPa)

	Springs					Sett (m)			
	Pile (kN/m)	Raft (kN/m/m2)	Pile length (m)	# of pile	Load (kPa)	Center	Corner	Total Pile Load	Pile/Total
Case 1-d	29,533	1,163	35	100	**700**	0.2497	0.2523	738,100	61.3%
	29,533	1,163	35	100	**500**	0.1834	0.1853	542,076	61.3%
	29,533	0	35	100	**700**	0.4073	0.4124	1,204,909	100.0%
	29,533	0	35	100	**500**	0.2991	0.3029	884,909	100.0%
Case 1-h	32,340	1,405	35	144	**700**	0.1505	0.2082	805,008	66.7%
	32,340	1,405	35	144	**500**	0.1107	0.1529	591,616	66.7%
	32,340	0	35	144	**700**	0.2181	0.3236	1,207,069	100.0%
	32,340	0	35	144	**500**	0.1607	0.2377	887,069	100.0%

For a more specific examination of the Sap2000 analyses, loads on center piles and corner piles are tabulated in Table 22 for Case 1-d (100piles, 35m, 700kPa) with corresponding arbitrary maximum allowable settlement values and calculated settlements at the head of the piles. Maximum allowable settlements are only used to calculate the spring constant of piles. Table 22 shows the change in loads for specific piles at the corner and center of the foundation. Main inference of the table is that; with additional raft springs there is a significant decrease in the axial load of the pile whether it is a center or corner pile.

Table 22 Comparison of loads and settlements of center and corner piles

	Spring Constants		Load (kN)		Settlement (m)		
Max. Allow. Sett.	Pile (kN/m)	Raft (kN/m/m2)	Center Pile	Corner Pile	Center Pile	Corner Pile	Sap. Ref.
0.010m	526100	0	11,942	12,379	0.0227	0.0235	46 S
	526100	1000	11,571	11,982	0.0220	0.0228	47 S
	526100	10000	9,040	9,293	0.0172	0.0177	50 S
0.015m	350733	0	11,932	12,341	0.0340	0.0352	86 S
	350733	1000	11,395	11,769	0.0325	0.0336	87 S
	350733	10000	8,109	8,303	0.0231	0.0237	90 S
0.005m	1052200	0	11,975	12,453	0.0114	0.0118	126 S
	1052200	1000	11,774	12,236	0.0112	0.0116	127 S
	1052200	10000	10,227	10,573	0.0097	0.0100	130 S
0.100m	52610	0	11,972	12,175	0.2276	0.2314	06 S
	52610	1000	9,173	9,310	0.1744	0.1770	07 S
	52610	10000	2,959	2,980	0.0563	0.0567	10 S
by Plaxis outputs	29,533	1,163	7,351	7,429	0.2489	0.2516	200

To compare Sap2000 and Plaxis results, pile loads and settlements and moment distribution in raft are plotted along two specific lines, i.e. Line 1 and Line 2, inner piles and outer piles respectively. The numbers of specific piles are also plotted along these axes as shown in Figure 61.Due to symmetry conditions, only a quarter of the foundation is taken into account. For the interpretation of Figure 62 and Figure 63, in Sap2000 outputs, it is observed that the bowl shape of the settlement, which is explicit in Plaxis, could not be achieved both for inner line 1 and for outer line 2. This is a result of actual soil behavior exists in Plaxis 3D which does not exist in Sap2000.Settlements occur at the edge piles are slightly higher than the center piles. This is because of the moment created by the cantilever part of the raft (2m for 100-pile-case, 3,5m for 144-pile-case), but almost negligible.

For the comparison of load distribution of piles, Figure 64 and Figure 65 are plotted. It is obvious that the outer piles take higher loads in Plaxis 3D comparing with Sap2000. In addition the behaviors of outer piles are more likely in both software. However, the axial load of the inner piles of Plaxis 3D are less that the Sap2000 piles. This result is also parallel with the settlement behavior of foundation considering the actual soil behavior. Loads are taken almost evenly in Sap2000, in which the settlements are in line with this even distribution. As an extract, maximum and minimum settlement values of the rafts are tabulated in Table 23. It can be clearly seen from the Figure 66 and Figure 67 that the moment distribution of raft is over estimated in Plaxis comparing with Sap2000. This may be because of not only the soil spring modeling of Sap2000 but also the taking the raft as more flexible in Plaxis. Also the moment difference is slightly decreasing in the outer sections of raft.

Also, it can be concluded that the differential settlements are underestimated in Sap2000 analyses comparing with Plaxis results. Please refer Appendix V for all Sap2000 outputs and Appendix VI for the figures of the deformed shapes.

Table 23 Maximum and minimum settlement of rafts

Software	Max. Sett. (mm)		Min. Sett. (mm)	
	Case 1-d (100piles, 35m, 700kPa)	Case 2 (Messe-Torhaus)	Case 1-d (100piles, 35m, 700kPa)	Case 2 (Messe-Torhaus)
Sap2000	253	86	249	82
Plaxis	234	76	165	65

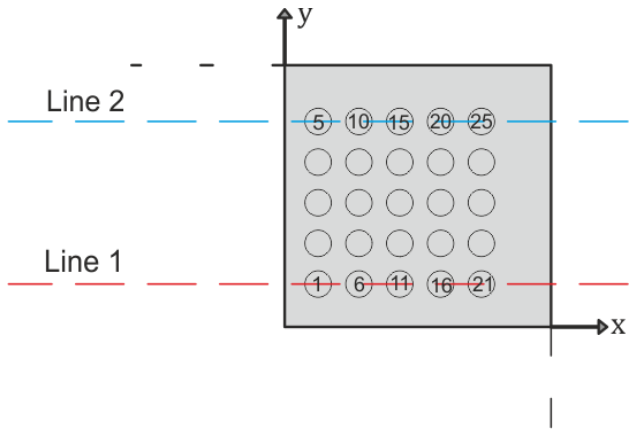

Figure 61 – Top view of the foundation as quarterly

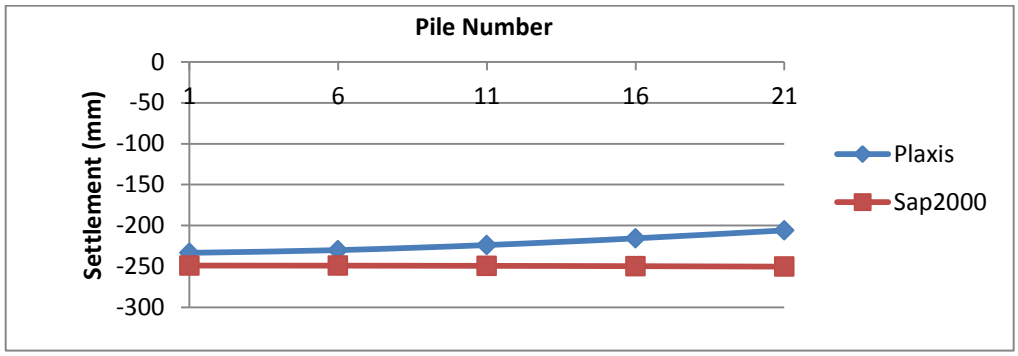

Figure 62 Settlements at the head of piles along Line 1 (i.e. inner piles)

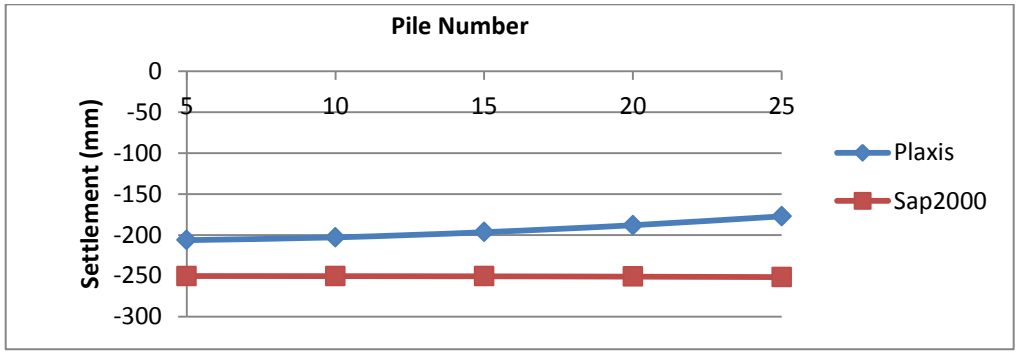

Figure 63 Settlements at the head of piles along Line 2 (i.e. outer piles)

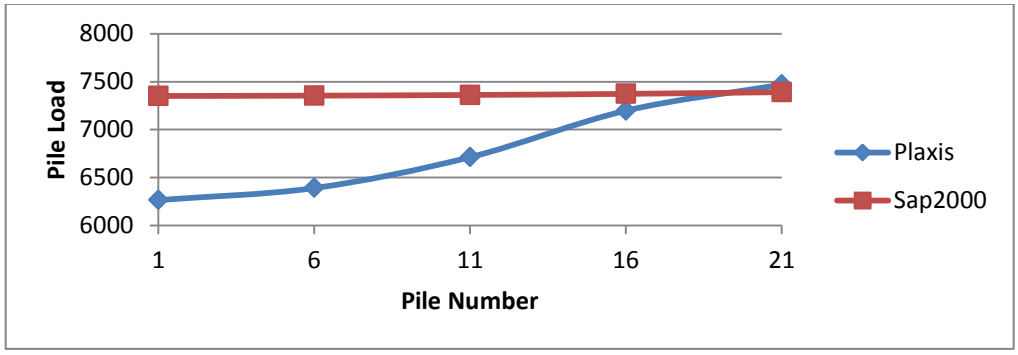

Figure 64 Pile loads along Line 1 (i.e. inner piles)

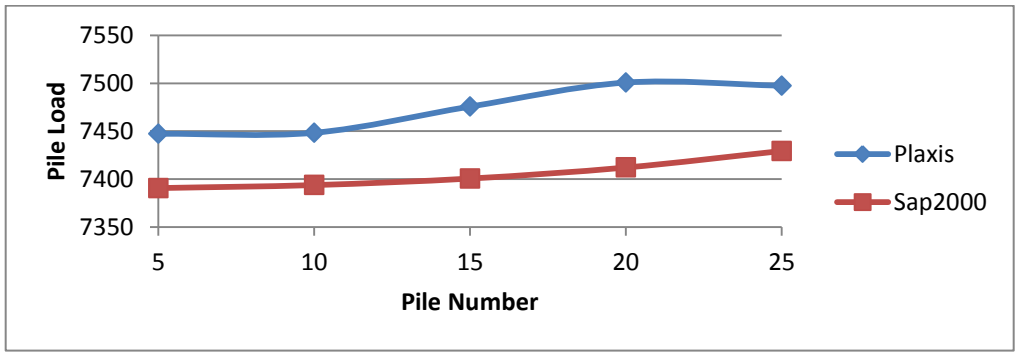

Figure 65 Pile loads along Line 2 (i.e. outer piles)

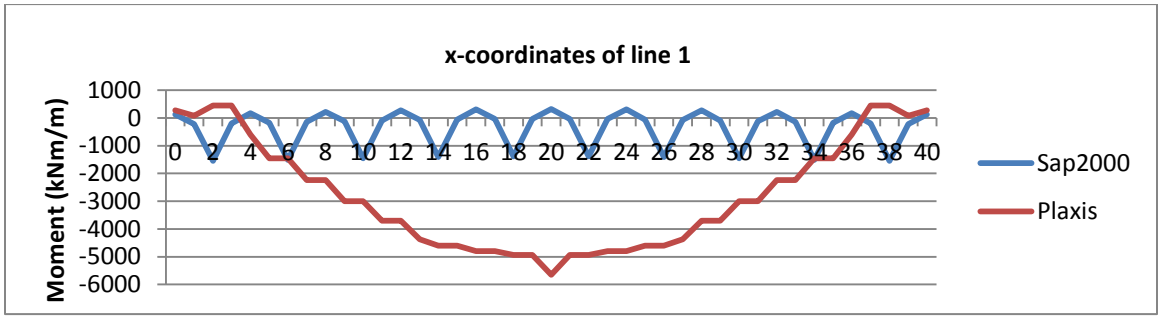

Figure 66 Moment distribution on raft along Line 1

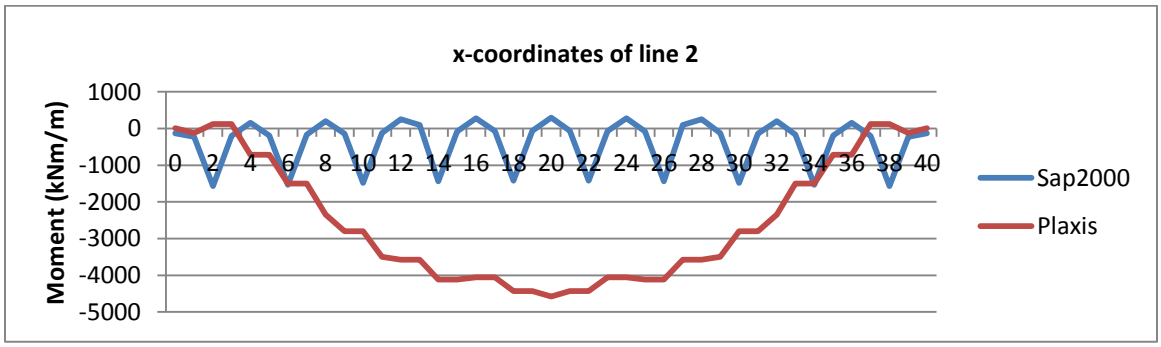

Figure 67 Moment distribution on raft along Line 2

CHAPTER 5

SUMMARY AND CONCLUSION

5.1 Summary

Piled raft systems are verified to be an economical foundation type comparing the conventional piled foundations, where, only the piles are used for the reducing of both total and differential settlements and the contribution of the raft is generally disregarded. In this study, the foundation settlement and the load sharing between raft and pile have been investigated to identify the contribution of raft to the total capacity of piled raft foundations.

In the first part of this study, a detailed literature review for the design of piled raft foundations has been presented. Advantages and disadvantages of different approaches have been discussed to model the piled raft foundation systems. Also the factors affecting the behavior of piled raft foundations have been discussed. Discussed factors are; the number of piles, length of piles, diameter of piles, pile spacing ratio, location of piles, stiffness of piles, distribution of load, level of load, raft thickness, raft dimensions and type of soil.

In the second part, a case has been created for Ankara clay and parametric analyses have been conducted with the help of Plaxis 3D software. Variables for the parametric analyses are pile number, pile length and level of the load applied. In addition, a case study, Messe-Torhaus in Frankfurt, has been solved to validate the method of the calculation. Results show that the calculation method is in line with the actual piled raft behavior.

5.2 Conclusions

A method presented to find the settlements in Sap2000 by using the outputs of the Plaxis. Using the embedded pile feature of Plaxis, raft and pile load sharing is calculated and the corresponding load-settlement curves are plotted. Taking the constant of the slope of this curve as the total spring of elements, corresponding average spring constants are assigned to the piles and raft in Sap2000.

The proposed method of analysis becomes more realistic with the additional soil springs connected to the raft. This may be helpful for structural/foundation engineers to calculate the deformations more accurate and the structural properties of raft more effective.

Average percentage of raft load share is 42.4% for the selected Case 1. For the Case 2, at the final design load, raft can carry up to 19.2% of applied load. The main reasons for the difference in these two cases are the excessive loading of Case 1, the foundation characteristic (number of piles and length of piles) and the soil stiffness difference between Ankara clay and Frankfurt clay.

General outcomes of the study can be listed as:

Load sharing is significantly increased in piled rafts, even small constants of soil springs are assigned to the raft in Sap2000.

The load sharing ratio of raft is the most ideal (or realistic) ratio when the load on pile approaches to the allowable capacity of pile with a F.S.=2.00.

Total load carried by the raft increases in higher load levels and when the longer piles are used it also increases with the increasing number of piles.

The usage of longer piles decreases the load share of raft. Also, with the usage of longer piles, the outer most piles take higher axial loads than the inner piles. This result is also parallel with the outcomes of the study of Lin and Feng (2006).

In addition, using longer piles reduced the differential settlement of raft in higher load levels.

At low load level; axial load of the center pile is smaller than the corner pile and at higher load level; axial load of the center pile is almost same with the corner pile. It is also observed that the number of piles does not have a significant effect on the settlements for low load levels. However, in higher load levels, increasing number of piles has a decreasing effect on settlements only for shorter piles (25 m).

Pile loads in Sap2000 are distributed almost evenly, due to the assignment of soil springs as the average of total piles.

Raft flexibility is higher in Plaxis comparing with Sap2000, under the same loading conditions within the proposed method.

As Cunha et al. (2001) stated, by decreasing the number of piles, displacements increase.

For increasing number of piles (in this study 144-pile case), it is observed that the axial load of the center pile is decreasing comparing the outer piles. Center pile can approach to the load level of outer piles after certain the depth and moves parallel after this point. This may be the effect of small ratio of pile spacing and pile diameter, which causes the block movement of soil just beneath the center of raft.

5.3 Recommendations for Future Researches

This study focuses on the axial and static loads on piles and rafts in piled raft foundations. Therefore, lateral and dynamic/cyclic loads can be considered in the further studies, which may lead to discover a proper/realistic behavior of piled rafts under dynamic conditions.

During the FE analyses of the model with Plaxis, it is important to consider the weight of the excavated material and other structural weights, like raft. In addition, the embedded pile feature of Plaxis may be used more accurately in calculations if the capacity of piles is taken from the field tests. The proposed method and the embedded piles are validated through a real case. In addition to this, separate validations may be done through different elements of Plaxis 3D, like, volume piles, beams etc.

With the intention of more detailed comparison and realistic behavior of piled raft foundation, Hardening Soil Model may be used with the help of elaborated soil data.

Uniform distributed loads have been applied to the model in this study and equally spaced identical piles have been used. However, this is not the actual case in day-to-day design of structures. As a general recommendation, it is needed to vary the pile spacing and/or pile diameters/length considering the pattern of the superstructure load. Therefore, load considerations are needed to be done on the project bases, by placing the piles strategically using a parametric study or trial and error. Local design codes/regulations should be taken into account during the design and construction stages.

In the back analyses by the Sap2000, the soil springs are chosen as linear springs. However, spring constants, increasing with the increasing depth and the lower values between the piles and non-linear springs may be used to show the actual pile-soil interaction in piled raft foundations.

REFERENCES

Bakholdin, B.V. (**2003**). Piled-Raft Foundations, Design and Characteristics of Construction Procedures. Soil Mechanics and Foundation Engineering, Vol. 40, No. 5, 185-189.

Barvashov, V. A., & Boldyrev, G. G. (**2009**). Experimental and theoretical research on analytical models of piled-raft foundations. Soil Mechanics and Foundation Engineering, Vol. 46, No. 5, 207-217.

Baziar, M.H., Ghorbani, A., & Katzenbach, R. (**2009**). Small-Scale Model Test and Three-Dimensional Analysis of Pile-Raft Foundation on Medium-Dense Sand. International Journal of Civil Engineerng. Vol. 7, No. 3, 170-175.

Bouzid, A., Vermeer, P.A., & Tiliouine, B. (**2005**). Finite Element Vertical Slices Model Validation and Application to an Embedded Square Footing Under Combined Loading.

Burland, J. B. (**1973**). Shaft friction of piles in clay: a simple fundamental approach. Ground Engineering, 6(3), 30 - 42.

Burland, J.B. (**1995**). Piles as settlement reducers. Keynote address 18th Italian congress on soil mechanics. Italy.

Cheng, Z. (**2011**). Prediction and Measurement of Settlement of a Piled Raft Foundation over Thick Soft Ground. The Electronic Journal of Geotechnical Engineering, Vol. 16, 125-136.

Chow, H.S.W. (**2007**). Analysis of Piled-Raft Foundations with Piles of Different Lengths and Diameters. University of Sydney.

Clancy, P. & Randolph, M. F. (**1993**), An approximate analysis procedure for piled raft foundations. Int. J. Numer. Anal. Meth. Geomech., 17: 849–869.

Comodromos, E.M., Papadopoulou, M.C., & Rentzeperis, I.K. (**2009**). Pile Foundation Analysis and Design Using Experimental Data and 3-D Numerical Analysis. Computers and Geotechnics, 36, 819–836.

Cunha, R.P., Poulos, H.G., & Small, J.C. (**2001**). Investigation of Design Alternatives for a Piled Raft Case History. Journal of Geotechnical and Geoenvironmental Engineering, August 2001, 635-641.

Davis, E.H. & Taylor, H. (**1962**). The movement of bridge approaches and abutment on soft foundation soils. In: Proceedings of the 1st Biennial Conference on Australian Road Research Board. p. 740.

Dennis, N.D, & Olson, R.E. (**1983**). Axial Capacity of Steel Pipe Piles in Sand. Proceedings of the Conference on Geotechnical Practice on Offshore Engineering, pp. 389-402. New York: American Society of Civil Engineers.

Ergun, M.U, & Turkmen, H.K. (**2007**). Kazıklı Radye Temellerin Etkin Tasarımı.

Engin, H.K., & Brinkgreve, R.B.J. (**2009**). Investigation of Pile Behaviour Using Embedded Piles. Proceedings of the 17th International Conference on Soil Mechanics and Geotechnical Engineering.

Fleming, K., Weltman, A., Randolph, K. & Elson, K. (**1992**). Piling engineering. Taylor & Francis.

Fraser, R.A. & Wardle, L. J. (**1976**). Numerical Analysis of Rectangular Rafts on Layered Foundations. Gêotechnique 26, No. 4, 613–630.

Gök, S. (**2007**). Kazıklı Radye Temellerin Tasarımı - Design of Piled Raft Foundations.

Gök, S., & Toğrol, E. (**2009**). Basitleştirilmiş Kazıklı Radye Hesabı. ITU Bulletin, Volume:8, Number:5, 149-156.

Guo, W.D., & Randolph, M.F. (**1998**). Rationality of Load Transfer Approach for Pile Analysis. Computers and Geotechnics, 23, 85-112.

Gupta, S.C. (**1997**). Design of Raft Foundations. New Age International Limited.

Katzenbach, R., Arslan, U., & Moormann, C. (**2000**). Piled raft foundation projects in Germany. Design applications of raft foundations, J. A. Hemsley, ed., Thomas Telford, London, 323–392.

Khelifi, Z., Berga, A., & Terfaya, N. (**2011**).Modeling the Behavior of Axially and Laterally Loaded Pile with a Contact Model. The Electronic Journal of Geotechnical Engineering, Vol. 16, 1239-1258.

Kim, K.N., Lee, S., Kim, K., & Chung, C. (**2001**). Optimal Pile Arrangement for Minimizing Differential Settlements in Piled Raft Foundations. Computers and Geotechnics, 28, 235–253.

Long, P.D. (**2010**). Piled Raft – A Cost-Effective Foundation Method for High- Rises. Geotechnical Engineering Journal of the SEAGS & AGSSEA Vol. 41 No.3, 1-12.

Lee, C. J., Bolton, M. D. & Al-Tabbaa, A. (**2002**). Numerical Modelling of Group Effects on the Distribution of Dragloads in Pile Foundations. Gêotechnique 52, No. 5, 325–335.

Lee, J., Kim, Y., & Jeong, S. (**2010**). Three-Dimensional Analysis of Bearing Behavior of Piled Raft on Soft Clay. Computers and Geotechnics, 37, 103–114.

Leung, Y.F., Klar, A., & Soga, K. (**2010**). Theoretical Study on Pile Length Optimization of Pile Groups and Piled Rafts. Journal of Geotechnical and Geoenvironmental Engineering, ASCE, 319-330.

Liang, F., Chen, L., & Han, J. (**2009**). Integral Equation Method for Analysis of Piled Rafts with Dissimilar Piles under Vertical Loading. Computers and Geotechnics, 36, 419–426.

Liang, F., Chena, L., & Shib, X. (**2003**). Numerical Analysis of Composite Piled Raft with Cushion Subjected to Vertical Load. Computers and Geotechnics, 30, 443–453.

Lin, D., & Feng, Z. (**2006**). A Numerical Study of Piled Raft Foundations. Journal of the Chinese Institute of Engineers, Vol. 29, No. 6, 1091-1097.

Madhira R. Madhav†, M.R., Sharma, J.K., & Sivakumar, V. (**2009**). Settlement of and Load Distribution in a Granular Piled Raft.

Makarchian. M., & Poulos, H.G. (**1996**). Simplified Method for Design of Underpinning Piles. Journal of Georechnical Engineering, September 1996, 745-751.

Meyerhof, G G (**1976**). Bearing capacity and settlement of pile foundations. Proceedings, American Society of Civil Engineers 102(GT3), pp 195-228

Meyerhof, G.G. (**1992**).Proceedings of the Conference on recent large-scale fully-instrumented pile test in clay. Institution of Civil Engineers, London.

Mroueh, H., & Shahrour, I. (**2002**). Three-Dimensional Finite Element Analysis of the Interaction between Tunneling and Pile Foundations. Int. J. Numer. Anal. Meth. Geomech., 2002, 26, 217–230.

Murthy, V.N.S (**2002**). Geotechnical Engineering. Taylor & Francis.

Niandou, H., & Breysse, D. (**2007**). Reliability Analysis of a Piled Raft Accounting for Soil Horizontal Variability. Computers and Geotechnics, 34, 71–80.

Nguyen, D.D.C, Jo, S.B, & Kim, D.S. (**2013**). Design method of piled-raft foundations under vertical load considering interaction effects. Computers and Geotechnics, Volume 47, Pages 16–27

Oh, E.Y., Hunag, M., Surarak, C., Adamec, R., & Balasurbamaniam, A.S. (**2008**). Finite Element Modeling for Piled Raft Foundation in Sand. Eleventh East Asia-Pacific Conference on Structural Engineering & Construction (EASEC-11) "Building a Sustainable Environment" November 19-21, 2008, Taipei, TAIWAN

Oh, E.Y., Lin, D.G., Bui, Q.M., & Huang, M. (**2009**). Numerical Analysis of Piled Raft Foundation in Sandy and Clayey Soils

Ozturk, S. (**2009**). Distribution of bending moments in laterally loaded passive pile groups a model study. M.S. Thesis in Civil Engineering, Middle East Technical University, Ankara, Turkey.

Poulos, H.G. (**2001**). Methods of Analysis of Piled Raft Foundations. International Society of Soil Mechanics and Geotechnical Engineering.

Poulos, H.G. (**2001**). Piled raft foundations design and applications. Gêotechnique 51, No. 2, 95–113.

Poulos, H.G., & Chen, L.T. (**1997**). Piles Response due to Excavation-Induced Lateral Soil Movement. Journal of Geotechnical and Geoenvironmental Engineering, February 1997, 94-99.

Poulos, H.G., & Davids, E. H. (**1980**). Pile Foundation Analysis and Design. John Wiley and Sons, New York.

Poulos, H.G., & Davids, A. J. (**2005**). Foundation design for the Emirates Twin Towers, Dubai. Can. Geotech. J. 46, 716–730.

Plaxis 3D Reference Manual. (**2012**). Plaxis bv.

Prakoso, W. A., & Kulhawy, F.H. (**2001**) Contribution to Piled Raft Foundation Design. Journal of Geotechnical and Geoenvironmental Engineering, 17-24.

Randolph, M.F. (**1994**). Design methods for pile groups and piled rafts.'' Proc., 13th Int. Conf. on Soil Mechanics and Foundation Engineering, Int. Society for Soil Mechanics and Foundation Engineering, 5, 61–82.

Reul, O. (**2004**). Numerical Study of the Bearing Behavior of Piled Rafts. International Journal of Geomechanics, ASCE, 59-68.

Reul, O., & Randolph, M.F. (**2003**). Piled rafts in overconsolidated clay comparison of in situ measurements and numerical analyses. Gêotechnique 53, No. 3, 301–315.

Reul, O., & Randolph, M.F. (**2004**). Design Strategies for Piled Rafts Subjected to Nonuniform Vertical Loading. Journal of Geotechnical and Geoenvironmental Engineering, ASCE, 1-13,

Russo, G. & Viggiani, C. (**1998**). Factors controlling soil-structure interaction for piled rafts. Proc. International Conference on Soil-Structure Interaction in Urban Civil Engineering, Ed. R. Katzenbach & U. Arslan, Darmstadt.

Sap2000 v.14 Reference Manual. (**2009**). Computers and Structures, Inc.

Sağlam, N. (2003). Settlement of piled rafts- a critical review of the case histories and calculation methods. M.S. Thesis in Civil Engineering, Middle East Technical University, Ankara, Turkey.

Sales, M. M., Small, J. C., & Poulos, H. G. (**2010**). Compensated Piled Rafts in Clayey Soils- Behaviour, Measurements, and Predictions. Can. Geotech. J. 47, 327–345.

Sanctis, L., & Mandolini, A. (**2006**). Bearing Capacity of Piled Rafts on Soft Clay Soils. Journal of Geotechnical and Geoenvironmental Engineering, ASCE, 1600-1610.

Schmitt, A., Turek, J., & Katzenbach, R. (**2003**). Reducing the Costs for Deep Foundaitons of High Rise Building by Advanced Numerical Modelling. ARI, the Bulletin of the Istanbul Technical University, Volume 53, Number 2, 81-87.

Skempton, A.W. (**1951**). The Bearing Capacity of Clays, Proc. Building Research Congress, Volume 1, pp. 180-189.

Small, J.C., & Liu, H.L. (**2008**). Time-Settlement Behaviour of Piled Raft Foundations Using Infinite Elements. Computers and Geotechnics, 35, 187–195.

Sonoda, R., Matsumoto, T., Kitiyodom, P., Moritaka, H., & Ono, T. (**2009**). Case Study of a Piled Raft Foundation Constructed Using a Reverse Construction Method and Its Post Analysis. Can. Geotech. J. 46, 142–159.

Stroud, M. A. (**1975**). The standard penetration test and the engineering properties of glacial material. Proceedings of the symposium on the engineering behaviour of glacial materials, Birmingham, pp. 1249–135.

Ta, L.D., & Small, J.C. (**1997**). An Approximation for Analysis of Raft and Piled Raft Foundations. Computers and Geotechnics, Vol. 20, No. 2, 105-123.

Tabsh, S.W., & Al-Shawa, A.R. (**2005**). Effect of Spread Footing Flexibility on Structural Response. Practice Periodical on Structural Design and Construction, May 2005, 109-114.

Tan, Y.C., & Chow, C.M. (**2004**) Design of Piled Raft Foundation on Soft Ground. GSM-IEM Forum: The roles of Engineering geology & geotechnical engineering in construction works, 21st October 2004, Department of Geology, University of Malaya, Kuala Lumpur.

Tomlinson, M. J. (**2004**). Pile Design and Construction Practice. E & FN Spon.

Viggiani, C. (**1993**). Further Experiences with Auger Piles in Naples Area. Proceedings of the 2nd International Geotechnical Seminar on Deep Foundations on Bored and Auger Piles, BAP II, W.F. Van Impe (ed.), Balkema, Rotterdam, pp. 77-94.Won, J., Ahn, S., Jeong, S., Lee, J., & Jang, S. (**2006**). Nonlinear Three-Dimensional Analysis of Pile Group Supported Columns Considering Pile Cap Flexibility. Computers and Geotechnics, 33, 355–370.

Xu, K.J., & Poulos, H.G. (**2001**). 3D Elastic Analysis of Vertical Piles Subjected to Passive Loadings. Computers and Geotechnics, 28, 349-375.

Yılmaz, B. (2010). An Analytical and Experimental Study on Piled Raft Foundations. M.S. Thesis in Civil Engineering, Middle East Technical University, Ankara, Turkey.

Zhang, G., & Zhang, J. (**2009**). Numerical Modeling of Soil–Structure Interface of a Concrete-Faced Rockfill Dam. Computers and Geotechnics, 36,762–772.

Ziaie-Moayed, R., Kama1zare, M., & Safavian, M. (**2010**). Evaluation of Piled Raft Foundations Behavior with Different Dimensions of Piles. Journal of Applied Sciences 10 (13), 1320-1325.

APPENDIX I

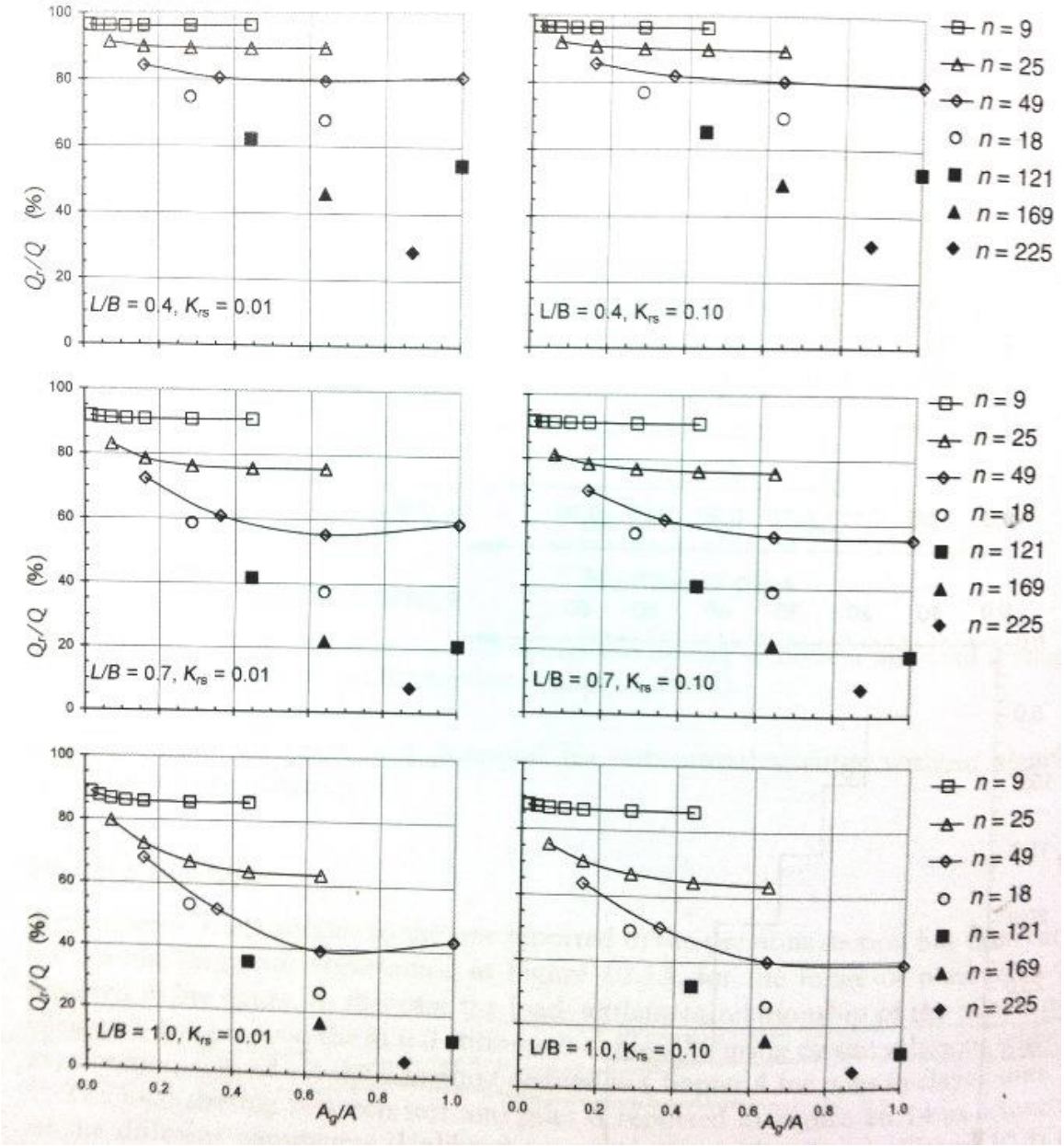

Figure 68 Load sharing for a large piled raft (Viggiani et. al. (2012))

APPENDIX II

The below table and figures are the outputs of the calculations made by disregarding the weight of the excavated soil and the structures (raft) for Case-1.

Table 24 Sub-cases with variable number of piles, pile length and load level (Disregarding the weight of the excavated soil and raft)

Case 1-	Number of Piles	Pile length (m)	Dist. Load (kPa)	Total load (kN)	Pile load (kN)	Raft load (kN)	Load on piles	Load on raft
a	25	25	500	200,000	138,405	61,595	69%	31%
b	25	25	700	280,000	148,827	131,173	53.15%	46.85%
c	25	35	500	200,000	167,181	32,819	83.59%	16.41%
d	25	35	700	280,000	209,771	70,229	74.92%	25.08%
e	36	25	500	200,000	144,725	55,275	72.36%	27.64%
f	36	25	700	280,000	177,752	102,248	63.48%	36.52%
g	36	35	500	200,000	158,122	41,878	79.06%	20.94%
h	36	35	700	280,000	202,101	77,899	72.18%	27.82%

Table 25 Settlement values for variable number of piles, pile length and load level (Disregarding the weight of the excavated soil and raft)

				Settlement (mm)			
Case 1-	Pile number	Pile length (m)	Dist. Load (kPa)	A	B	C	D
a	25	25	500	111	107	113	99
b	25	25	700	232	223	214	181
c	25	35	500	72	68	73	63
d	25	35	700	128	122	125	108
e	36	25	500	106	103	116	111
f	36	25	700	173	169	183	181
g	36	35	500	68	65	79	77
h	36	35	700	116	111	124	120

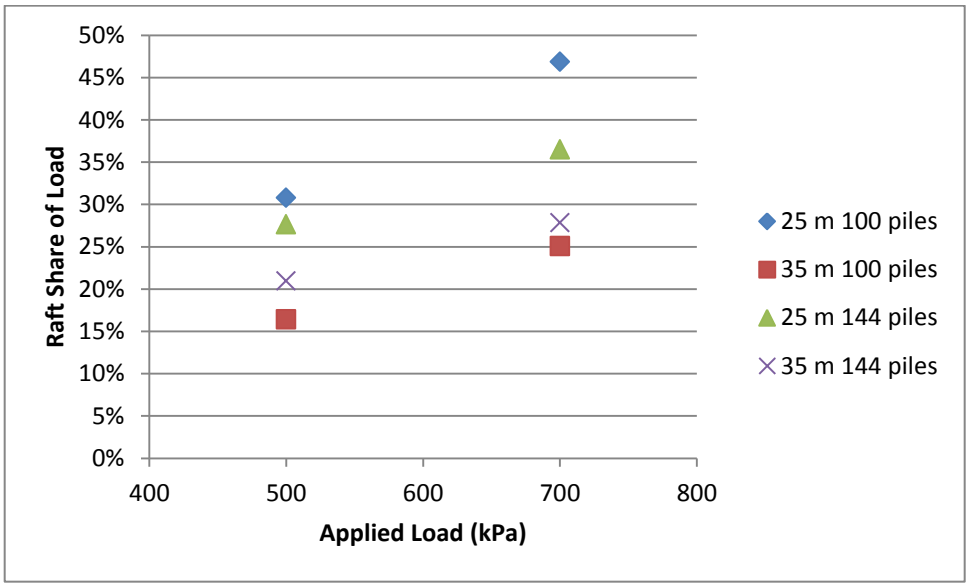

Figure 69 Load carried by raft vs. applied load (Disregarding the weight of the excavated soil and raft)

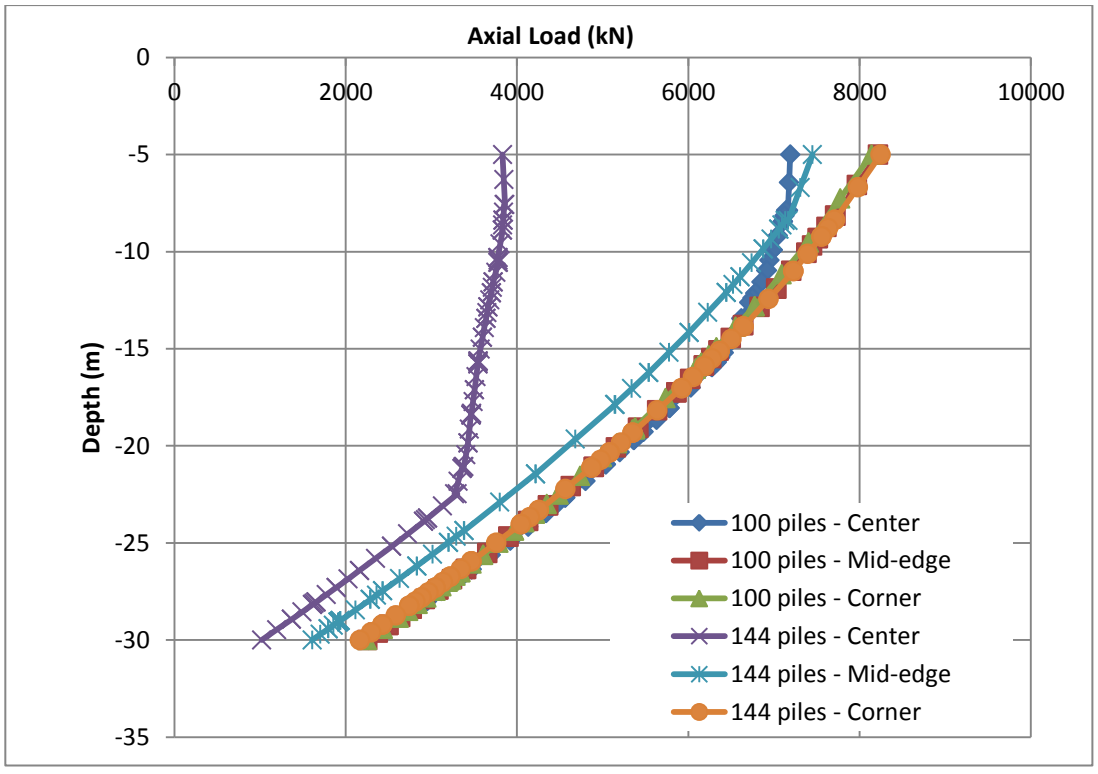

Figure 70 Comparison of axial load distributions along piles for different number of piles (Case 1-a (100piles, 25m, 500kPa) vs. Case 1-e (144piles, 25m, 500kPa)) (Disregarding the weight of the excavated soil and raft)

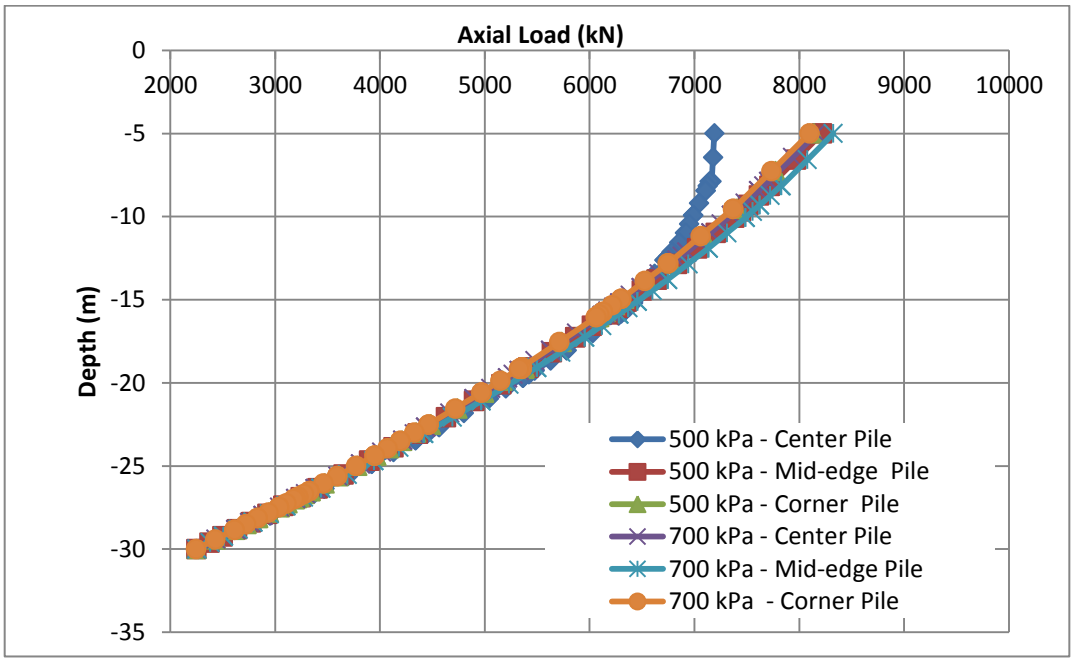

Figure 71 Comparison of axial load distributions along piles for different load levels (Case 1-a (100piles, 25m, 500kPa) vs. Case 1-b (100piles, 25m, 700kPa)) (Disregarding the weight of the excavated soil and raft)

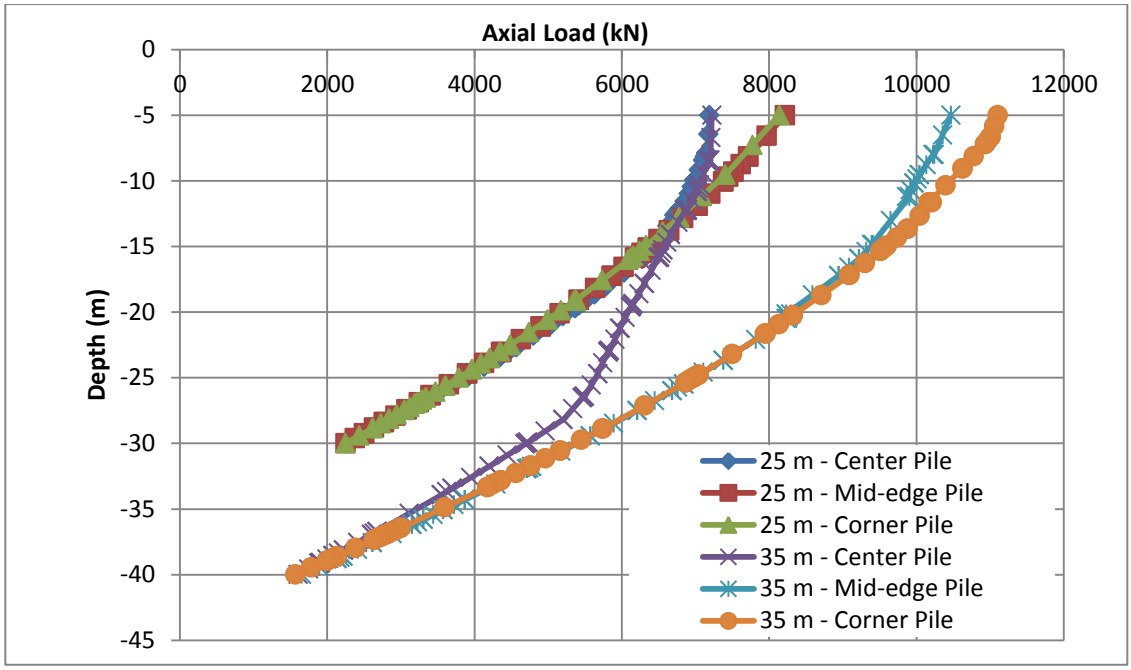

Figure 72 Comparison of axial load distributions along piles for different length of piles (Case 1-a (100piles, 25m, 500kPa) vs. Case 1-c (100piles, 35m, 500kPa)) (Disregarding the weight of the excavated soil and raft)

APPENDIX III - EFFECT OF MESH COARSENESS

				Settlement (mm)				
Case 1-	Mesh Coarseness	Number of elements	Number of nodes	A	B	C	D	Plaxis ref.
a	Coarse	11101	17300	195	186	166	135	*251*
b	Coarse	11101	17300	343	327	294	238	*252*
c	Coarse	14836	23404	153	144	122	96	*253*
d	Coarse	14836	23404	234	223	201	168	*254*
e	Coarse	16466	25304	189	182	166	143	*255*
f	Coarse	16466	25304	277	271	259	234	*256*
g	Coarse	16397	26403	153	146	129	110	*257*
h	Coarse	16397	26403	216	207	191	170	*258*
a	Medium	19901	30112	195	188	165	136	*201*
b	Medium	19901	30112	343	330	290	239	*202*
c	Medium	19806	30379	153	146	122	94	*203*
d	Medium	19806	30379	234	226	200	164	*204*
e	Medium	26673	40196	189	182	166	145	*205*
f	Medium	26673	40196	277	271	266	238	*206*
g	Medium	27126	41551	151	143	127	109	*207*
h	Medium	27126	41551	213	204	188	169	*208*
a	Fine	36016	53318	196	188	166	137	*241*
b	Fine	36016	53318	344	329	294	240	*242*
c	Fine	36045	53885	151	142	120	93	*243*
d	Fine	36045	53885	235	225	201	168	*244*
e	Fine	47761	71053	189	183	166	146	*245*
f	Fine	47761	71053	278	272	260	241	*246*
g	Fine	47421	71633	151	145	128	110	*247*
h	Fine	47421	71633	213	205	189	171	*248*
a	Very fine	84103	120839	197	189	169	142	*231*
b	Very fine	84103	120839	346	332	299	255	*232*
c	Very fine	84257	121493	152	143	121	96	*233*
d	Very fine	84257	121493	237	228	205	175	*234*
e	Very fine	103221	149458	187	180	165	146	*235*
f	Very fine	103221	149458	278	272	264	248	*236*
g	Very fine	103812	151285	152	145	130	113	*237*
h	Very fine	103812	151285	215	206	192	175	*238*

APPENDIX IV - EFFECT OF MODEL SIZE

Case 1-	Model size	Number of elements	Number of nodes	Settlement (mm) A	B	C	D	Plaxis ref.
a	3x (60m)	14653	22875	196	188	167	139	*211*
b	3x (60m)	14653	22875	346	333	301	253	*212*
c	3x (60m)	14768	23464	151	142	120	94	*213*
d	3x (60m)	14768	23464	236	226	204	173	*214*
e	3x (60m)	22147	34683	187	179	164	147	*215*
f	3x (60m)	22147	34683	278	273	264	251	*216*
g	3x (60m)	22149	35603	151	144	128	111	*217*
h	3x (60m)	22149	35603	213	205	190	177	*218*
a	5x (100m)	19901	30112	195	188	165	136	*201*
b	5x (100m)	19901	30112	343	330	290	239	*202*
c	5x (100m)	19806	30379	153	146	122	94	*203*
d	5x (100m)	19806	30379	234	226	200	164	*204*
e	5x (100m)	26673	40196	189	182	166	145	*205*
f	5x (100m)	26673	40196	277	271	266	238	*206*
g	5x (100m)	27126	41551	151	143	127	109	*207*
h	5x (100m)	27126	41551	213	204	188	169	*208*
a	8x (160m)	19690	29845	195	186	166	130	*221*
b	8x (160m)	19690	29845	341	324	291	223	*222*
c	8x (160m)	19447	30142	154	144	122	95	*223*
d	8x (160m)	19447	30142	235	224	203	164	*224*
e	8x (160m)	27364	41173	189	183	166	140	*225*
f	8x (160m)	27364	41173	277	270	256	226	*226*
g	8x (160m)	26903	41714	154	147	131	110	*227*
h	8x (160m)	26903	41714	217	209	192	169	*228*

APPENDIX V – SAP2000 ANALYSES AND OUTPUTS

Table 26 – Results for maximum allowable settlement taken as **0.1m**

	Spring constants					Sett (m)				
	Pile (kN/m)	Raft (kN/m/ m2)	Pile length (m)	# of piles	Load (kPa)	Center	Corner	Total Pile Load	Pile Load / Total Load	Sap. Ref.
Case 1-b	35810	0	25	100	**700**	0.3361	0.3423	1,204,908	100.0%	01 S
	35810	1000	25	100	**700**	0.2321	0.2359	831,635	69.0%	02 S
	35810	2000	25	100	**700**	0.1772	0.1799	634,939	52.7%	03 S
	35810	5000	25	100	**700**	0.1039	0.1050	371,411	30.8%	04 S
	35810	10000	25	100	**700**	0.0615	0.0620	219,548	18.2%	05 S
Case 1-d	**52610**	**0**	**35**	**100**	**700**	**0.2291**	**0.2342**	**1,204,908**	**100.0%**	**06 S**
	52610	1000	35	100	700	0.1755	0.1790	922,420	76.6%	07 S
	52610	2000	35	100	700	0.1423	0.1448	747,235	62.0%	08 S
	52610	5000	35	100	700	0.0908	0.0920	476,025	39.5%	09 S
	52610	**10000**	**35**	**100**	**700**	**0.0566**	**0.0572**	**296,610**	**24.6%**	**10 S**
Case 1-f	35810	0	25	144	**700**	0.1938	0.3369	1,207,068	100.0%	11 S
	35810	1000	25	144	**700**	0.1508	0.2449	912,750	75.6%	12 S
	35810	2000	25	144	**700**	0.1241	0.1911	734,872	60.9%	13 S
	35810	5000	25	144	**700**	0.0819	0.1133	465,204	38.5%	14 S
	35810	10000	25	144	**700**	0.0527	0.0664	289,544	24.0%	15 S
Case 1-h	**52610**	**0**	**35**	**144**	**700**	**0.1252**	**0.2502**	**1,207,068**	**100.0%**	**16 S**
	52610	1000	35	144	**700**	0.1059	0.1965	987,588	81.8%	17 S
	52610	2000	35	144	**700**	0.0920	0.1609	836,722	69.3%	18 S
	52610	5000	35	144	**700**	0.0667	0.1028	575,646	47.7%	19 S
	52610	**10000**	**35**	**144**	**700**	**0.0460**	**0.0631**	**380,069**	**31.5%**	**20 S**
Case 1-a	35810	0	25	100	500	0.2469	0.2512	884,908	100.0%	21 S
	35810	1000	25	100	500	0.1704	0.1733	610,770	69.0%	22 S
	35810	2000	25	100	500	0.1302	0.1321	466,313	52.7%	23 S
	35810	5000	25	100	500	0.0763	0.0771	272,774	30.8%	24 S
	35810	10000	25	100	500	0.0451	0.0455	161,243	18.2%	25 S
Case 1-c	52610	0	35	100	500	0.1682	0.1720	884,908	100.0%	26 S
	52610	1000	35	100	500	0.1289	0.1315	677,445	76.6%	27 S
	52610	2000	35	100	500	0.1045	0.1064	548,786	62.0%	28 S
	52610	5000	35	100	500	0.0666	0.0676	349,606	39.5%	29 S
	52610	10000	35	100	500	0.0416	0.0420	217,840	24.6%	30 S
Case 1-e	35810	0	25	144	500	0.1425	0.2474	887,068	100.0%	31 S
	35810	1000	25	144	500	0.1109	0.1799	670,792	75.6%	32 S
	35810	2000	25	144	500	0.0912	0.1403	540,078	60.9%	33 S
	35810	5000	25	144	500	0.0602	0.0832	341,905	38.5%	34 S
	35810	10000	25	144	500	0.0388	0.0487	212,812	24.0%	35 S
Case 1-g	52610	0	35	144	500	0.0920	0.1837	887,068	100.0%	36 S
	52610	1000	35	144	500	0.0779	0.1429	725,790	81.8%	37 S
	52610	2000	35	144	500	0.0677	0.1181	614,928	69.3%	38 S
	52610	5000	35	144	500	0.0490	0.0755	423,074	47.7%	39 S
	52610	10000	35	144	500	0.0339	0.0463	279,346	31.5%	40 S

Table 27 Results for maximum allowable settlement taken as **0.01m**

	Spring constants					Sett (m)				
	Pile (kN/m)	Raft (kN/m/ m2)	Pile length (m)	# of piles	Load (kPa)	Center	Corner	Total Pile Load	Pile Load / Total Load	Sap. Ref.
Case 1-b	358100	0	25	100	**700**	0.0348	0.0358	1,204,908	100.0%	41 S
	358100	1000	25	100	**700**	0.0333	0.0341	1,151,045	95.5%	42 S
	358100	2000	25	100	**700**	0.0318	0.0326	1,101,791	91.4%	43 S
	358100	5000	25	100	**700**	0.0283	0.0289	976,448	81.0%	44 S
	358100	10000	25	100	**700**	0.0237	0.0242	820,826	68.1%	45 S
Case 1-d	**526100**	**0**	**35**	**100**	**700**	**0.0239**	**0.0248**	**1,204,908**	**100.0%**	**46 S**
	526100	1000	35	100	**700**	0.0234	0.0240	1,166,951	96.8%	47 S
	526100	2000	35	100	**700**	0.0227	0.0232	1,131,313	93.9%	48 S
	526100	5000	35	100	**700**	0.0208	0.0212	1,036,366	86.0%	49 S
	526100	**10000**	**35**	**100**	**700**	**0.0183**	**0.0186**	**909,198**	**75.5%**	**50 S**
Case 1-f	358100	0	25	144	**700**	0.0160	0.0427	1,207,069	100.0%	51 S
	358100	1000	25	144	**700**	0.0158	0.0404	1,164,682	96.5%	52 S
	358100	2000	25	144	**700**	0.0156	0.0384	1,125,452	93.2%	53 S
	358100	5000	25	144	**700**	0.0150	0.0334	1,023,320	84.8%	54 S
	358100	10000	25	144	**700**	0.0139	0.0274	891,059	73.8%	55 S
Case 1-h	**526100**	**0**	**35**	**144**	**700**	**0.0114**	**0.0310**	**1,207,069**	**100.0%**	**56 S**
	526100	1000	35	144	**700**	0.0111	0.0298	1,176,769	97.5%	57 S
	526100	2000	35	144	**700**	0.0111	0.0287	1,148,135	95.1%	58 S
	526100	5000	35	144	**700**	0.0108	0.0257	1,070,848	88.7%	59 S
	526100	**10000**	**35**	**144**	**700**	**0.0103**	**0.0219**	**964,591**	**79.9%**	**60 S**
Case 1-a	358100	0	25	100	500	0.0256	0.0263	884,909	100.0%	61 S
	358100	1000	25	100	500	0.0244	0.0251	845,351	95.5%	62 S
	358100	2000	25	100	500	0.0234	0.0240	809,180	91.4%	63 S
	358100	5000	25	100	500	0.0208	0.0212	717,130	81.0%	64 S
	358100	10000	25	100	500	0.0175	0.0178	602,842	68.1%	65 S
Case 1-c	526100	0	35	100	500	0.0178	0.0182	884,909	100.0%	66 S
	526100	1000	35	100	500	0.0173	0.0177	857,034	96.9%	67 S
	526100	2000	35	100	500	0.0167	0.0171	830,862	93.9%	68 S
	526100	5000	35	100	500	0.0153	0.0156	761,135	86.0%	69 S
	526100	10000	35	100	500	0.0134	0.0137	667,746	75.5%	70 S
Case 1-e	358100	0	25	144	500	0.0118	0.0313	887,069	100.0%	71 S
	358100	1000	25	144	500	0.0117	0.0297	855,928	96.5%	72 S
	358100	2000	25	144	500	0.0156	0.0282	827,105	93.2%	73 S
	358100	5000	25	144	500	0.0110	0.0245	752,067	84.8%	74 S
	358100	10000	25	144	500	0.0102	0.0201	654,889	73.8%	75 S
Case 1-g	526100	0	35	144	500	0.0083	0.0228	887,069	100.0%	76 S
	526100	1000	35	144	500	0.0083	0.0219	864,809	97.5%	77 S
	526100	2000	35	144	500	0.0082	0.0210	843,773	95.1%	78 S
	526100	5000	35	144	500	0.0080	0.0189	786,992	88.7%	79 S
	526100	10000	35	144	500	0.0076	0.0161	708,925	79.9%	80 S

Table 28 Results for maximum allowable settlement taken as **0.015m**

	Spring constants					Sett (m)		
	Pile (kN/m)	Raft (kN/m/m2)	Pile length (m)	# of piles	Load (kPa)	Center	Corner	Sap. Ref.
Case 1-b	238733	0	25	100	**700**	0.0510	0.0528	81 S
	238733	1000	25	100	**700**	0.0482	0.0494	82 S
	238733	2000	25	100	**700**	0.0453	0.0463	83 S
	238733	5000	25	100	**700**	0.0382	0.0391	84 S
	238733	10000	25	100	**700**	0.0304	0.0310	85 S
Case 1-d	**350733**	**0**	**35**	**100**	700	**0.0353**	**0.0365**	**86 S**
	350733	1000	35	100	**700**	0.0337	0.0348	87 S
	350733	2000	35	100	**700**	0.0322	0.0333	88 S
	350733	5000	35	100	**700**	0.0286	0.0294	89 S
	350733	**10000**	**35**	**100**	700	**0.0240**	**0.0246**	**90 S**
Case 1-f	238733	0	25	144	**700**	0.0238	0.0600	91 S
	238733	1000	25	144	**700**	0.0232	0.0557	92 S
	238733	2000	25	144	**700**	0.0227	0.0521	93 S
	238733	5000	25	144	**700**	0.0214	0.0434	94 S
	238733	10000	25	144	**700**	0.0189	0.0338	95 S
Case 1-h	**350733**	**0**	**35**	**144**	700	**0.0164**	**0.0434**	**96 S**
	350733	1000	35	144	**700**	0.0161	0.0411	97 S
	350733	2000	35	144	**700**	0.0160	0.0390	98 S
	350733	5000	35	144	**700**	0.0153	0.0339	99 S
	350733	**10000**	**35**	**144**	700	**0.0141**	**0.0277**	**100 S**
Case 1-a	238733	0	25	100	500	0.0376	0.0388	101 S
	238733	1000	25	100	500	0.0352	0.0363	102 S
	238733	2000	25	100	500	0.0331	0.0340	103 S
	238733	5000	25	100	500	0.0281	0.0287	104 S
	238733	10000	25	100	500	0.0223	0.0229	105 S
Case 1-c	350733	0	35	100	500	0.0259	0.0268	106 S
	350733	1000	35	100	500	0.0247	0.0256	107 S
	350733	2000	35	100	500	0.0237	0.0244	108 S
	350733	5000	35	100	500	0.0210	0.0216	109 S
	350733	10000	35	100	500	0.0176	0.0180	110 S
Case 1-e	238733	0	25	144	500	0.0177	0.0440	111 S
	238733	1000	25	144	500	0.0173	0.0402	112 S
	238733	2000	25	144	500	0.0168	0.0382	113 S
	238733	5000	25	144	500	0.0157	0.0318	114 S
	238733	10000	25	144	500	0.0139	0.0245	115 S
Case 1-g	350733	0	35	144	500	0.0121	0.0319	116 S
	350733	1000	35	144	500	0.0120	0.0312	117 S
	350733	2000	35	144	500	0.0118	0.0287	118 S
	350733	5000	35	144	500	0.0112	0.0249	119 S
	350733	10000	35	144	500	0.0104	0.0203	120 S

Table 29 Results for maximum allowable settlement taken as **0.005m**

	Spring constants					Sett (m)		
	Pile (kN/m)	Raft (kN/m/m2)	Pile length (m)	# of piles	Load (kPa)	Center	Corner	Sap. Ref.
Case 1-b	716200	0	25	100	**700**	0.0180	0.0186	121 S
	716200	1000	25	100	**700**	0.0175	0.0182	122 S
	716200	2000	25	100	**700**	0.0171	0.0178	123 S
	716200	5000	25	100	**700**	0.0160	0.0166	124 S
	716200	10000	25	100	**700**	0.0145	0.0149	125 S
Case 1-d	**1052200**	**0**	**35**	**100**	**700**	**0.0126**	**0.0132**	**126 S**
	1052200	1000	35	100	**700**	0.0124	0.0129	127 S
	1052200	2000	35	100	**700**	0.0122	0.0127	128 S
	1052200	5000	35	100	**700**	0.0117	0.0122	129 S
	1052200	**10000**	**35**	**100**	**700**	**0.0108**	**0.0112**	**130 S**
Case 1-f	716200	0	25	144	**700**	0.0087	0.0241	131 S
	716200	1000	25	144	**700**	0.0087	0.0234	132 S
	716200	2000	25	144	**700**	0.0086	0.0226	133 S
	716200	5000	25	144	**700**	0.0084	0.0207	134 S
	716200	10000	25	144	**700**	0.0081	0.0181	135 S
Case 1-h	**1052200**	**0**	**35**	**144**	**700**	**0.0063**	**0.0178**	**136 S**
	1052200	1000	35	144	**700**	0.0063	0.0174	137 S
	1052200	2000	35	144	**700**	0.0062	0.0169	138 S
	1052200	5000	35	144	**700**	0.0061	0.0154	139 S
	1052200	**10000**	**35**	**144**	**700**	**0.0059**	**0.0142**	**140 S**
Case 1-a	716200	0	25	100	500	0.0132	0.0137	141 S
	716200	1000	25	100	500	0.0129	0.0134	142 S
	716200	2000	25	100	500	0.0126	0.0130	143 S
	716200	5000	25	100	500	0.0118	0.0122	144 S
	716200	10000	25	100	500	0.0106	0.0109	145 S
Case 1-c	1052200	0	35	100	500	0.0093	0.0097	146 S
	1052200	1000	35	100	500	0.0091	0.0095	147 S
	1052200	2000	35	100	500	0.0090	0.0093	148 S
	1052200	5000	35	100	500	0.0086	0.0089	149 S
	1052200	10000	35	100	500	0.0079	0.0082	150 S
Case 1-e	716200	0	25	144	500	0.0063	0.0177	151 S
	716200	1000	25	144	500	0.0063	0.0171	152 S
	716200	2000	25	144	500	0.0062	0.0166	153 S
	716200	5000	25	144	500	0.0061	0.0152	154 S
	716200	10000	25	144	500	0.0059	0.0133	155 S
Case 1-g	1052200	0	35	144	500	0.0047	0.0131	156 S
	1052200	1000	35	144	500	0.0046	0.0127	157 S
	1052200	2000	35	144	500	0.0046	0.0124	158 S
	1052200	5000	35	144	500	0.0046	0.0116	159 S
	1052200	10000	35	144	500	0.0044	0.0104	160 S

APPENDIX VI

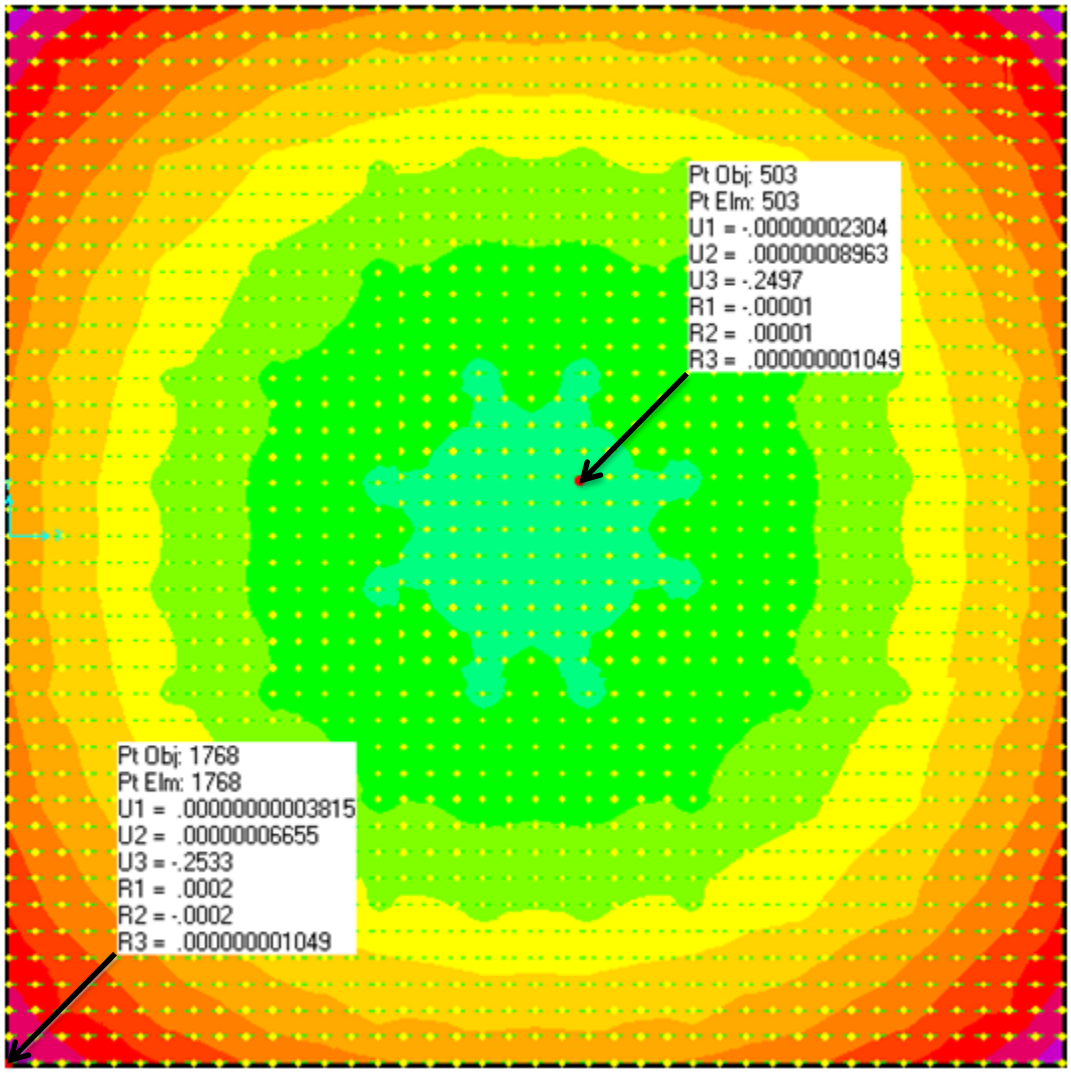

Figure 73 Deformed shape in Sap2000 for Case 1-d (100piles, 35m, 700kPa)

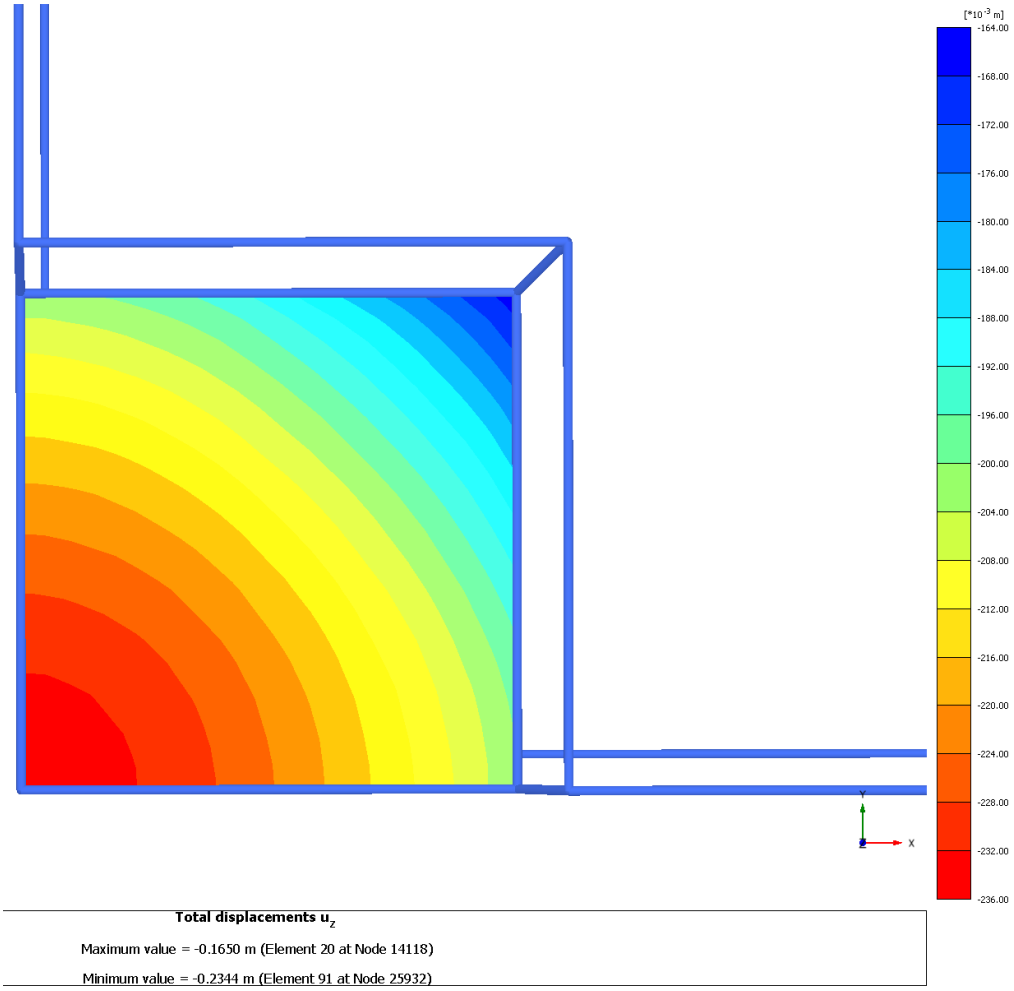

Figure 74 Deformed shape in Plaxis for Case 1-d (100piles, 35m, 700kPa)

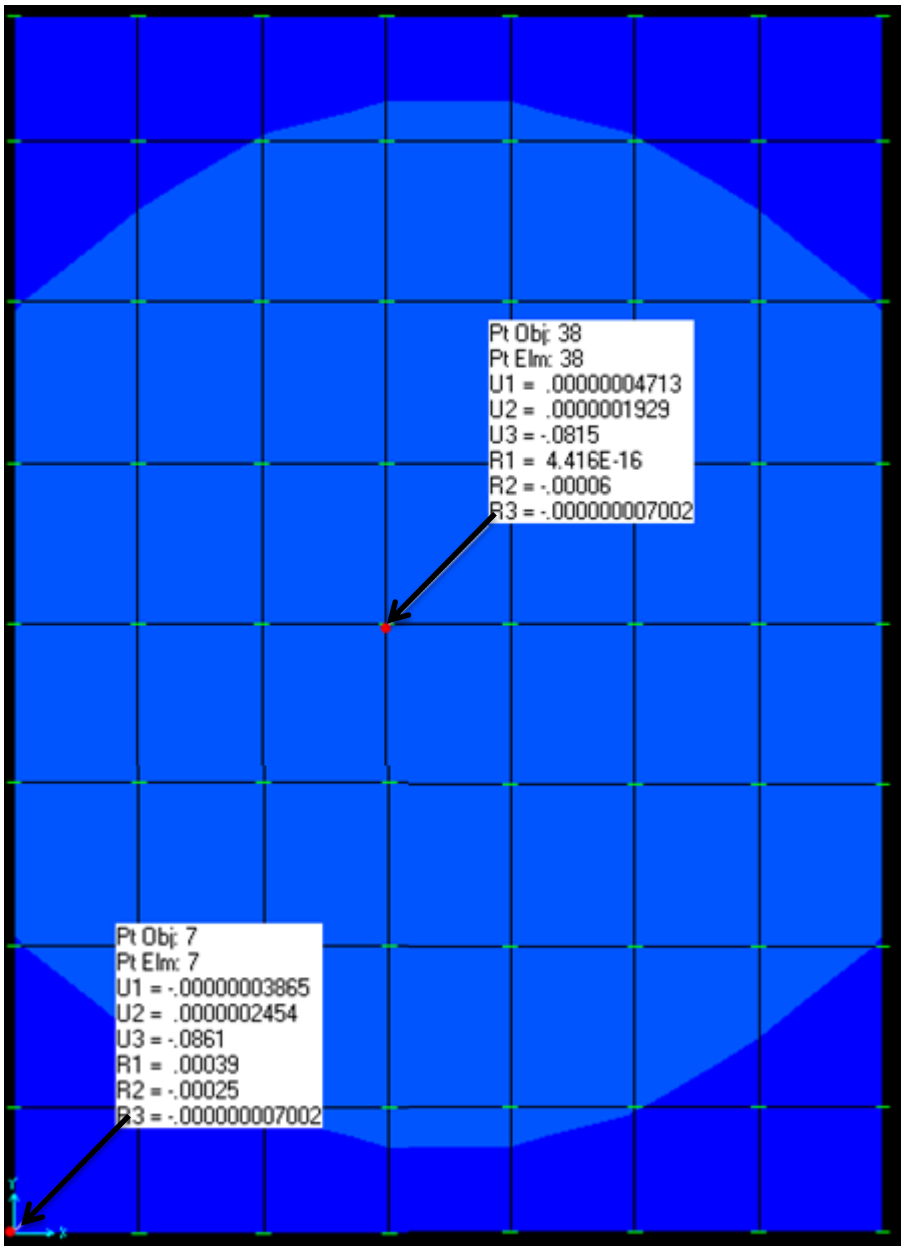

Figure 75 Deformed shape in Sap2000 for Case 2

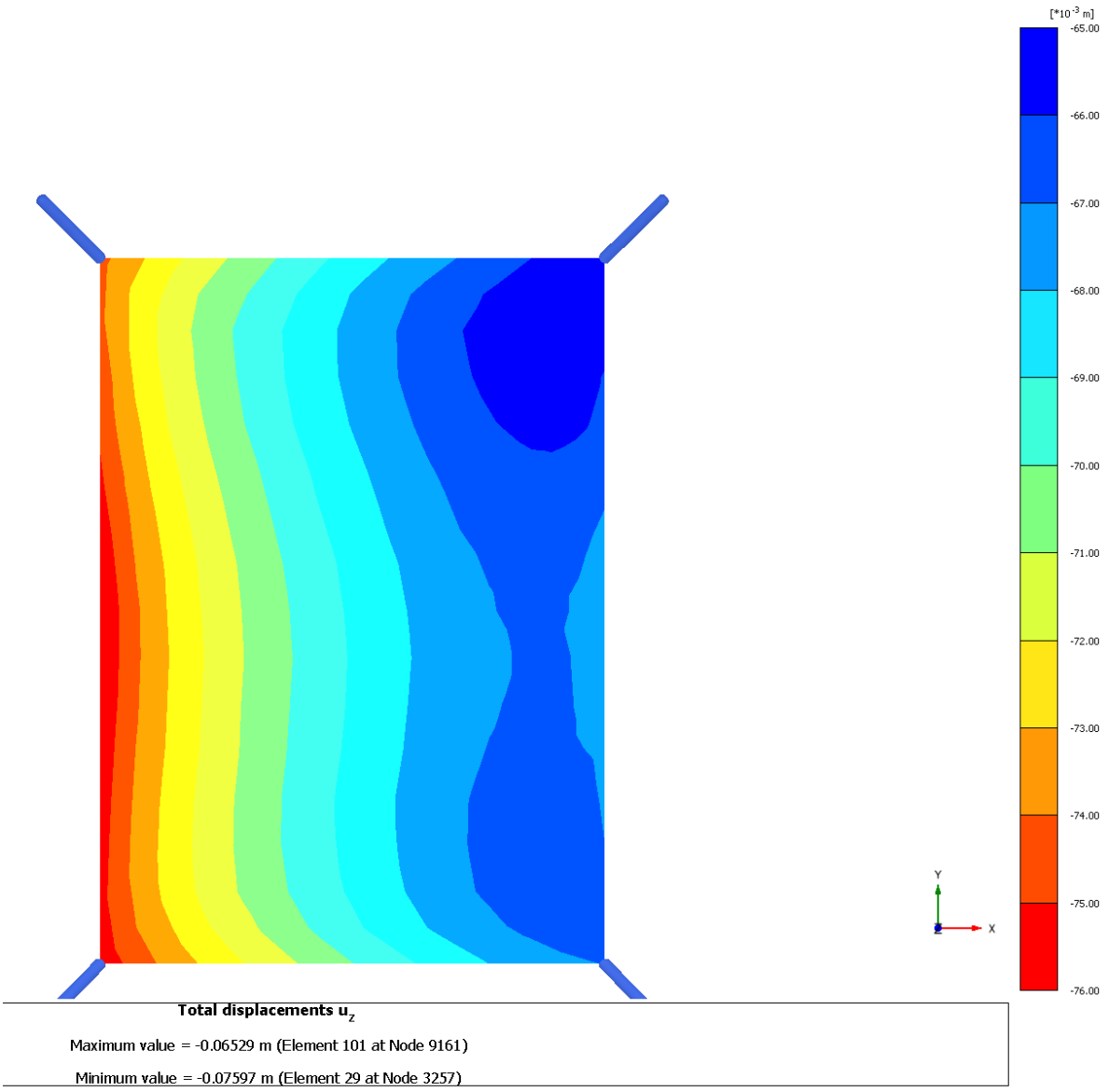

Figure 76 Deformed shape in Plaxis for Case 2

APPENDIX VII – ALTERNATIVE RESULT

The below table is the alternative output of the analyses made by taking the stiffness parameter of Ankara clay as shown in Figure 77 (E' increases averagely 1.175 MPa per one meter depth, starting from the 20.550 MPa at ground level).

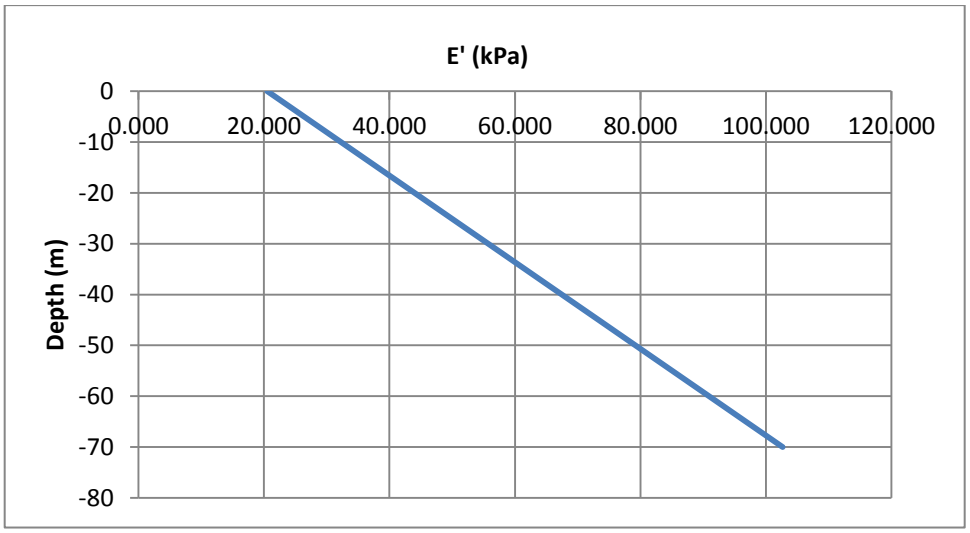

Figure 77 E' (MPa) vs. depth (m).

Table 30 Settlement values for variable number of piles, pile length and load level

				Settlement (mm)			
Case 1-	Number of piles*	Pile length (m)	Dist. Load (kPa)	A	B	C	D
a	25	25	500	-147	-140	-118	-91
b	25	25	700	-242	-232	-204	-165
c	25	35	500	-119	-113	-92	-69
d	25	35	700	-172	-163	-137	-106
e	36	25	500	-147	-141	-127	-108
f	36	25	700	-211	-204	-186	-169
g	36	35	500	-117	-111	-98	-81
h	36	35	700	-165	-157	-141	-122

*number of piles represents the piles in the model which is a quarter of the actual model.

Table 31 Sub-cases with variable number of piles, pile length and load level

Case 1-	Number of piles*	Pile length (m)	Dist. Load (kPa)	Total load (kN)	Pile load (kN)	Raft load (kN)	Load on piles	Load on raft
a	25	25	500	200,000	120,473	79,527	60.2%	39.8%
b	25	25	700	280,000	149,546	130,454	53.4%	46.6%
c	25	35	500	200,000	141,857	58,143	70.9%	29.1%
d	25	35	700	280,000	190,758	89,242	68.1%	31.9%
e	36	25	500	200,000	125,514	74,486	62.8%	37.2%
f	36	25	700	280,000	162,702	117,298	58.1%	41.9%
g	36	35	500	200,000	133,733	66,267	66.9%	33.1%
h	36	35	700	280,000	181,323	98,677	64.8%	35.2%

*number of piles represents the piles in the model which is a quarter of the actual model.